行政院國家科學委員會補助專題研究計畫 □成 果 報 告
□期中進度報告

光電系統促進芬頓程序處理高濃度廢液之反應動力與反應槽設計

計畫類別：□ 個別型計畫 □ 整合型計畫
計畫編號：NSC 96－2628－E－041－002－MY3
執行期間： 96 年 8 月 1 日至 99 年 7 月 31 日

計畫主持人： 盧明俊 教授
共同主持人： 黃耀輝 副教授
計畫參與人員： 丁涴屏、莊宗霖、趙敏傑、陳建瑋、**Nalinrut Masomboon**

成果報告類型(依經費核定清單規定繳交)：□精簡報告 □完整報告

本成果報告包括以下應繳交之附件：
□赴國外出差或研習心得報告一份
□赴大陸地區出差或研習心得報告一份
□出席國際學術會議心得報告及發表之論文各一份
□國際合作研究計畫國外研究報告書一份

處理方式：除產學合作研究計畫、提升產業技術及人才培育研究計畫、列管計畫及下列情形者外，得立即公開查詢
□涉及專利或其他智慧財產權，□一年□二年後可公開查詢

執行單位： 嘉南藥理科技大學

中 華 民 國 九十九 年 八 月 十七 日

摘要

本團隊近年來致力於光電促進芬頓程序的相關發展與研究，發現以光電促進芬頓程序可有效提高芬頓程序的處理效能。其主要原因為傳統芬頓程序中的亞鐵在反應進行之初會快速與過氧化氫反應，一方面產生氫氧自由基氧化有機物，另一方面產生三價鐵離子與氫氧化鐵污泥。當系統中的鐵離子自二價氧化成三價後，可提供給過氧化氫的催化能力隨即大幅下降，並容易與副產物產生錯合，惟此類錯合物可接受光與電所提供的電子，再次還原成亞鐵離子供系統循環使用。是故欲提高氫氧自由基濃度，首先需提高系統中的鐵離子還原速率。

相關文獻指出芳香族類的化合物在經過傳統的芬頓程序氧化後，通常礦化效果不佳，污染物多半轉而以小分子型態的有機酸存在於系統中。研究發現這些有機酸多半為草酸及其他少量甲酸及醋酸，三價鐵易與此類副產物發生錯合反應，而這些錯合物在紫外光至可見光範圍的吸收度很高，故可接受光能量還原成亞鐵離子再次參與芬頓反應。研究中以電流及長波長紫外光源促進系統中的鐵還原反應，目標以節省能源為方向進行一系列的電化學反應槽篩選。

有鑑於過去與電解相關的電解槽裝置一般均為單一陰極與陽極相對，可提供的反應面積受限於陰陽極板相對之處。本研究以單、雙層陰極電解槽與極板間距為變因，評估反應槽效能與操作經費，尋求最佳電解槽設計參數，並透過反應時間、pH、Fe^{2+}/H_2O_2 莫爾比、電流與過氧化氫進藥模式等變因的探討，瞭解最適電-芬頓程序操作參數，最後以生物可分解程度(BOD/COD；BOD/TOC)對芬頓，電-芬頓與光電-芬頓程序進行評估。並於研究中分析污染物降解情形，以決定污染物在不同操作參數與氧化程序中之反應速率及速率常數，藉以瞭解相關設計參數，最後進行中間產物鑑定，推導污染物的氧化機制。

關鍵詞: 光電-芬頓程序，芳香族類化合物、生物可分解、中間產物、反應動力模式

Abstract

A new approach of photoelectro assisted Fenton process has been developed in our laboratory. It is found that the Fenton reaction can be efficiency enhanced in photoelectro assisted Fenton process since Fe(Ⅲ) may complex with certain target compounds or byproducts, especially those acting as ligands, produced by UVA light and current. The new design of our system came from the concept of promoting the ferric reduction rate, which can increase the amount of hydroxyl radicals.

Literatures reported that oxalic, formic and acetic acids are the major products of aromatic compound degradation, which can complex with ferric ions. These complexes typically have higher molar absorption coefficients in the UV and visible regions to generate ferrous ions. Meanwhile, the ferrous ion is regenerated via the reduction of ferric ion on the cathode. However, the reaction mechanism of ferric ion reduction is still unclear. Therefore, a functional reactor was designed to save energy and to clarify the mechanism of ferric reduction with UVA light and electricity.

A new electro-chemical cell was developed to increase the working area and promote the current efficiency. The operation parameters, such as single and double electrode effect, electrode distance, initial pH, Fe^{2+}/H_2O_2 molar ratio, applied current, H_2O_2 feeding mode were investigated, firstly. Then the test of biodegradability (BOD/COD; BOD/TOC) was used to explore the effect of Fenton, electro-Fenton and photoelectro assisted Fenton process. Finally, in this dissertation, the intermediate of oxidation process was identified and the mechanisms were proposed.

Key word: Photoelectro-Fenton process, aromatic compound, biodegradability, kinetic, intermediate

CONTENTS

LIST OF TABLES

LIST OF FIGURES

CHAPTER 1 INTROUCTION

1.1. Background

2,6-Dimethylaniline (2,6-DMA) and benzene sulfonic acid (BSA) are usually used as intermediates in the manufacture of azo dyestuffs, pharmaceuticals, agrochemicals, coloring agents and tanning agents. Large amounts of aromatic compounds have been produced as building blocks for the synthesis of dyes and detergents, and released into the environment as waste during their manufacture and use (Bossmann et al., 1998; Takeo et al., 1997; Alonso et al., 2005). Most of them are not biodegradable. Although 2,6-DMA and BSA have been produced and applied for a long time, little information is available on their toxicology and environmental behavior.

Aromatic sulfonated compounds are surface-active and very soluble in water. In contrast to the linear alkylbenzenesulfonates (LAS), which have been found to be readily biodegradable, the aromatic sulfonates without long alkyl side chains are reported to be persistent (Takada and Ishiwatari, 1990). Consequently, it is difficult to remove them from water and they are transported from sewers to surface waters. In the previous study, the photocatalytic degradation of sodium benzenesulfonate and its substituted compounds were investigated (Ollis and Al-Ekabi, 1993). Photochemical or thermal processes also can enhance the Fenton reaction in the presence of 2,4-dimethylaniline (2,4-DMA) (Bossmann et al., 1998).

More demanding requirements imposed by law to the treatment plants have forced to the development of new alternatives, like stronger oxidizing agents or advanced oxidation processes (AOPs) (Safarzadeh-Amiri et al., 1996; Walling, 1975; Pignatello et al., 2006; Lu et al., 2001). AOPs are defined as the oxidation processes that generate hydroxyl

radicals in sufficient quantity to effect wastewater treatment (Chou et al., 1999; Lu et al., 2003; Ting et al., 2007; Sengil and ozacar, 2006). Although AOPs were classified as expensive treatment option, the cost can be minimized and optimized from different aspects, such as apply methodologies for catalyst recycling and integration of chemical and biological treatment processes (Brillas et al., 2002; Badellino et al., 2006; Sirés et al., 2007a; Sirés et al., 2007b; Esplugas and Ollis, 1997).

Hydrogen peroxide was first used to reduce odor in wastewater treatment plants, and from then on, hydrogen peroxide entered the realm of wastewater treatment. Hydrogen peroxide is a non-contaminating oxidant because its products are non-toxic substances, and can conform to strict environmental regulations (Elizardo, 1991). Besides, some contaminants may be oxidized into biologically degradable matter using hydrogen peroxide, and oxygen produced from hydrogen peroxide is also supplied to enhance the biodegradability.

The Fenton reaction is a widely used and studied catalytic process based on an electron transfer between H_2O_2 and a metal acting as a homogeneous catalyst (Safarzadeh-Amiri et al., 1996). The reactivity of this system was first observed in 1894 by its inventor H.J.H. Fenton, but its utility was not recognized until the 1930s when a mechanism based on hydroxyl radicals was proposed (Walling, 1975). The process may be applied to wastewaters, sludge, and contaminated soils to reduce toxicity, improve biodegradability, and remove odor and color (Pignatello et al., 2006; Lu et al., 2001; Lu et al., 2003). During the Fenton process, hydrogen peroxide is catalyzed by ferrous ion to produce hydroxyl radicals (Walling, 1975).

$$Fe^{2+} + H_2O_2 \rightarrow Fe^{3+} + OH^- + HO^{\bullet} \qquad (1.1)$$

This reaction is propagated from ferrous ion regeneration mainly by the reduction of the produced ferric species with hydrogen peroxide (Walling, 1973),

$$H_2O_2 + Fe^{3+} \rightarrow Fe^{2+} + HO_2^{\bullet} + H^+ \quad (1.2)$$

However, in the Fenton chain reactions, the rate constant of equation (1.1) is between 53 and 76 $M^{-1}s^{-1}$ (Walling, 1975; Rigg, et al., 1954; Metelitsa, 1971), while that of equation (1.2) is only 0.01 $M^{-1}s^{-1}$ (Walling, 1973). This means that ferrous ions are consumed more rapidly than they are produced. This results in the formation of a large amount of ferric hydroxide sludge during the neutralization stage of the Fenton process, which requires additional separation and disposal processes (Chou et al., 1999).

Recently, an electrochemical application method in the Fenton process, named the electro-Fenton method, has been reported. These studies can be generally divided into four categories (Pignatello et al., 2006). In Type 1, hydrogen peroxide is externally applied while a sacrificial iron anode is used as a ferrous ion source (Kannan et al., 2006; Sengil and ozacar, 2006; Kurt et al., 2007).

$$Fe^0 \rightarrow Fe^{2+} + 2e^- \quad (1.3)$$

In Type 2, ferrous ion is externally applied, and hydrogen peroxide is generated by an oxygen sparging cathode (Badellino et al., 2006; Kusvuran et al., 2005).

$$O_2 + 2H^+ + 2e^- \rightarrow H_2O_2 \quad (1.5)$$

In Type 3, Fenton's regent was utilized to produce hydroxyl radical in the electrolytic cell, and ferrous ion was regenerated via the reduction of ferric ion on the cathode (Zhang et al., 2006; Zhang et al., 2007; Li et al., 2007).

$$Fe^{3+} + e^- \rightarrow Fe^{2+} \quad (1.4)$$

In Type 4, ferrous ion and hydrogen peroxide are electro-generated using a sacrificial anode and an oxygen sparging cathode respectively (Brillas et al., 2002).

Different authors have shown that in aqueous mediums, several organic pollutants lead to weak decontamination because of the formation of carboxylic acids in both the Fenton and electro-Fenton processes (Pignatello et al., 2006; Chou et al., 1999; Sirés et al.,

2007b; Brillas et al., 2000; Brillas et al., 2003; Brillas et al., 2007). More potent electro-Fenton methods with UV irradiation are also being developed for wastewater remediation, so-called photoelectro-Fenton process (Sirés et al., 2007a; Brillas et al., 2003; Brillas et al., 2000; Brillas et al., 2007; Brillas et al., 1998). The process was irradiated with UV light under electro-Fenton conditions. The action of this irradiation is complex and can be described as: (i) the production of a greater amount of hydroxyl radicals from the photoreduction of $Fe(OH)^{2+}$, the predominant Fe^{3+} species in acid medium (Pignatello et al., 2006), by equation (1.6) and (ii) the photolysis of complexes of Fe(Ⅲ) with generated carboxylic acids, as shown in equation (1.7) (Pignatello et al., 2006; Exposito et al., 2007).

$$Fe(OH)^{2+} \xrightarrow{h\nu} Fe^{2+} + HO^{\bullet} \quad (1.6)$$

$$R(CO_2) - Fe(\text{Ⅲ}) + h\nu \rightarrow R(CO_2^{\bullet}) + Fe(\text{Ⅱ}) \rightarrow R^{\bullet} + CO_2 \quad (1.7)$$

The maximum adsorption wavelength of $Fe(OH)^{2+}$ species is less than 360 nm, hence visible irradiation may not drive the reaction of equation (1.6). An interesting and potentially useful modification of the photoreduction reaction takes advantage of the photo-lability of Fe(Ⅲ)-oxalate complexes, which can be efficiently decomposed up to 500 nm (Pignatello et al., 2006). Oxalic acid is produced during the oxidation of most organics. Under these conditions, it is also feasible to used sunlight as an alternative inexpensive source, so-called sunlight-assisted electro-Fenton technology (Casado et al., 2005).

1.2. Research Objective

BSA and 2,6-DMA are usually used as an intermediate of azo dyestuffs, pharmaceuticals, agrochemicals, coloring agents and tanning agents. Large amounts of aromatic compounds have been produced and released into the environment as waste during their manufacture and use. Some BSA has been detected at high concentration levels in hazardous waste sites, landfill leachates textile and tannery wastewaters (Kim et al., 1990; Suter et al., 1999; Altenbach and Giger, 1995; Alonso et al., 1999). Although 2,6-DMA and BSA have been produced and applied for a long time, little information is available on their toxicology and environmental behavior.

In addition most electro-Fenton studies primarily focus on the electro-regeneration of Fe^{2+} is largely neglected. Generation of iron sludge limits the applicability of Fenton oxidation processes. Therefore a novel electrochemical cell was developed to enhance the electro-regeneration rate of ferrous ions and the oxidation efficiency of two aromatic compounds. In this study, we employed a novel photoelectro-Fenton method, in which Fenton's reagent was utilized to produce hydroxyl radical in the electrochemical cell and ferrous ion was regenerated via the reduction of ferric ion on the light source and cathode. This research investigates the removal of the BSA and 2,6-DMA by different oxidation technology. The ferrous ions were generated at the new electrochemical reactor. The constant current mode was adopted to evaluate the current efficiency (ferric reduction efficiency) and energy consumption. We are concerned with the reactor efficiency, the performance of the kinetics, mechanism and the influences of several operating parameters. At the same time, a very interesting field is what to do with BSA and 2,6-DMA that they are either toxic and nonbiodegradable. Advanced oxidation technologies for wastewater treatment show high efficiency but work at high consume of energy and reagents. Partial chemical oxidation of a toxic wastewater may increase its biodegradability up to high

levels. Consequently, detection of intermediates and biodegradable efficiencies of Fenton, electro-Fenton and photoelectro-Fenton processes were also investigated in the study.

CHAPTER 2 LITERATURE REVIEW

Fenton and related reactions encompass reactions of peroxides (usually H_2O_2) with iron ions to form active oxygen species that oxidize organic or inorganic compounds when they are present. Recently, Fenton and related reactions have become of great interest for their relevance to biological chemistry, synthesis, chemistry of natural waters, and treatment of hazardous wastes. A search of the keyword “Fenton reaction” yielded over 2500 scientific articles since 1945 (Pignatello et al., 2006).

2.1. The use of hydrogen peroxide

Hydrogen peroxide is a strong oxidant (standard potential 1.80 and 0.87 V at pH 0 and 14, respectively) (Degussa Corporation) and its application in the treatment of various inorganic and organic pollutants is well established. Numerous applications of hydrogen peroxide in the removal of pollutants from wastewater, such as sulphites, hypochlorites, nitrites, cyanides, and chlorine, are known (Venkatadri and Peeters, 1993).

Hydrogen peroxide is also useful in the treatment of the gaseous sulphur oxides and nitrogen oxides being converted to the corresponding acids. Other related uses include the bleaching of pulp and paper and organic synthesis. Hydrogen peroxide has applications in the surface treatment industry involving cleaning, decorating, protecting and etching of metals.

By dissociation into oxygen and water, hydrogen peroxide can also supply oxygen to micro organisms in biological treatment facilities and in the bioremediation of contaminated sites. It can be used as a disinfecting agent in the control of undesirable biofilm growth. Since the oxygen concentration is generally rate limiting during the in situ biodegradation of organic contaminants, several applications using injection of hydrogen

peroxide into the subsurface have been successfully attempted to enhance the biodegradation activity (Calabrese and Kostecki, 1989). Hydrogen peroxide can be decomposed into water and oxygen by enzymatic and nonenzymatic routes.

Oxidation by hydrogen peroxide alone is not effective for high concentrations of certain refractory contaminants, such as highly chlorinated aromatic compounds and inorganic compounds (e.g. cyanides), because of low rates of reaction at reasonable hydrogen peroxide concentrations. Transition metal salts (e.g. iron salts), ozone and UV-light can activate hydrogen peroxide to form hydroxyl radicals which are strong oxidants:

Ozone and hydrogen peroxide

$$O_3 + H_2O_2 \rightarrow HO^{\bullet} + O_2 + HO_2^{\bullet} \qquad (2.1)$$

Iron salts and hydrogen peroxide

$$Fe^{2+} + H_2O_2 \rightarrow Fe^{3+} + OH^- + HO^{\bullet} \qquad (1.1)$$

UV-light and hydrogen peroxide

$$H_2O_2 + UV \rightarrow 2HO^{\bullet} \qquad (2.2)$$

The oxidation processes utilizing activation of hydrogen peroxide by iron salts, referred to as Fenton's reagent, are discussed below.

In general, oxidation processes which are based on the generation of radical intermediates are termed advanced oxidation techniques (Venkatadri and Peeters, 1993). Hydroxyl radicals (oxidation potential: 2.8 V) are stronger oxidants than ozone and hydrogen peroxide. Hydroxyl radicals non-specifically oxidize target compounds at high reaction rates (of the order of $10^9\ M^{-1}s^{-1}$ as described later).

2.2. Fenton's reagent

2.2.1. Fundamental chemistry of the Fenton reaction

Fenton's reagent was discovered about 100 years ago, but its application as an oxidizing process for destroying toxic organics was not applied until the late 1960s (Huang et al., 1993). Fenton reaction wastewater treatment processes are known to be very effective in the removal of many hazardous organic pollutants from water. The main advantage is the complete destruction of contaminants to harmless compounds, e.g. CO_2, water and inorganic salts. The Fenton reaction causes the dissociation of the oxidant and the formation of highly reactive hydroxyl radicals that attack and destroy the organic pollutants.

2.2.2. Kinetic scheme

Fenton's reagent is a mixture of hydrogen peroxide and ferrous ion, which generates hydroxyl radicals according to equation (1.1) (Kitis et al., 1999; Yoon et al., 2001; Lu et al., 2001). The ferrous ion initiates and catalyzes the decomposition of hydrogen peroxide, resulting in the generation of hydroxyl radicals. The generation of the radicals involves a complex reaction sequence in an aqueous solution (Rigg et al., 1954; Buxton and Greenstock, 1988)

$Fe^{2+} + H_2O_2 \rightarrow Fe^{3+} + OH^- + HO^\bullet$ (chain initiation) $k_1 \approx 58\sim70\ M^{-1}s^{-1}$ (1.1)

$HO^\bullet + Fe^{2+} \rightarrow OH^- + Fe^{3+}$ (chain termination) $k_2 = 3.2\times10^8\ M^{-1}s^{-1}$ (2.3)

Moreover, the newly formed ferric ions may catalyze hydrogen peroxide, causing it to be decomposed into water and oxygen. Ferrous ions and radicals are also formed in the reactions. The reactions are as shown in below (Walling and Goosen, 1973; Bielski et al., 1985; Buxton and Greenstock, 1988).

$Fe^{3+} + H_2O_2 \rightarrow Fe\text{-}OOH^{2+} + H^+$ $k_3 = 0.001\sim 0.01 M^{-1}s^{-1}$ (2.4)

$Fe\text{-}OOH^{2+} \rightarrow HO_2^\bullet + Fe^{2+}$ (2.5)

$$Fe^{2+} + HO_2^{\bullet} \rightarrow Fe^{3+} + HO_2^- \qquad k_4 = 1.3\times10^6\ M^{-1}s^{-1} \quad (2.6)$$

$$Fe^{3+} + HO_2^{\bullet} \rightarrow Fe^{2+} + O_2 + H^+ \qquad k_5 = 1.2\times10^6\ M^{-1}s^{-1} \quad (2.7)$$

$$HO^{\bullet} + H_2O_2 \rightarrow H_2O + HO_2^{\bullet} \qquad k_6 = 3.3\times10^7\ M^{-1}s^{-1} \quad (2.8)$$

As seen in equation (2.8), hydrogen peroxide can act as a hydroxyl radical's scavenger as well as an initiator (equation (1.1)). Hydroxyl radicals can oxidize organics (*RH*) by abstraction of protons producing organic radicals ($R^{\bullet}$), which are highly reactive and can be further oxidized (Walling and Kato, 1971; Venkatadri and Peters, 1993; Lin and Lo, 1997).

$$RH + HO^{\bullet} \rightarrow H_2O + R^{\bullet} \rightarrow \textit{further oxidation} \quad (2.9)$$

Since $k_6 = 10^7\ M^{-1}s^{-1}$ while $k_2 > 10^8$ (equation (2.3)) can be made unimportant by maintaining a high $[RH]/[H_2O_2]$ ratio.

Walling (1975) simplified the overall Fenton chemistry by accounting for the dissociation water:

$$2Fe^{2+} + H_2O_2 + 2H^+ \rightarrow 2Fe^{3+} + 2H_2O \quad (2.10)$$

This equation suggests that the presence of H^+ is required in the decomposition of H_2O_2, indicating the need for an acid environment to produce the maximum amount of hydroxyl radicals. Previous Fenton studies have shown that acidic pH levels near 3 are usually optimum for Fenton oxidations (Hickey et al., 1995). In the presence of organic substrates (RH), excess ferrous ion, and at low pH, hydroxyl radicals can add to the aromatic or heterocyclic rings (as well as to the unsaturated bonds of alkenes or alkynes)

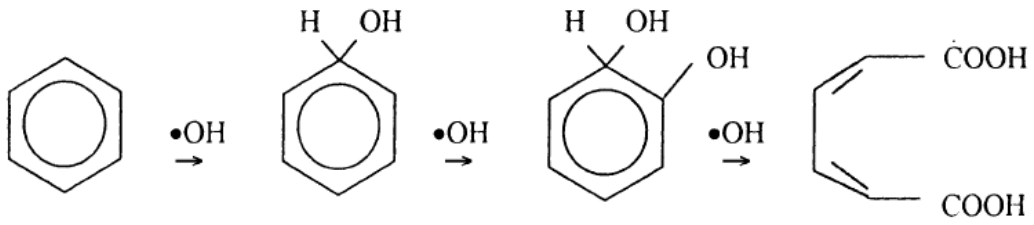

They can also abstract a hydrogen atom, initiating a radical chain oxidation (Walling, 1975;

Lipczynska-Kochany et al., 1995)

$$RH + HO^{\bullet} \rightarrow H_2O + R^{\bullet} \quad (chain\ propagation) \tag{2.9}$$

$$R^{\bullet} + H_2O_2 \rightarrow ROH + HO^{\bullet} \tag{2.11}$$

$$R^{\bullet} + O_2 \rightarrow ROO^{\bullet} \tag{2.12}$$

The organic free radicals produced in equation (2.9) may then be oxidized by Fe^{3+}, reduced by Fe^{2+}, or dimerized according to the following reactions (Tang and Tassos, 1997)

$$R^{\bullet} + Fe^{3+} - oxidation \rightarrow R^{+} + Fe^{2+} \tag{2.13}$$

$$R^{\bullet} + Fe^{2+} - reduction \rightarrow R^{-} + Fe^{3+} \tag{2.14}$$

$$2R^{\bullet} - dimerization \rightarrow R\text{-}R \tag{2.15}$$

2.2.3. Stoichiometric relationship

The key features of the Fenton system are believed to be its reagent conditions, i.e. $[Fe^{2+}]$, $[Fe^{3+}]$, $[H_2O_2]$ and the reaction characteristics (pH, temperature and the quantity of organic and inorganic constituents). Because these parameters determine the overall reaction efficiency, it is important to understand the mutual relationships between these parameters in terms of hydroxyl radical production and consumption. Yoon et al. (2001) studied these relationships and classified them in three categories according to the quantity of the $[Fe^{2+}]_0/[H_2O_2]_0$ ratio (initial concentration of Fe^{2+} versus initial concentration of H_2O_2). Their results are now summarized.

2.2.3.1. High ratio of $[Fe^{2+}]_0/[H_2O_2]_0$ (≥2)

The Fenton reaction begins by producing hydroxyl radicals from the reaction between ferrous ion and hydrogen peroxide (equation (1.1)). When the Fenton reaction in the absence of organics is initiated under $[Fe^{2+}]_0/[H_2O_2]_0$ (≥2), the consumption ratio of ferrous ion to hydrogen peroxide ($\triangle[Fe^{2+}]/\triangle[H_2O_2]$) becomes about 2, and radical chain reactions are quickly terminated.

This is because the hydroxyl radicals produced as a result of equation (1.1) mainly react with the ferrous ion (equation (2.3)) instead of hydrogen peroxide (equation (2.8)). This explanation is supported by the fact that the reaction between hydroxyl radical and the ferrous ion is ten times faster than that between hydroxyl radicals and hydrogen peroxide ($k_2 = 3.2\times10^8$ $M^{-1}s^{-1}$ and $k_7 = 3.3\times10^7$ $M^{-1}s^{-1}$).

$$HO^{\bullet} + Fe^{2+} \rightarrow OH^{-} + Fe^{3+} \quad \textit{(chain termination)} \qquad k_2 = 3.2\times10^8 \ M^{-1}s^{-1} \quad (2.3)$$

$$HO^{\bullet} + H_2O_2 \rightarrow H_2O + HO_2^{\bullet} \qquad k_6 = 3.3\times10^7 \ M^{-1}s^{-1} \quad (2.8)$$

$$RH + HO^{\bullet} \rightarrow H_2O + R^{\bullet} \rightarrow \textit{further oxidation} \quad (2.9)$$

On the other hand, the presence of RH affects only the behavior of the ferrous ion, not the hydrogen peroxide. This is because the organics compete with ferrous ion for hydroxyl radicals (equations (2.3) and (2.9)). The presence of organics reduces the △[Fe2+]/△[H2O2] ratio to less than two (△[Fe2+]/△[H2O2] ≈ 1.3), which means that the ferrous ion is utilized as a major reactant, not as a catalyst in the Fenton reaction.

Yoon et al. (2001) studied the effect of the Fenton reaction in the removal of landfill leachate organics. They used a $[Fe^{2+}]_0/[H_2O_2]_0$ ratio of 1.25. In that case, the Fenton reaction can be divided into two processes. The first process is an initial oxidation at a low pH of about 3. The second process, which follows the oxidation process, is coagulation at a high pH of 7~8. It is interpreted that the coagulation step in the Fenton reaction had a primary role in the selective removal of organics, even though the Fenton reaction is not a coagulation one.

However, since the efficiency of organic removal in the Fenton reaction was higher than coagulation, the Fenton reaction in landfill leachate treatment process may be called a type of “enhanced coagulation”.

2.2.3.2. Medium ratio of $[Fe^{2+}]_0/[H_2O_2]_0$ (=1)

Regardless of the presence of organics, hydrogen peroxide rapidly converts all ferrous to ferric ions via equation (1.1). In the absence of *RH*, hydrogen peroxide decomposes slowly through ferric ion induced radical chain reactions (equation (2.4)) just after the rapid consumption of hydrogen peroxide. The reduction of the ferric ion (equation (2.4) and (2.5)) is significantly lower than equation (1.1) and is the rate-determining step. To have a continued decrease of hydrogen peroxide, ferrous ion must be formed by the reduction of ferric ion. Then, the Fenton reaction can be characterized by two specific systems, i.e. the ferrous system and the ferric system, which depend on the oxidation stage of the iron initially added or the major oxidation state of the iron present. The ferrous system refers to the case where the primary reaction, which produces hydroxyl radicals, is the reaction between the ferrous ion and hydrogen peroxide (equation (1.1)). The ferric system refers to the case in which the ferric ion induced equation (2.4) and (2.5) must be preceded in order to produce hydroxyl radicals via equation (1.1).

$$Fe^{2+} + H_2O_2 \rightarrow Fe^{3+} + OH^- + HO^{\bullet} \quad (1.1)$$

$$Fe^{3+} + H_2O_2 \rightleftharpoons Fe\text{-}OOH^{2+} + H^+ \qquad k_3 = 0.001 \sim 0.01\ M^{-1}s^{-1} \quad (2.4)$$

$$Fe\text{-}OOH^{2+} \rightarrow HO_2^{\bullet} + Fe^{2+} \quad (2.5)$$

$$HO^{\bullet} + H_2O_2 \rightarrow H_2O + HO_2^{\bullet} \qquad k_6 = 3.3\times10^7\ M^{-1}s^{-1} \quad (2.8)$$

$$RH + HO^{\bullet} \rightarrow H_2O + R^{\bullet} \rightarrow \textit{further oxidation} \quad (2.9)$$

However, the presence of *RH* has an impact on the behavior of the hydrogen peroxide in two ways: (i) no further hydrogen peroxide decomposition occurs just after the initial decrease of hydrogen peroxide, since the reaction of *RH* with hydroxyl radicals (equation (2.9)) overwhelms the reaction of hydrogen peroxide with hydroxyl radicals (equation (2.8)); (ii) the presence of excess *RH* can hinder the reaction between hydroxyl radicals

and the ferrous ion, which may have been the major route of hydroxyl radicals consumption in the absence of *RH*. Therefore, the remaining ferrous ion can react with the hydrogen peroxide and show a slightly higher consumption of hydrogen peroxide at the initial stage of the reaction as compared with that observed in the absence of *RH*.

2.2.3.3. Low ratio of $[Fe^{2+}]_0/[H_2O_2]_0$ (<<1)

In the absence of *RH*, a slow decomposition of hydrogen peroxide occurs caused by ferric ion, which induces radical chain reactions (ferric system) immediately after the initial rapid depletion of hydrogen peroxide. However, the presence of *RH* almost stops the decomposition of hydrogen peroxide by ferric ion (ferric system). At a low ratio of $\triangle[Fe^{2+}]_0/\triangle[H_2O_2]_0$ (<<1), hydroxyl radicals react to a greater extent with hydrogen peroxide, producing $HO^{\bullet}_2$ via equation (2.8). Therefore, additional $HO^{\bullet}_2$ can participate in propagating radical chain reactions by reducing ferric to ferrous ion (equation (2.7)), and can result in larger consumption of hydrogen peroxide than that occurs in the absence of *RH*.

$$Fe^{3+} + HO_2^{\bullet} \rightarrow Fe^{2+} + O_2 + H^+ \qquad k_5 = 1.2\times10^6\ M^{-1}s^{-1} \quad (2.7)$$

2.2.3.4. Influence of the structure of hazardous components

Kinetic degradation of aromatic pollutants with the system Fe^{2+}/H_2O_2 was reported earlier (Yoon et al., 1998; Wei et al., 1990; Lipczynska-Kochany, 1991) but less attention was given to the mineralization of these substances. The degradation of alicyclic compounds was given little attention since most of the water pollutants with a low biodegradability have an aromatic structure.

Ruppert and Bauer (1993) studied the influence of the structure of several organic pollutants on the way they are mineralized by OH-radicals. All of the aromatic substances

studied were strongly degraded after several hours, while the organic carbon of cyclohexanol and cyclohexanone was hardly attacked. In alicyclic compounds the attack of the electrophilic OH-radicals cannot occur at conjugated C=C double bonds in contrast to aromatic compounds where ring opening and further degradation take place.

2.3. Electrochemical oxidation processes

The intensification of industrial activities, since the latter half of the 19 century and throughout the 20 century, has inevitably caused severe environmental pollution with dramatic consequences in atmosphere, water and soils. The consequent restrictions imposed by new legislation require effective initiatives for pollution reduction, not only in gaseous emissions and industrial aqueous effluents but also adequate decontamination in soils. Typically, in the case of the latter, different classes of pollutants may have accumulated during long periods of uncontrolled waste disposal and reclamation may represent a serious technological problem. Due to the extremely diverse features of pollution phenomena, universal strategies of reclamation have not been found (Manahan, 1994). Generally, wastewater treatment is carried out using primary, secondary or tertiary methods, depending on the nature of pollutants. As far as organic pollutants in wastewaters are concerned, biological abatement may sometimes be impossible, due to the bio-refractory character of the substrates. For this reason, physical-chemical methods are preferably applied, but an oxidation with ozone or chlorine dioxide is not always effective and also transportation and storage of reactants may be a significant inconvenience for safe processing (Rajeshwar et al., 1994). An alternative can be the application of electrochemical technologies for wastewater treatment, benefiting from advantages such as versatility, environmental compatibility and potential cost effectiveness among others described below (Rajeshwar et al., 1994). Both direct and mediated electrochemical

oxidation can be considered, and have proved to be interesting subjects for different research groups and industries seeking new technologies for wastewater treatment (Chen, 2004; Carlos et al., 2006).

In recent years, the applications of electrochemistry for environmental pollution have been thoroughly investigated (Chen, 2004; Juttner et al., 2000). The feasibility of electrochemical destruction of organic substrates in wastewater, in particular, has attracted much attention since pioneering studies by Comninellis in the 60s, Dabrowski in the 70s, Kirk, Stucki, Kotz, Chettiar and Watkinson in the 80s to the present day. In these studies, the influence of the electrode material has been considered in detail, showing that optimal conditions for the process are obtained at high-oxygen-overpotential anodes (Carlos et al., 2006).

Electrochemistry, as a branch of physical chemistry plays an important role in most areas of science and technology (Grimm et al., 1998). Electrochemistry offers promising approaches for the prevention of pollution problems in the process industry. The inherent advantage is its environmental compatibility, due to the fact that it uses a clean reagent, the electron. The strategies include both the treatment of effluents and waste and the development of new processes or products with less harmful effects, often denoted as process-integrated environmental protection. The promising characteristics of approaches for the prevention and remediation of pollution problems have been explained in detail: (Rajeshwar et al., 1994, 1997).

(i) Versatility: Several techniques can be applied such as direct and/or indirect oxidations and reductions, phase separations, biocide functions, concentrations (or dilutions), and electrochemical methods can deal with many pollutants and treat from microliters to millions of liters.

(ii) Energy efficiency: These processes generally require lower temperature with respect to

equivalent nonelectrochemical counterparts (e.g., thermal incineration), the potential can be easily controlled and operational parameters can be designed to minimize power losses.

(iii) Amenability to automation: The electrical variables used in the electrochemical processes are particularly suited for facilitating data acquisition, process automation and control.

(iv) Environmental compatibility: The electron is a clean and very effective reagent, whose reactivity may be tuned by choosing a suitable electrocatalyst, in order to prevent the production of undesirable metabolites.

(v) Cost effectiveness: The required equipment and operations are generally simple and inexpensive, but diverse considerations must be studied for optimal efficiency.

For the above reasons, electrochemistry can be considered as an alternative for the prevention of pollution problems. Therefore, intensive research proceeds with the goal of discovering more efficient techniques, processes, materials, technologies and applications of electrochemistry for remediation and/or prevention of pollution problems (Carlos et al., 2006).

During the last two decades, research work has focused on the efficiency in oxidizing various pollutants at different electrodes, on the improvement of the electrocatalytic activity and electrochemical stability of the electrode materials, on the investigation of factors affecting the process performance and on the exploration of mechanisms and kinetics of pollutant degradation (Chen, 2004).

2.3.1. Anodic oxidation mechanism

Electrochemical oxidation of pollutants can occur directly at anodes through the generation of physically adsorbed "active oxygen" (adsorbed hydroxyl radicals, HO·) or chemisorbed "active oxygen" (oxygen in the oxide lattice, MO_{x+1}) (Comninellis, 1994). This process is usually called "anodic oxidation" or "direct oxidation" and the course for the anodic oxidation was described by Comninellis (1994), the complete destruction of the organic substrate or its selective conversion into oxidation products is schematically represented in Figure 2.1.

When a toxic, non-biocompatible pollutant is treated, the electrochemical conversion transforms the organic substrate into a variety of metabolites; often, biocompatible organics are generated, and biological treatment is still required after the electrochemical oxidation. In contrast, electrochemical degradation yields water and CO_2, no further purification being necessary. Nevertheless, the feasibility of this process depends on three parameters: (i) the generation of chemically or physically adsorbed hydroxyl radicals, (ii) the nature of the anodic material and (iii) the process competition with the oxygen evolution reaction (Carlos et al., 2006).

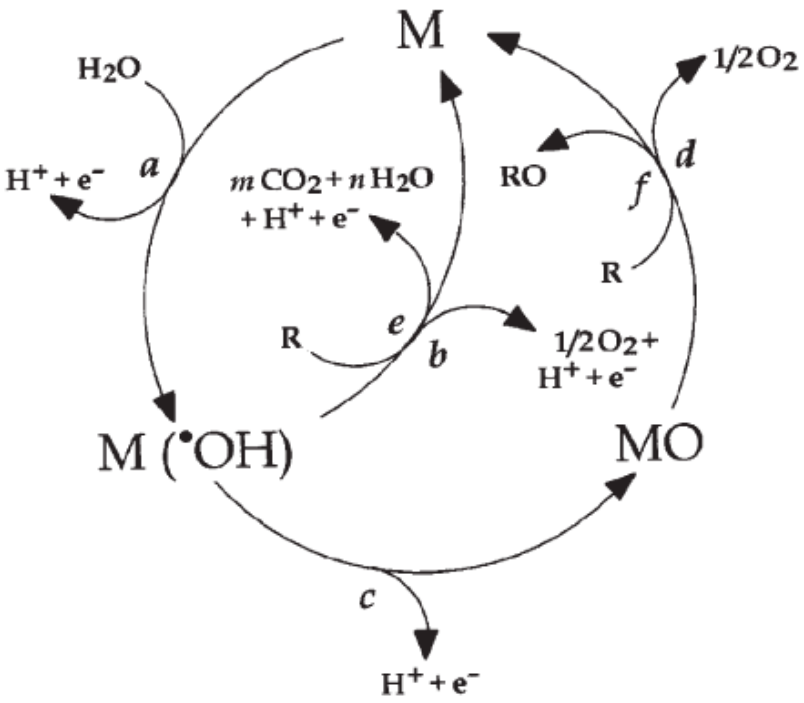

Figure 2.1 Mechanistic scheme of anodic oxidation of organic compounds with simultaneous oxygen evolution on non-active anodes (reactions a, b and e) and on active anodes (reactions a, c, d and f).

(a) Formation of hydroxyl radicals, HO·.

(b) Oxygen evolution by electrochemical oxidation of hydroxyl radicals.

(c) Formation of the higher metal oxide, MO.

(d) Oxygen evolution by chemical decomposition of the higher metal oxide.

(e) Electrochemical combustion of the organic compound via hydroxyl radicals.

(f) Electrochemical conversion of the organic compound, R, via the higher metal oxide.

The electrochemical oxidation of some organics in aqueous media may take place without any loss in electrode activity, except at high potentials, and with concomitant evolution of oxygen (Comninellis et al., 1995, 1996, 1998; Thar et al., 1998). Furthermore, it has been described that the nature of the electrode material strongly influences both the selectivity and the efficiency of the process. To interpret these observations, a comprehensive model for the anodic oxidation of organics in acidic medium, including the competition with the oxygen evolution reaction, has been proposed (Comninellis et al., 1994, 1996; Foti, 1997; Simond, 1997). More recent results, obtained at conductive diamond electrodes (which are characterized by very high oxygen overpotential), fit the model predictions quite well (Marselli et al., 2003). Based on these results, Comninellis explained the differences considering two limiting cases, i.e. the so-called "active" and "non-active" anodes.

In both cases, the first equation (2.16) is the oxidation of water molecules leading to the formation of adsorbed hydroxyl radicals:

$$M + H_2O \rightarrow M(HO^{\bullet}) + H^+ + e^- \qquad (2.16)$$

Both the electrochemical and chemical reactivities of adsorbed hydroxyl radicals depend strongly on the nature of the used electrode material. With active electrodes there is a strong interaction between the electrode (*M*) and the hydroxyl radical. Adsorbed hydroxyl radicals may interact with the anode, forming a higher oxide *MO* (equation (2.17)).

$$M(HO^{\bullet}) \rightarrow MO + H^+ + e^- \qquad (2.17)$$

These may be the case when higher oxidation states are available, for the electrode material, above the thermo-dynamic potential for the oxygen evolution (1.23 V vs. SHE) (Comninellis et al., 1994).

With active electrodes, the redox couple *MO/M* acts as a mediator in the oxidation of organics (equation (2.18)). This reaction is in competition with the side reaction of oxygen

evolution, which is due to the chemical decomposition of the higher oxide (equation (2.19)).

$$MO + R \rightarrow M + RO \tag{2.18}$$

$$MO \rightarrow M + 1/2O_2 \tag{2.19}$$

The oxidative reaction via the surface redox couple *MO/M* (equation (2.18)) may be much more selective than the reaction involving hydroxyl radicals (equation (2.20)). A typical example of an active electrode is the case of IrO_2 (Comninellis et al., 1994). With a non-active electrode, weak interactions exist between the hydroxyl radical and the electrode surface. In this case, the oxidation of organics is mediated by hydroxyl radicals and may result in fully oxidized reaction products such as CO_2 (Carlos et a;., 2006).

$$M(HO^{\bullet}) + R \rightarrow M + mCO_2 + nH_2O + H^+ + e^- \tag{2.20}$$

In the above schematic equation, *R* is a fraction of an organic compound containing no heteroatoms, which needs one oxygen atom to be fully transformed into CO_2. This reaction competes with the side reaction of hydroxyl radicals (direct or indirect consumption, through the formation of hydrogen peroxide as intermediate) to oxygen (equation (2.21)) without any participation of the anode surface (Carlos et al., 2006):

$$M(HO^{\bullet}) \rightarrow M + 1/2O_2 + H^+ + e^- \tag{2.21}$$

A non-active electrode does not participate in the anodic reaction and does not provide any catalytic active site for the adsorption of reactants and/or products from the aqueous medium. In this case, the anode serves only as an inert substrate, which can act as a sink for the removal of electrons. In principle, only outer-sphere reactions and water oxidation are possible with this kind of anode. Intermediates produced by the water oxidation are subsequently involved in the oxidation of organics in aqueous medium (Marselli et al., 2003).

The electrochemical activity (which may be related to the overpotential for oxygen

evolution) and chemical reactivity (rate of the organics oxidation with electrogenerated hydroxyl radicals) of adsorbed HO· are strongly linked to the strength of the *M-HO·* interaction. As a general rule, the weaker the interaction, the higher the anode reactivity for organics oxidation (fast chemical reaction); boron-doped diamond electrodes (BDD) are typical non-active electrodes, characterized by high stability and acceptable conductivity. This model assumes that the electrochemical oxidation is mediated by hydroxyl radicals, either adsorbed at the surface (in the case of active electrodes) or free, in the case of the non-active ones (Marselli et al., 2003).

2.3.2. Electro-Fenton method

Electro-Fenton methods broadly include electrochemical reactions that are used to generate in situ one or both of the reagents for the Fenton reaction. The reagent(s) generated depend on cell potential, solution conditions and the nature of the electrodes. Several different types of electro-Fenton reactions have been described, as summarized in Table 2.1.

Table 2.1 Types of electrochemical Fenton reaction

Type	Anode reaction	Cathode reaction	Reagent externally
1	$Fe^0 \rightarrow Fe^{2+} + 2e^-$	$2H_2O + 2e^- \rightarrow H^2 + 2OH^-$	H_2O_2
2	$2H_2O \rightarrow 4H^+ + O_2 + 2e^-$	$O_2 + 2H^+ + 2e^- \rightarrow H_2O_2$	Fe^{2+}
3	$2H_2O \rightarrow 4H^+ + O_2 + 2e^-$	$Fe^{3+} + e^- \rightarrow Fe^{2+}$	Fe^{2+}; H_2O_2
4	$Fe^0 \rightarrow Fe^{2+} + 2e^-$	$O_2 + 2H^+ + 2e^- \rightarrow H_2O_2$ $Fe^{3+} + e^- \rightarrow Fe^{2+}$	-

Ferrous ions may be produced by oxidative dissolution of sacrificial anodes such as iron metal (Pratap and Lemley, 1994; Roe and Lemley, 1997; Wang and Lemley, 2001; Saltmiras and Lemley, 2001; Chou et al., 1999; Arienzo et al., 2001a, 2001b) or titanium and iron (Huang et al., 1999):

$$Fe^0 \rightarrow Fe^{2+} + 2e^- \qquad (1.3)$$

The electrodes must have sufficiently high specific surface area to achieve optimum dissolved iron concentrations (Savall, 1995). Ferrous ion may also be produced by reduction of ferric ions at an inert cathode, such as platinum (Hsaio and Nobe, 1993; Oturan et al., 1999; Brillas, et al., 1998b; Qiang et al., 2003):

$$Fe^{3+} + e^{-} \rightarrow Fe^{2+} \tag{1.4}$$

Hydrogen peroxide may be produced by reduction of oxygen at the cathode (Chou et al., 1999; Brillas et al., 1998b, 2000; Oturan et al., 1999; Sudoh et al., 1986; Casado et al., 2005):

$$O_2 + 2H^{+} + 2e^{-} \rightarrow H_2O_2 \tag{1.5}$$

In situ generation of reagents might be an advantage in some applications over pumping the same reagents from an external reservoir using conventional technology. However, the electro-Fenton reaction faces several obstacles that must be overcome first. The production of hydrogen peroxide in equation (1.5) is slow because oxygen has low solubility in water (Savall, 1995) and because current efficiency under acidic conditions is low (Chou et al., 1999). Porous gas dispersion electrodes appear to be a promising solution to the former problem (Shen et al., 2005). Stoichiometric electro-generated Fe^{2+} can be carried out near neutral pH (Pratap and Lemley, 1998), thus overcoming the need for acidic conditions, a fundamental disadvantage of Fenton reactions in general. However, formation of ferric oxyhydroxide sludge is still a problem here. The sludge can be electrochemically reduced to Fe^{2+}, but this requires a step in which the pH is lowered below 1 (Qiang et al., 2003; Chou et al., 1999). Gradual corrosion of electrodes can be expected in many electro-Fenton applications. Hydrogen peroxide produced at the cathode is destroyed at the anode unless the cells are separated by an electrolyte bridge. Shen et al. (2005) studied acid red B dye degradation in such a dual-chamber cell. They achieved both anodic oxidation of the dye in the anode chamber and hydrogen peroxide oxidation

(accelerated by addition of Fe^{2+}) in the cathode chamber.

In principle the most promising electro-Fenton mode is Type 3 (Table 2.1), in which ferric ion is reduced to ferrous at the cathode. However, Fe^{2+} regeneration is slow even at optimal current density, and both current density and current efficiency drop off precipitously above pH~2.5. As an active area of research, further advances are expected in electro-Fenton reactions.

2.4. The photo assisted Fenton reaction

Irradiation of reaction solutions with ultraviolet (UV) or UV/visible light almost invariably leads to faster rates and higher yields of inorganic products (e.g., Pignatello, 1992; Ruppert et al., 1993; Kiwi et al., 1994; Lei et al., 1998; DeLaat et al., 1999; Balanosky et al., 2000; Benitez et al., 2000). Photoenhancement will be observed even in the presence of ordinary overhead fluorescent light used to illuminate laboratory space. Enhancement is due nearly entirely to the photochemistry of Fe(III). Fe(II) complexes undergo ligand-to-metal charge transfer (LMCT) excitation, dissociating to give Fe(II) and an oxidized ligand, L_{ox} (Balzani and Carassiti, 1970; Sima and Makanova, 1997):

$$Fe^{III}(L)_n + h\upsilon \rightarrow Fe^{II}(L)_{n-1} + L_{ox}^{\bullet} \qquad (2.22)$$

The photochemistry of Fe(III) is advantageous to Fenton AOPs because the reduced iron can then react with hydrogen peroxide to produce hydroxyl radicals (equation (1.1)) and because oxidation of the ligand may lead to further degradation of the target pollutant (e.g., Pignatello, 1992; Sun and Pignatello, 1993; Safarzadeh-Amiri et al., 1996; Bandara et al., 1997; Bossmann et al., 1998). The photolysis of Fe(II) species is unimportant at wavelengths employed in Fenton AOPs. Hydrogen peroxide also photolyzes with UV light:

$$H_2O_2 + h\upsilon \rightarrow 2HO^{\bullet} \quad (2.2)$$

2.4.1. Photolysis of aquated Fe(III) species

Fe(III) hydroxy complexes present in mildly acidic solution, such as $Fe(OH)^{2+}$ and $Fe_2(OH)_2^{4+}$, absorb light appreciably in the UV and into the visible region. These complexes undergo photoreduction to give hydroxyl radicals and ferrous ions. The most important species is $Fe(OH)^{2+}$ due to a combination of its relatively high absorption coefficient and concentration relative to other Fe(III) species under typical conditions:

$$Fe^{III}(L)_n + h\upsilon \rightarrow Fe^{II}(L)_{n-1} + L^{\bullet}_{ox} \quad (2.22)$$

$$Fe(OH)^{2+} \xrightarrow{h\upsilon} Fe^{2+} + HO^{\bullet} \quad (1.6)$$

In technical applications, quantum efficiency under polychromatic irradiation, symbolized by (Φ), is of interest. The quantum yield (Φ) for Fe^{2+} formation in equation (2.22) is wavelength dependent (Faust and Hoigne, 1990; Langford and Carey, 1975; Benkelberg and Wameck, 1995): It is 0.14-0.19 at 313 nm and 0.017 at 360 nm (Faust and Hoigne, 1990). The (Φ) for Fe^{2+} production from ferric sulfate at pH 3 using a medium-pressure mercury arc (Heraeus Noblelight, TQ 718) is 0.21 (Bossmann et al., 1998).

Excitation of Fe(III) aquo complexes alone (i.e., without peroxide) can be used to promote degradation of pollutants since $HO^{\cdot}$ is formed (Larson et al., 1991; Kawaguchi and Inagaki, 1994; Mazellier et al., 1997, 1999; Brand et al., 1998, 2000a, 2000b; Mailhot et al., 1999). However, photolysis of Fe(III) alone appears to offer little, if any, advantage over the photo-Fenton reaction. Fe(III) is required in stoichiometric amount unless a pathway for its regeneration from Fe^{2+} is available. While regeneration is possible from intermediates in the reaction**,** or air, it is not very efficient. Furthermore, care has to be taken to keep the pH in a range (2.5<pH<3~4) where the $Fe(OH)^{2+}$ species exists in appreciable concentration and the bulk of the iron remains soluble.

2.4.2. Photolysis of Fe(III) complexes with organic ligands

Fe(II) may complex with certain target compounds or their byproducts, especially those acting as polydentate ligands. These complexes typically have higher molar absorption coefficients in the near-UV and visible regions than do the aquo complexes. Their excitation leads to the production of Fe^{2+} and a ligand radical by the generalized equation (2.26) with quantum yields that are wavelength dependent. Polychromatic quantum efficiencies in the UV/visible for different complexes range from ~0.05 to ~0.95 (Ronco and Aymonino, 1987; Pohl et al., 1988; Andrianirinaharivelo et al., 1995; Bandara et al., 1996; Van der Zee et al., 1993).

The photoreactivity of Fe(III)-carboxylate or Fe(Ill)-polycarboxylate complexes is well-known and usually leads to decarboxylation of the organic ligand (Balzani and Carassiti, 1970):

$$R(CO_2)-Fe(\text{Ⅲ})+h\nu \rightarrow R(CO_2^{\bullet})+Fe(\text{Ⅱ}) \rightarrow R^{\bullet}+CO_2 \qquad (1.7)$$

An interesting and potentially useful modification of the photo-Fenton reaction takes advantage of the photo-lability of Fe(III)-oxalate complexes (Safarzadeh-Amiri et al., 1996, 1997; Hislop and Bolton, 1999), which is efficient up to 500 nm (Φ) = 1.0~1.2). Ferric oxalate is commonly used as a chemical actinometer (Hatchard and Parker, 1956; Braun et al., 1991). Bolton and coworkers added oxalate to reaction solutions and obtained photoreduction of the resulting ferrioxalate complexes in situ, such as

$$[Fe(C_2O_4)_3]^{3-} \rightarrow Fe^{2+}+2C_2O_4^{2-}+C_2O_4^{-\bullet} \qquad (2.23)$$

and obtained degradation of aromatic and chlorinated aromatic hydrocarbons, chlorinated ethenes, ethers, alcohols, and ketones (Safarzadeh-Amiri et al., 1996, 1997). Oxalate addition also enhanced photo-Fenton degradation of the herbicide diuron in goethite suspensions by accelerating photoreductive dissolution of iron (Mazellier and Sulzberger, 2001):

$$\equiv Fe(III)-(C_2O_4^{-})+h\upsilon \rightarrow Fe^{2+}{}_{(aq)}+C_2O_4^{-\bullet} \quad (2.24)$$

where ≡represents the surface-bound metal.

At low Fe(III) concentrations, the oxalyl radical anion rapidly decomposes to give carbon dioxide and the carboxylate radical anion. The latter reacts with dioxygen (when present) to yield the superoxide anion:

$$C_2O_4^{-\bullet} \rightarrow CO_2+CO_2^{-\bullet} \quad (2.25)$$

$$O_2+CO_2^{-\bullet} \rightarrow CO_2+O_2^{-\bullet} \quad (2.26)$$

At high Fe(III) concentrations, $C_2O_4^{-\bullet}$ reduces Fe(III) to Fe(II).

The carboxylate radical anion ($CO_2^{-\bullet}$) is a sufficiently strong reducing agent that it can, in the absence of peroxide and dioxygen, reduce perchloroalkanes such as tetrachloromethane and hexachloroethane, which are normally inert to hydroxyl radicals (Huston and Pignatello, 1996):

2.4.3. Contribution of different photochemical reactions to the enhancement of the Fenton reaction

Clearly, many photochemical reactions are possible in irradiated Fenton systems. The contribution of a given reaction to degradation depends on the emission spectrum of the source, the concentration and absorbance of the photoactive species, the quantum efficiency for the given reaction, and the presence and concentration of other light-absorbing species in the system that is the inner filter effect. The inner filter effect limits the reactor volume. The concentration and absorbance of photoactive and non-photoactive species change during the course of the reaction. Further research is needed to establish the contributions of individual reactions. However, a few conclusions may be reached from existing knowledge.

First, Fe(III) complexes often exhibit higher absorbances and higher quantum yields than simple aquated Fe(III) species, and therefore may be more important in photo-Fenton systems. For example, the mixture of 2,4-dimethylaniline and Fe(III) at pH 3 photolyzes with a quantum yield of 0.92 for Fe(II) production (Bossmann et al., 1998), compared to <0.2 for aquated complexes. The photolysis of Fe(III)-carboxylate or -polycarboxylate complexes likely play a dominant role when they are present. Photodecarboxylation, in fact, often accounts for a substantial fraction of carbon mineralization, especially when the target compound is aromatic (Casado et al., 2005; Sun and Pignatello, 1993b, 1993c). For example, 60% of CO_2 evolved from 2,4-D was attributed to Fe(III)-catalyzed photodecarboxylation principally of oxalic acid resulting from advanced degradation of the aromatic ring (Sun and Pignatello, 1993b, 1993c). Oxalic acid is a major product of aromatic ring degradation and its complexes with Fe(III) are very stable to hydroxyl radicals attack in the dark. These examples help explain why complete mineralization often cannot be achieved using the Fenton reaction in the dark.

$$H_2O_2 + h\upsilon \rightarrow 2HO^{\bullet} \qquad (2.2)$$

Second, although photolysis of hydrogen peroxide (equation (2.21)) has a relatively high quantum yield, its contribution in photo-Fenton applications is limited by the weak absorption of light by hydrogen peroxide and the strong “inner filter effect” due to absorption of light by iron and organic solutes (especially aromatics). However, hydrogen peroxide photolysis may contribute to hydroxyl radical production at low concentration of iron and organic absorbers or at very large concentrations of hydrogen peroxide.

Third, while in theory rate should increase with radiant power, in practice there may be an upper limit reached when photoreduction of iron outpaces its reoxidation, that is, when iron in the +III state becomes a small fraction of total iron.

2.5. The photo assisted electro-Fenton reaction

2.5.1. Fundamental chemistry of the Fenton reaction

In general, the Fenton processes operate through the interaction of the hydrogen peroxide with the iron present in solution, generating the hydroxyl radicals according to the following reaction (Brillas et al., 1998; Brillas et al., 2003a):

$$Fe^{2+} + H_2O_2 \rightarrow Fe^{3+} + OH^- + HO^{\bullet} \quad (1.1)$$

Furthermore, it has been shown that the application of UV light to this system, i.e. in the photo-Fenton processes, produces additional hydroxyl radicals through the reduction of ferric ions, which could be coupled to other parallel reactions such as the photolytic breakdown of the $Fe(OH)^{2+}$ complex:

$$Fe(OH)^{2+} \xrightarrow{h\nu} Fe^{2+} + HO^{\bullet} \quad (1.6)$$

The catalytic effect of Fe^{2+} in the electro-Fenton process can be enhanced by solution irradiation with UV light. Thus, the combination of the electrochemical generation of hydrogen peroxide with the photochemical production of hydroxyl radicals, called the Photoelectro-Fenton process, generates a greater quantity of free radicals because of the contribution of both mechanisms (Boye et al., 2002). Direct photolysis of acid solutions containing peroxide on the other hand generates hydroxyl radicals through the hemolytic breakdown of the peroxide molecule according to equation (2.2):

$$H_2O_2 + UV \rightarrow 2HO^{\bullet} \quad (2.2)$$

This reaction increases oxidative capability of the process due to the rise of the hydroxyl radicals in the process. In addition to all of these mechanisms in the photoelectro-Fenton process, two hydroxyl radicals can be produced from hydrogen peroxide by photocatalytic effect of UV light (253 nm).

The degradation of the target organic substrate can be enhanced when the solution is irradiated by UV light in parallel to the application of the electro-Fenton process

(photoelectro- Fenton). Photochemical regeneration of Fe^{2+} by the photoreduction of Fe^{3+} ions and p-activation of complexes renders the photoelectro-Fenton system more efficient (Brillas et al., 2003a; Boye et al., 2003). At acidic pH, oxalic acids behave as photo-active complexes in the presence of ferric ions which undergo photo-decarboxylation reaction (Pignatello et al., 2006):

$$R(CO_2) - Fe(\text{Ⅲ}) + h\nu \rightarrow R(CO_2^{\bullet}) + Fe(\text{Ⅱ}) \rightarrow R^{\bullet} + CO_2 \quad (1.7)$$

Environmental application of the photoelectro-Fenton process is fairly a new topic and previous studies are quite limited. The most part of these studies have comprised to treatability of some specific pollutants such as some kinds of herbicides (Boye et al., 2002; Irmak et al., 2006; Boye et al., 2003; Brillas et al., 2003b), some kinds of dyes (Flox et al., 2006; Rao et al., 2006) and some kinds of organics (Brillas et al., 2002; Boye et al., 2006). In addition, Flox et al. (2007) have recently used solar energy as photon source, and reduced operating costs of the process substantially. However, in order to increase the environmental application of the process, researchers should focus on real wastewaters.

2.5.2. Overview of the earlier work of the photoelectro-Fenton process

In conclusion, the use of photoelectro-Fenton technique for the destruction of pollutants is new to the researchers. Table 2.2 gives the list of chemicals degraded by the photoelectro-Fenton process and the references. Some of the illustrative works in recent years have been discussed in detail so as to establish the optimum operating parameters and other critical considerations for attaining maximum efficiency of this hybrid oxidation technique.

Table 2.2 List of the chemicals degraded by photoelectro-Fenton oxidation process

Year	Title and Source	Experimental conditions						Significant conclusion
		Pollutant	Anode	Cathode	Current	UV	$[Fe^{2+}]$	
1998	Aniline mineralization by AOP's: anodic oxidation, photocatalysis, electro-Fenton and photoelectro-Fenton processes ***Appl. Catal. B-Envoron. 16, 31-42***	Aniline TOC=100 ppm	Pt	Carbon-PTFE	0.1 A	λ=360 nm 125 W	1 mM	- The photoelectro-Fenton process allows to destroy 92 % of TOC after 6 hr. - Electro-Fenton reaction only leads to 68% of mineralization.
2000	Mineralization of 2,4-D by advanced electrochemical oxidation processes ***Water Res. 8, 2253-2262***	2,4-D TOC=100 ppm	Pt	Carbon-PTFE	0.1 A	λ=360 nm 6 W	1 mM	- The photoelectro-Fenton process allows to destroy 97 % of TOC after 4 hr.
2003	Anodic oxidation, electro-Fenton and photoelectro-Fenton treatment of 2,4,5-trichlorophenoxyacetic acid ***J. Electroanal. Chem.557, 135-146***	Herbicide TOC=100 ppm	Pt	Carbon-PTFE	0.1 A	λ=360 nm 6 W	1 mM	- The photoelectro-Fenton process allows to destroy 99 % of TOC after 3 hr. - Electro-Fenton reaction only leads to 60~65% of mineralization. - The herbicide decay always follows a pseudo first-order reaction.
2003	Mineralization of herbicide 3,6-dichloro-2-methoxybenzoic acid in aqueous medium by anodic oxidation, electro-Fenton and photoelectro-Fenton ***Electrochimica Acta. 48, 1697-1705***	Herbicide TOC=50 ppm	Pt	Carbon-PTFE	0.1 A	λ=360 nm 6 W	1 mM	- The photoelectro-Fenton process allows to destroy 98 % of TOC after 4 hr. - While electro-Fenton only yields 60~70% mineralization, photoelectro-Fenton allows a fast and complete depollution.

2006	Electro-Fenton and photoelectro-Fenton degradation of indigo carmine in acidic aqueous medium ***Appl. Catal. B-Envoron.. 63, 243-248***	Dye TOC=100 ppm	Pt BDD	Carbon-PTFE	0.1 A	λ=360 nm 6 W	1 mM	- Complete mineralization is feasible using electro-Fenton with a BDD anode and 1.0 mM Fe^{2+} and 0.25 mM Cu^{2+} are combined as catalysts in photoelectro-Fenton with a Pt anode.
2006	Electrochemical removal of gallic acid from aqueous solutions ***Electrochimica Acta. 52, 256-262***	gallic acid TOC=155 ppm	Ti-Pt	Carbon-PTFE	0.08 A	λ=360 nm 6 W	1 mM	- The elector-Fenton process allows a TOC and COD abatement aloes to 70% at maximum after 4 hr. - The photoelectro-Fenton process allows to destroy 90 % of TOC after 4 hr.
2007	Degradation of clofibric acid in acidic aqueous medium by electro-Fenton and photoelectro-Fenton ***Chemosphere. 66, 1660-1669***	Clofibric TOC=100 ppm	Pt	Carbon-PTFE	0.1 A	λ=360 nm 6 W	1 mM	- 96% TOC decay and complete dechlorination were observed. - The decay kinetics of clofibric acid always follows a pseudo-first-order reaction. - The similar rate constant in electro-Fenton and photoelectro-Fenton processes.
2007	Mineralization of herbicide mecoprop by photoelectro-Fenton with UVA and solar light ***Catalysis Today. 129, 29-36***	Herbicide TOC=58 ppm	BDD	Carbon-PTFE	0.05 A	λ=360 nm 160 W	0.5 mM	- PEF with UVA or solar light yields complete mineralization (>96% TOC removal). - The kinetics for the herbicide decay follows a pseudo-first-order reaction.

2007	Solar photoelectro-Fenton degradation of cresols using a flow reactor with a boron-doped diamond anode ***Appl. Catal. B-Envoron. 75, 17-28***	Cresols TOC=100 ppm	BDD	Carbon-PTFE	0.1 A	-	1 mM	- The decay kinetics for all cresols follows a pseudo-first-order reaction. - The aromatic intermediates are rapidly converted into a mixture of carboxylic acids, being oxalic and acids the most persistent final products.
2007	Mineralization of clofibric acid by electrochemical advanced oxidation processes using a boron-doped diamond anode and Fe^{2+} and UVA light as catalysts ***Appl. Catal. B-Envoron. 72, 373-381***	Clofibric TOC=100 ppm	BDD	Carbon-PTFE	0.1 A	λ=360 nm 6 W	1 mM	- Total mineralization is achieved at Q=12 Ah^{-1} (4 hr) in photoelectro-Fenton process. - The decay kinetics for clofibric follows a pseudo-first-order reaction.
2007	Degradation of the herbicide 2,4-DP by anodic oxidation, electro-Fenton and photoelectro-Fenton using platinum and boron-doped diamond anodes ***Chemosphere. 68, 199-209***	2,4-DP TOC=100 ppm	Pt BDD	Carbon-PTFE	0.1 A	λ=360 nm 6 W	1 mM	TOC removal (4 hr): - AO-Pt: 17% - AO-BDD: 63% - EF-Pt: 48% - EF-BDD: 82% - PEF-Pt: 70% - PEF-BDD: 83%
2008	Mineralization of the biocide chloroxylenol by electrochemical advanced oxidation processes ***Chemosphere. 71, 1718-1729***	2,4-DP TOC=60 ppm	Pt BDD	Carbon-PTFE	0.1 A	λ=360 nm 6 W	1 mM	TOC removal: - PEF-BDD> PEF-Pt> EF-BDD> EF-Pt> AO-BDD> AO-Pt

2008	Mineralization of salyic acid in acidic aqueous medium by electrochemical advanced oxidation processes using platinum and boron-doped diamond as anode and cathodically generated hydrogen peroxide ***Water Res. 42, 499-511***	Salyic acid TOC=100 ppm	Pt BDD	Carbon-PTFE	0.1 A	λ=360 nm 6 W	1 mM	TOC removal (3 hr): - AO-Pt: 12% - AO-BDD: 69% - EF-Pt: 62% - EF-BDD: 85% - PEF-Pt: -% - PEF-BDD: -%

CHAPTER 3 EXPERIMENTAL METHODS

3.1 Chemicals and analytical methods

3.1.1 Chemicals

All the reagents used in the experiments were in analytical quality. BSA, $C_6H_5SO_3H \cdot H_2O$; it was 97% pure, and had a molecular weight of 176.19 (g/mole). 2,6-DMA, $C_8H_{11}N$; it was 98% pure, and had a molecular weight of 121.18 (g/mole). BSA and 2,6-DMA were obtained from Kanto Chemical Company and Merck Company, respectively. The physical properties and chemical structures are shown in Table 3.1 and Figure 3.1. Ferrous sulfate ($FeSO_4 \cdot 7H_2O$), H_2O_2 (35%), NaOH, $HClO_4$ and $NaClO_4$ were all purchased from Merck Company.

3.1.2 Analytical methods

1. 2,6-DMA

All the preparations and experiments were conducted at room temperature. The samples taken at predetermined time intervals were immediately injected into tubes containing sodium hydroxide solution to quench the reaction by increasing the pH to 11. Then all the samples were filtered with 0.45 μm mixed cellulose ester filters (Toyo) before analysis. The 2,6-DMA was analyzed by an HP4890 gas chromatography with a flame ionization detector and an HP-5 column (0.53 mm in inside diameter, 15 m long).

2. BSA

All the preparations and experiments were conducted at room temperature. The samples taken at predetermined time intervals were immediately injected into tubes containing sodium hydroxide solution to quench the reaction by increasing the pH to 11. Then all the samples were filtered with 0.45 μm mixed cellulose ester filters (Toyo), and kept for 12 hours in the refrigerator before chemical oxygen demand (COD) analysis was conducted. This work has been carried out to correct quantitative the effect of the

concentration of hydrogen peroxide on the COD value. COD was determined using a closed-reflux titrimetic method based on Standard Methods (APHA, 1998).

3. Ferrous ions concentration

The investigation of accumulated ferrous ions during the reaction at different current densities on cathode and 1 mM of Fe^{3+} and pH_i=2.0. The Fe^{2+} concentration was determined by light absorbance measurement at 510 nm after complexing with 1,10-phenanthroline using a Unicam UV-Visible spectrophotometer (APHA, 1998).

4. Hydrogen peroxide concentration

The residual H_2O_2 was determined photometrically using potassium titanium oxalate in mineral acid (Wagner and Ruck, 1984; Roland et al., 1997). The formula of titanium reagent was described as follows: 272 ml H_2SO_4 and 35.4 g $K_2TiO(C_2O_4)_2 \cdot 2H_2O$ were placed in 300 ml D.I. water and then diluted the mixture with D.I. water to 1000 ml. Finally, mix this titanium reagent with the sample. The titanium-H_2O_2 complex was analyzed photometrically at 400 nm. Before the measurements were made, calibration curve was plotted using standard H_2O_2 of known concentration.

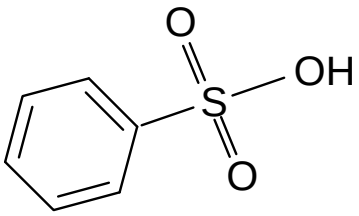

BSA

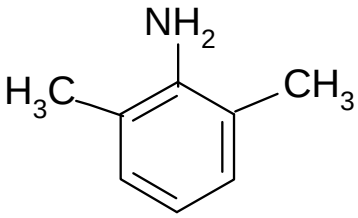

2,6-DMA

Figure 3.1 The structures of BSA and 2,6-DMA.

Table 3.1 The characteristics of BSA and 2,6-DMA.

Chemical names	2,6-DMA	BSA
CAS No	87-62-7	98-11-3
Molecular weight	121.18	176.19
Properties	colorless to light yellow oily liquid	needle solid
Assay	≥99%	≥99%
Boiling point	216˚C	190˚C
Melting point	11.2˚C	43-44˚C
Solubility in water	moderate	appreciable (10%)
LD_{50}	oral rat 698 mg/kg	oral rat 890 mg/kg

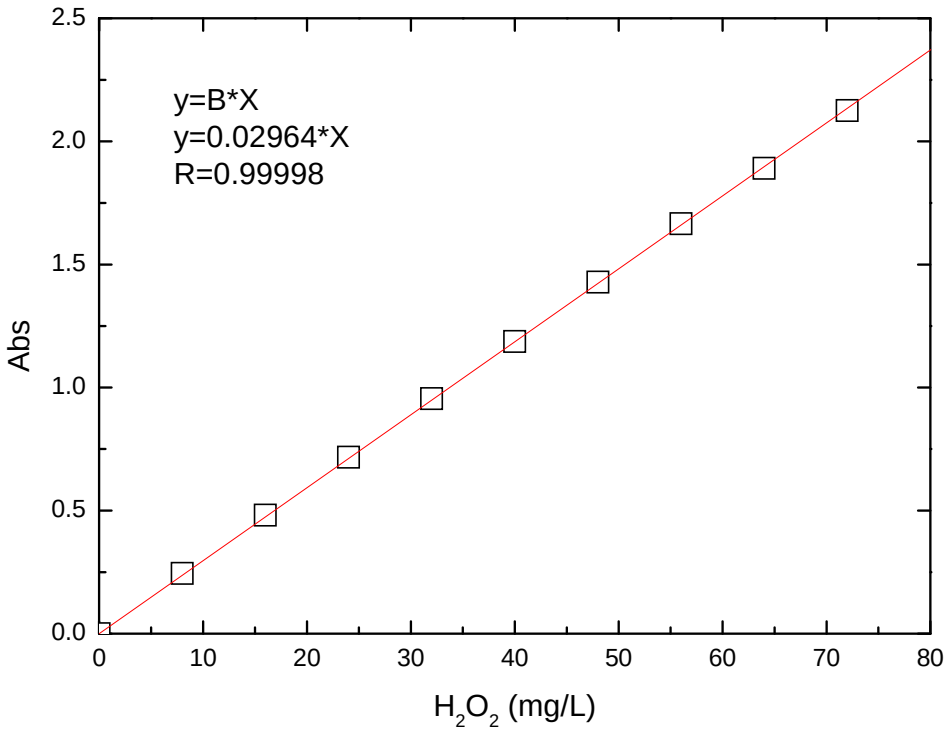

Figure 3.2 Calibration curve of the H_2O_2 concentration.

5. Biochemical oxygen demand (BOD)

The reaction final solution was used for the BOD test after being neutralized. BOD was measured according to the procedures in Standard Methods (APHA, 1998).

6. Total/Dissolved organic carbon (TOC/DOC)

TOC/DOC was determined on a TOC analyzer The TOC was determined with an Elementer-liquid TOC (Germany) total organic carbon analyzer.

7. Organic acids

Organic acids were analyzed using a Dionex DX-120 ion chromatograph (IC) with an IonPac® AS 17 anion column at 30 °C. The eluent concentration was generated by an RFIC eluent generation system. Sample analysis with a RFIC system using a potassium hydroxide eluent gradient proved to be the ideal choice to meet the separation and detection requirements of this application. Analytes were detected at concentrations less than 1 μg/l. The present application note describes an RFIC method using a carbonate removal device to determine a similar set of 14 anions common in electronic component extracts. This method allows more reliable quantification of sulfate, oxalate, and other anions eluting just after carbonate.

8. Intermediates

Oxidation products were detected by gas chromatography mass spectrometry (GC-MS) using an HP 6890 gas chromatography and an HP 5975 mass spectrometer. DB-5MS capillary column (30 m x 0.25 mm i.d., 0.25 lm film, from J&W, USA) was used. The GC temperature program was as follows: 40 °C for 2 min, followed by a 15 °C/min ramp to 280 °C, and hold for 5 min.

3.2 Experimental apparatus

Figure 3.3 shows the schematic experimental setup of this study. The cylindrical reactor (radius: 6.5 cm and height: 35 cm) was operated at a constant current mode. The total volume of the reactor was 3.5 liters. The anode used was titanium net coated with RuO_2/IrO_2 (DSA), and the cathode was made of stainless steel. The double electrode cell had a DSA anode with an inside diameter of 7 cm, and the cathode had 2 cm and 13 cm stainless steel walls.

3.3 Experiment procedures

3.3.1 Fenton process

All the reactions were carried out in a 3.5 L reactor (Figure 3.2) at room temperature, 28(±2˚C). The pH of the reaction solution was adjusted by using $HClO_4$ or NaOH. A predetermined quantity of ferrous concentration was added after the pH was adjusted to the desired value. Solution pH was not controlled during the reaction. The hydrogen peroxide was added to initiate the reaction. The oxidation reaction was stopped instantly by adding NaOH to the reaction mixtures after sampling. The samples were then filtered with 0.45 μm to remove precipitates before analysis.

3.3.2 Electrolysis process

All the reactions were carried out in a 3.5 L reactor (Figure 3.3) at room temperature, 28(±2˚C). The pH of the solution was adjusted by using $HClO_4$ or NaOH. The solution pH was not controlled during the reaction. The power supply was turned on to initiate the reaction. The oxidation reaction was stopped instantly by adding NaOH to the reaction mixtures after sampling. The samples were then filtered with 0.45 μm to remove precipitates before analysis.

3.3.3 Electro-Fenton process

The reaction solution was poured into the system. The ferrous ion was added after the pH was adjusted to the desired value. The pH of the solution was not controlled during the reaction. In the meantime, hydrogen peroxide was added to the solution, and the power supply was turned on to initiate the reaction. The oxidation reaction was stopped instantly by adding NaOH to the reaction mixtures after sampling. The samples were then filtered with 0.45 μm to remove precipitates before analysis.

3.3.4 Photoelectro-Fenton process

The irradiation source was a set of sixteen 3 W UVA lamps (Sunbeamtech. com) fixed inside a cylindrical Pyrex tube (allowing wavelengths λ>320 nm to penetrate). This setup prevented the formation of HO˙ radicals by the direct photolysis of H_2O_2. Figure 3.4 shows the UV–vis spectrum of the UVA lamp. In addition to all the experimental conditions mentioned above, UV light with maximum wavelength of 360 nm was irradiated inside the reactor, supplying a photoionization energy input of 48 W to the solution.

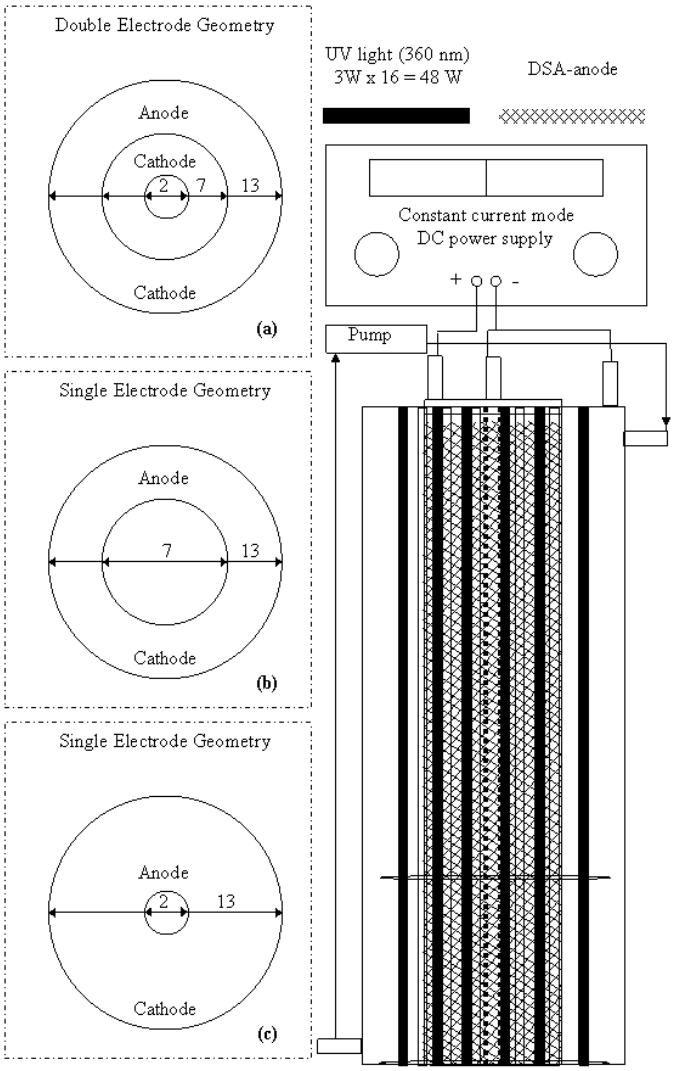

Figure 3.3 Schematic diagram of reaction system.

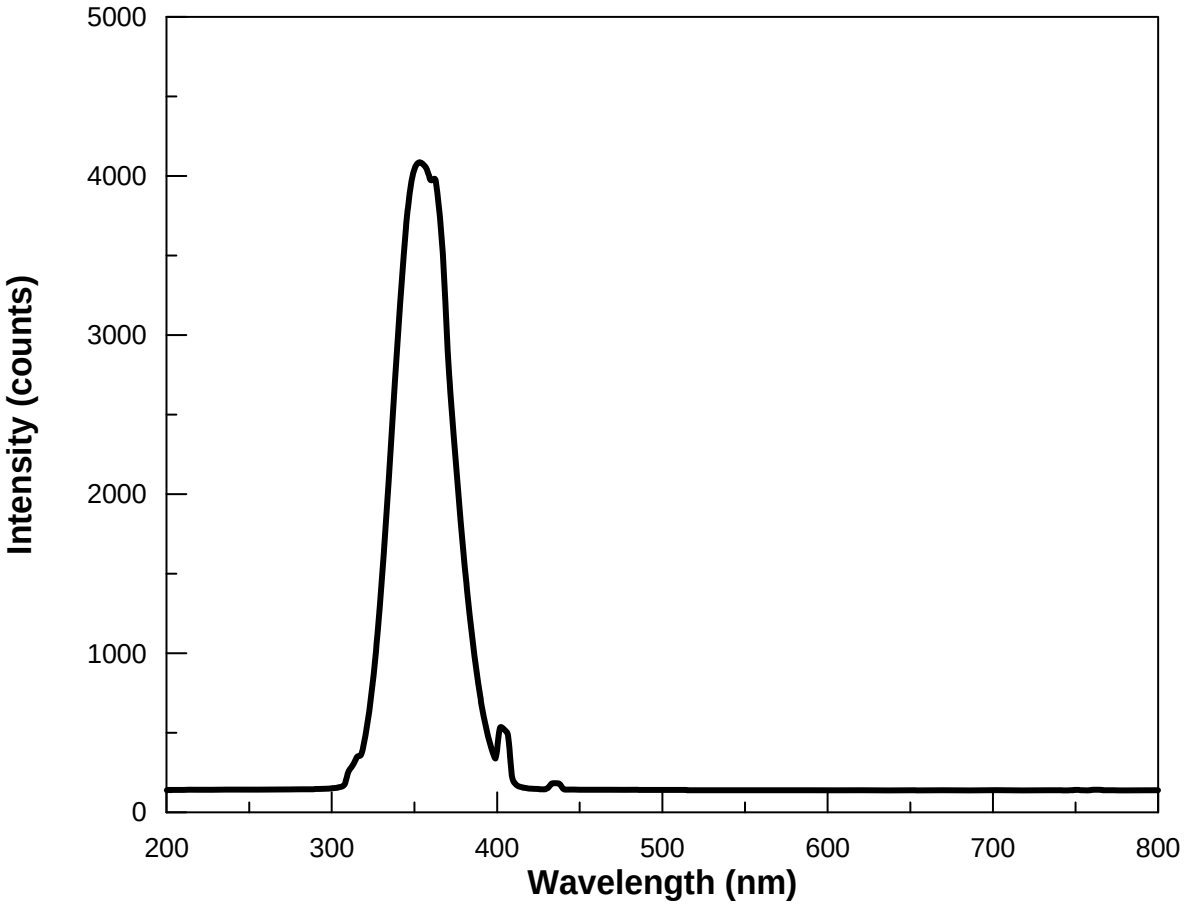

Figure 3.4 The UV–vis spectrum of the UVA lamp.

CHAPTER 4 RESULTS AND DISCUSSION

Framework of the results and discussion

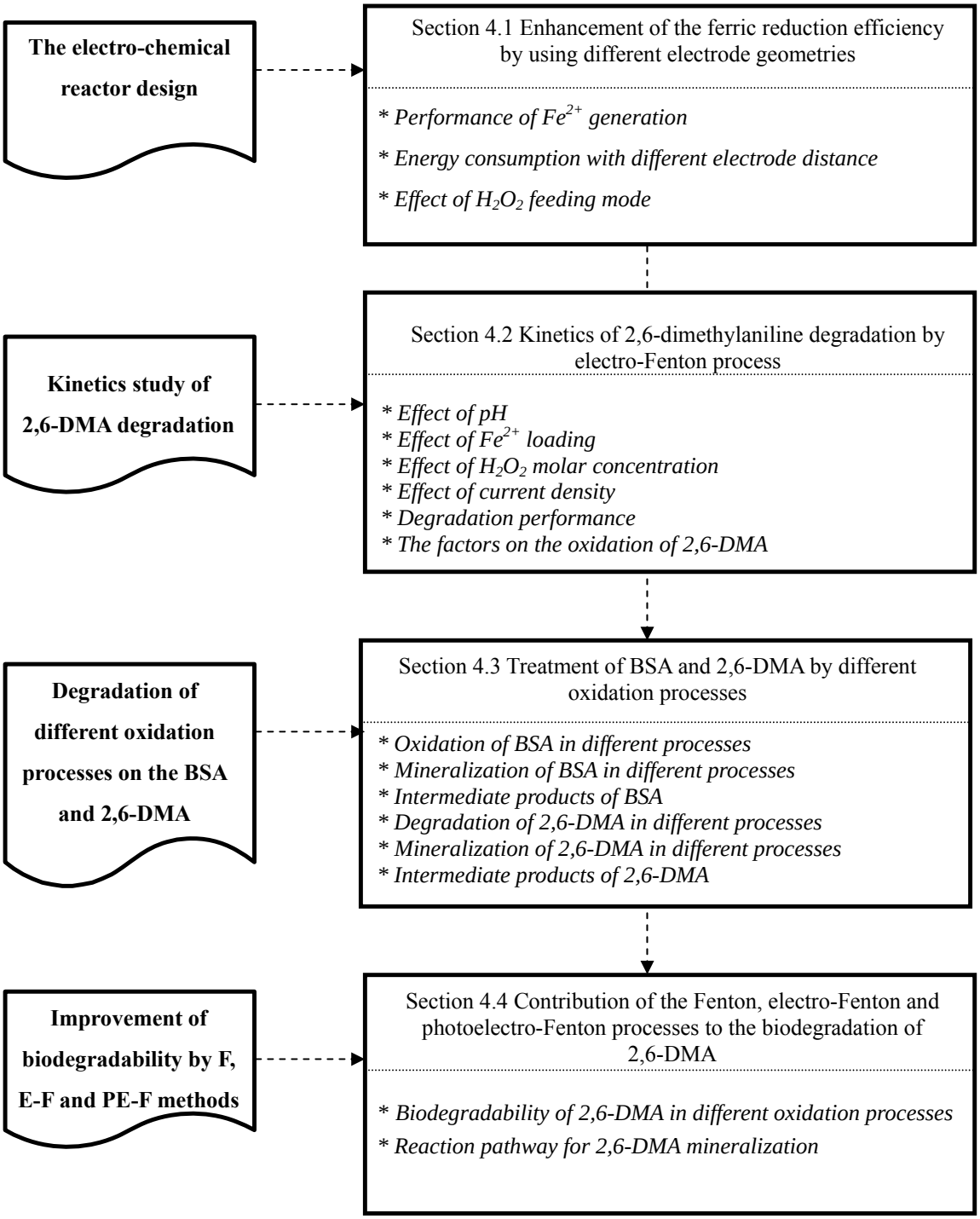

Figure 4.1 The schematic diagram of this study

4.1. Enhancement of the Ferric Reduction Efficiency by Using Different Electrode Geometries

In this part of the research, we would like to investigate the role of the electrode geometry playing in the electrochemical system. The parameters including the electrode working area, electrode distance and energy consumption were investigated to evaluate the reactor design.

4.1.1. Performance of Fe^{2+} generation

The proposed reactions in the electrolytic system are (Chou et al., 1999)

(1) on the anode side:

$$H_2O \rightarrow HO^{\bullet} + H^+ + e^- \quad (4.1)$$

$$H_2O \rightarrow 2H^+ + 1/2O_2 + 2e^- \quad (4.2)$$

$$H_2O_2 \rightarrow O_2 + 2H^+ + 2e^- \quad (4.3)$$

$$Fe^{2+} \rightarrow Fe^{3+} + e^- \quad (4.4)$$

(2) on the cathode side:

$$Fe^{3+} + e^- \rightarrow Fe^{2+} \quad (1.4)$$

$$H_2O + e^- \rightarrow 1/2H_2 + OH^- \quad (4.5)$$

$$2H^+ + 2e^- \rightarrow H_2 \quad (4.6)$$

The performance was evaluated by the instantaneous current efficiency (CE %) of ferrous ion generation, which is defined as equation (4.7) (Chou et al., 1999)

$$CE\% = (FV/A)(dC_{Fe}/dt) \times 100\% \quad (4.7)$$

where F is Faraday's constant, C_{Fe} represents the molar concentration of generated ferrous

ion, *V* is the volume of the solution, *A* is the operating current, and *t* is the reaction time. Since the current was kept constant, the amount of generated Fe^{2+} was proportional to the electrolysis time.

Figure 4.2 shows the effect of cathode geometry on the generated ferrous concentration. According to our past experience, a single working electrode does not significantly enhance the electro-regeneration of ferrous ions. For this reason, we developed a double cathode electrolysis cell (Figure 3.3 (a)) to increase the working area and to promote current efficiency. As shown in equations (4.4) and (1.4), the small working area on the anode was designed to minimize the oxidation of ferrous ions and to promote the reduction of ferric ions on the cathode. At the cathode, ferric ions were electrochemically reduced to ferrous ions in an acidic solution. Simultaneously, H_2 evolution may occur as the side reaction which reduces the current efficiency. At the anode, the oxidation of H_2O leads to oxygen evolution and proton release. Consequently the ferrous concentration increased with increasing in the cathode working area. Figure 4.3 shows the effect of cathode geometry on initial current efficiency (Figure 3.3 (a) and (b)). The double cathode reactor could increase the current efficiency by 7 %, which would translate to greater ferrous production and a higher degradation rate of organic compounds in the electro-Fenton process. A 41 % current efficiency was observed using the double cathode electrochemical cell when CD_c= 71.0 A/m^2 and CD_a= 75.8 A/m^2. The CD_c and CD_a denote the current densities of the cathode and anode, respectively. Chou et al. (1999) reported that the initial current efficiency of Fe^{2+} regeneration was 39 % at $[Fe^{3+}]_0$ = 1000 mg/L, CD_c= 98 A/m^2 and CD_a= 980 A/m^2 in the constant current mode. It should be pointed out that the double cathode electrochemical cell has more potential for the improvement of the efficiency of electricity utilization.

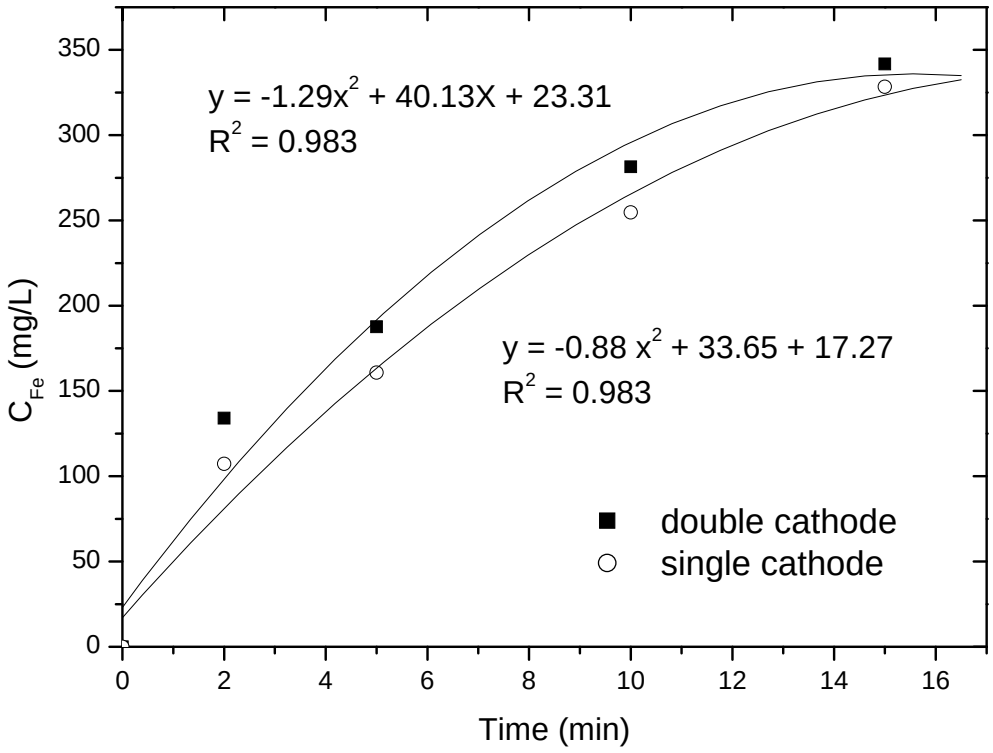

Figure 4.2 Effect of cathode geometry on ferrous concentration.

The solid line is the fit of second-order polynomial model (Fe^{3+}=1000 mg/L; pH_i=2.0; CDa= 75.8 A/m^2; (■) double electrode (Fig. 3.4 (a)) : CDc= 71.0 A/m^2; (○) single electrode (Fig 3.4 (b)): CD_c= 81.6 A/m^2; CD_a and CDc denote the current densities of anode and cathode, respectively)

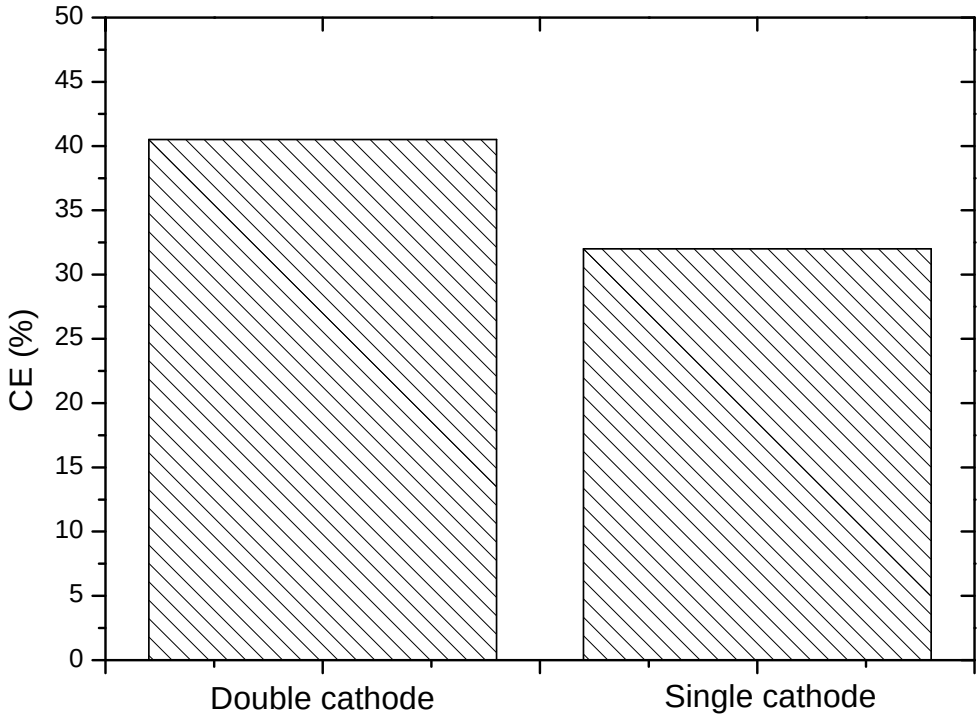

Figure 4.3 Effect of cathode geometry on initial current efficiency.

(Fe^{3+}=1000 mg/L; pH_i=2.0; CD_a= 75.8 A/m^2; double cathode reactor (Fig. 3.4 (a)): CD_c= 71.0 A/m^2; single cathode (Fig. 3.4 (b)): CD_c= 81.6 A/m^2).

The ferrous ions were oxidized to ferric ion on the anode by equation (4.4). Fe^{2+} regeneration was controlled either by the electron transfer between Fe^{3+} and the cathode or by the mass transfer of Fe^{3+} across the cathode-solution interface. As shown in Figure 4. 4 two geometries of electrode distance 3.0 cm and 5.5 cm (Figure 3.3 (b) and (c)) were employed to investigate the effect of electrode distance on Fe^{2+} regeneration. Figure 4.5 shows the effect of electrode distance on current efficiency. A 52 % current efficiency was observed in the trial using an electrode gap of 5.5 cm, and approximately 33 % was detected in the trial using 3.0 cm. This shows a 19 % increase in current efficiency which indicates that long electrode distance can avoid the oxidation of ferrous ion on the anode.

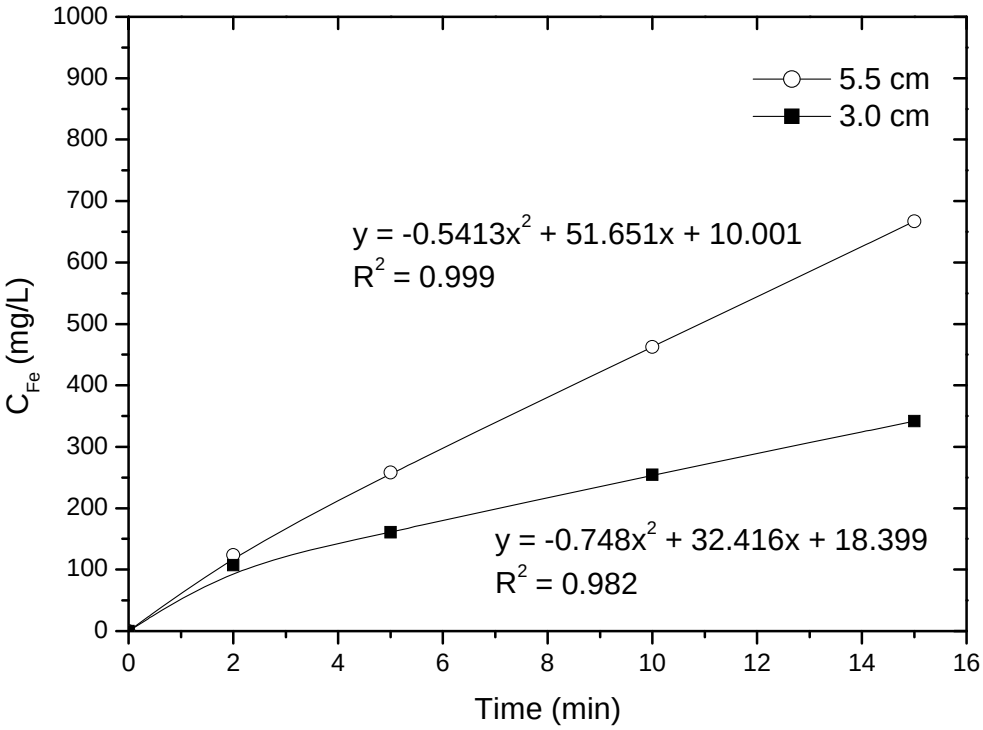

Figure 4. 4 Effect of electrode distance on ferrous concentration.
The solid line is the fit of second-order polynomial model (Fe^{3+}=1000 mg/L; pH_i=2.0; CD_a= 75.8 A/m^2; double cathode reactor (Fig. 3.4 (a)): CD_c= 71.0 A/m^2; single cathode (Fig. 3.4 (b)): CD_c= 81.6 A/m^2)

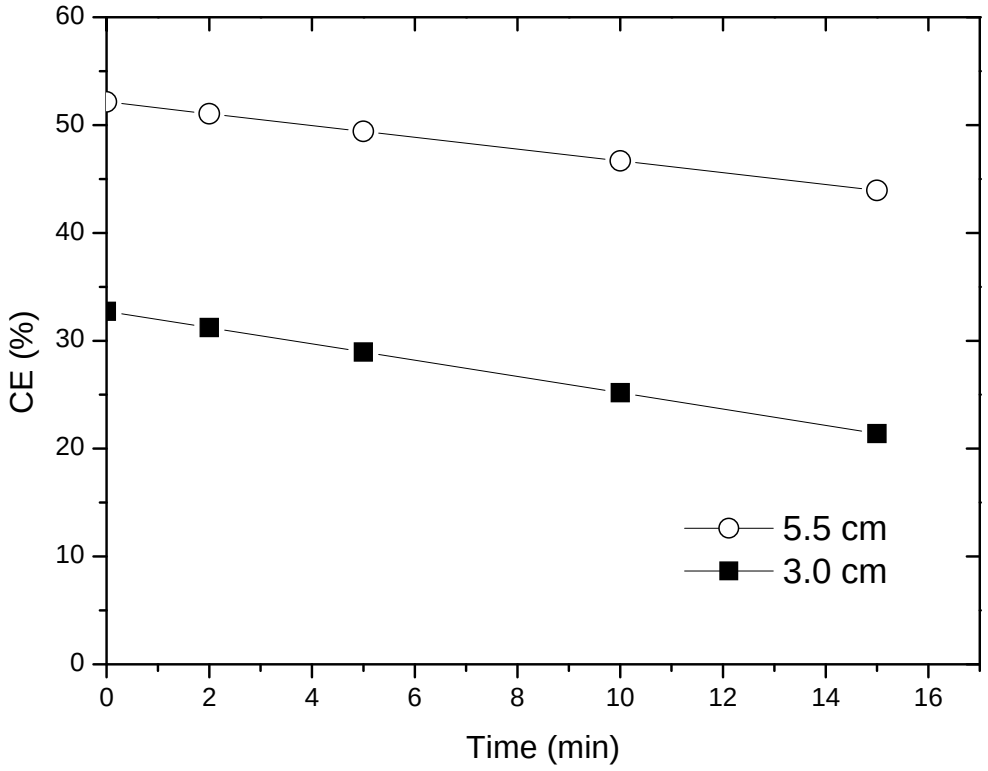

Figure 4.5 Effect of electrode distance on current efficiency.

(Fe^{3+}=1000 mg/L; pH_i=2.0; current=10 A; single cathode reactor (Fig. 3.4 (a)): 3.0 cm; single cathode reactor (Fig. 3.4 (b)): 5.5 cm)

4.1.2. Energy consumption with different electrode distance

To simplify the analysis, only electricity was considered. The energy consumption was calculated for electrode distances of 3.0 cm and 5.5 cm for the electro-Fenton process, respectively, when 1 kg COD needs to be removed. The energy cost for each device was obtained from equation (4.8).

$$\text{Energy conmption } (kWh/kg\ COD) = AV_{oltage}t/\Delta CODV \quad (4.8)$$

$$\text{Resistance} = V_{oltage}/C_{urrent} \quad (4.9)$$

Where A is the operating current, V_{oltage} is the voltage, V is the volume of the solution, t is the reaction time and ΔCOD denotes the experimental COD decay in solution. The experimental results with regard to COD removal and energy consumption are shown in Table 4.1. Although the current efficiency of the 5.5 cm device is 19 % higher than 3.0 cm, results show that after 2 hours of electrolysis the electronic expense using an electrode gap of 5.5 cm is much higher than 3.0 cm. The result suggests that the electrode distance 3.0 cm device can provide more economical operation.

This phenomenon is due to equation (4.9). Long electrode distance will increace the resistance causing the voltage and electricity cost to be higher. The results were compared with the results obtained by Brillas et al, when aniline was treated with Ti/Pt anode and carbon-PTFE cathode (Brillas et al., 2002). The electro-Fenton process used by Brillas has a higher energy cost (45 $kWhm^{-3}$ for 2 hrs) than this system (39 $kWhm^{-3}$ at 2 hr, the data calculated from 3.0 cm device: Figure 3.3 (b)).

Table 4.1 Effect of electrode distance on energy consumption ([$C_6H_5SO_3H$]=10 mM; [Fe^{2+}]=8 mM; [H_2O_2]=166 mM; pH_i=2.0; current=10 A; H_2O_2 feeding time= 0, 5, 10, 15, 20, 30, 40, 60, 80, 100 min; single cathode reactor: 3.0 cm, Fig. 3.4 (b); 5.5 cm, Fig. 3.4 (c))

Time (hr)	Current (A)	Voltage (V)	Electrode distance (cm)	COD residual (%)	Energy consumption (kWh/kg COD)
0.5	9.99	8.1	3.0	50	12.58
1	9.99	7.2	3.0	37	17.60
2	9.99	6.9	3.0	29	28.35
0.5	10.00	19.6	5.5	45	26.59
1	10.00	16.8	5.5	34	38.53
2	9.99	16.5	5.5	26	62.59

4.1.3. Effect of hydrogen peroxide feeding mode

As shown in Figure 4.6, the residues in turn depend on the method of chemical addition, for example, single-step or multi-step addition; thus, affect the process performance. Multi-step addition of chemical was considered due to that the initial application of one reactant might be in excess of the other. To avoid the excessive application or rather the waste of chemical, the step additions appears to be attractive. Bowers et al. (1989) and Mohanty and Wei (1993) used the Fenton process for degradation of toxic organics and reported that multi-step addition of H_2O_2 shows a removal efficiency better than one-step addition, without further explanation of cause and effect. Hence, it is also desirable to know if the multi-step addition of hydrogen peroxide will lead to any improvement in the performance of Fenton, electro-Fenton and photoelectro-Fenton processes.

Figure 4.6 presents the comparison of single-step and multi-step additions of H_2O_2 by electro-Fenton process. The amount of H_2O_2 applied was 166 mM in one-step addition, and 16.6 mM in ten-step addition at times of 0, 5, 10, 15, 20, 30, 40, 60, 80 and 100 min. Multi-step addition of H_2O_2 was slightly better in front of 80 min compared with single step addition. Similar observations were derived when multi-step H_2O_2 addition was employed to treat landfill leachate by electro-Fenton process (Zhang et al., 2006). The COD removal ratio was improved by multi-step addition as much as 10% in electro-Fenton process at the first 20 min. That is because the ferrous ion is regenerated via the reduction of ferric ion on the cathode induce the Fenton chain reaction. Thus, stepwise addition keeps the hydrogen peroxide concentration at relatively low levels, reducing the detrimental effect of hydroxyl radical scavenging (equation (2.8)).

$$HO^{\bullet} + H_2O_2 \rightarrow H_2O + HO_2^{\bullet} \qquad k = 3.3\times10^7\ M^{-1}s^{-1} \quad (2.8)$$

In addition, BSA led to weak decontamination after 80 min because of the formation of carboxylic acids. Oxalic acid is a major product of aromatic ring degradation and its complexes with Fe(Ⅲ) are very fast (see in 4.2.3). This indicates that almost zero residues of ferrous ion after 80 min.

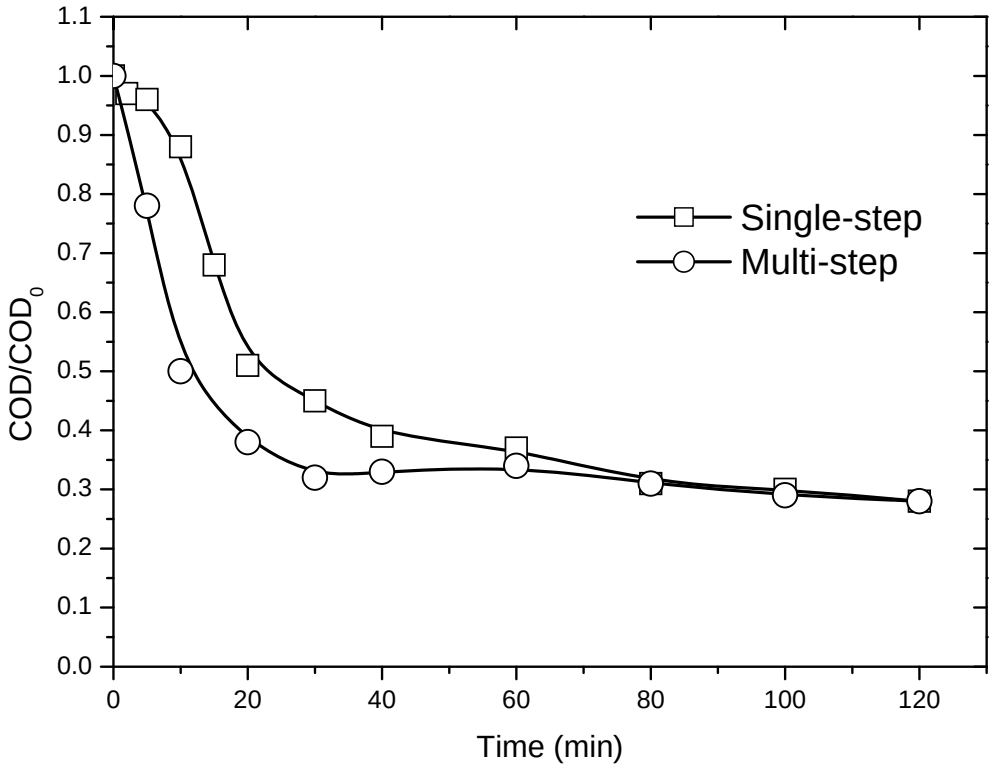

Figure 4.6 Effect of H_2O_2 feeding mode on COD removal by electro-Fenton process. ($[C_6H_5SO_3H]$=10 mM; $[Fe^{2+}]$=8 mM; $[H_2O_2]$=166 mM; pH_i=2.0; CD_a= 75.8 A/m^2; CD_c=71.0 A/m^2; H_2O_2 feeding time= 0, 5, 10, 15, 20, 30, 40, 60, 80, 100 min)

4.1.4. Summary

The effect of electrode geometry and different oxidation methods were investigated to evaluate reactor design and mineralization efficiency. The double cathode reactor could increase the working area and enhance the current efficiency by 7 %, which would translate to greater ferrous production and a higher degradation rate of organic compounds in the electro-Fenton process. It should be pointed out that the double cathode electrochemical cell has more potential for the improvement of the efficiency of electricity utilization. The result also suggests that the electrode distance 3.0 cm device can provide more economical operation.

4.2. Kinetics of 2,6-DMA degradation by electro-Fenton process

Based on the results of current efficiency and energy consumption, the double cathode device (Figure 3.3 (a)) should be used for further oxidation research. In this part of research, the effects of initial pH (pH_i), Fe^{2+} loading, H_2O_2 concentration and current density on the processes were investigated. In addition, the study also concerned the degradation performance of the Fenton, electro-Fenton and photoelectro-Fenton processes.

4.2.1. Effect of pH

The pH of the solution controls the production of the hydroxyl radical and the concentration of ferrous ions (Pignatello et al., 2006; Abad et al., 2007; Muruganandham and Swaminathan, 2004; Sun et al., 2007). Hence, pH is an important parameter for the electro-Fenton process. The effect of pH on the degradation of 2,6-DMA is shown in Figure 4.7. Increasing the pHi from 1.5 to 2.0 decreased the remaining from 36% to 25% in 2 hours. A further increase of pH_i from 2 to 4 increased the remaining from 25% to 85%. At pH_i 3, only a small amount of Fe^{2+} is observed. Above this pH, Fe^{3+} started to be precipitated in the form of amorphous $Fe(OH)_{3(s)}$. The formation of $Fe(OH)_{3(s)}$ not only decreased the dissolved Fe^{3+} concentration, but also inhibited Fe^{2+} regeneration by partially coating the electrode surface. The optimum pH was found to be about 2. It is in good agreement with early reports (Lu et al., 2003; Chou et al., 1999; Sirés et al., 2007a; Li et al., 2007; Qiang et al., 2003).

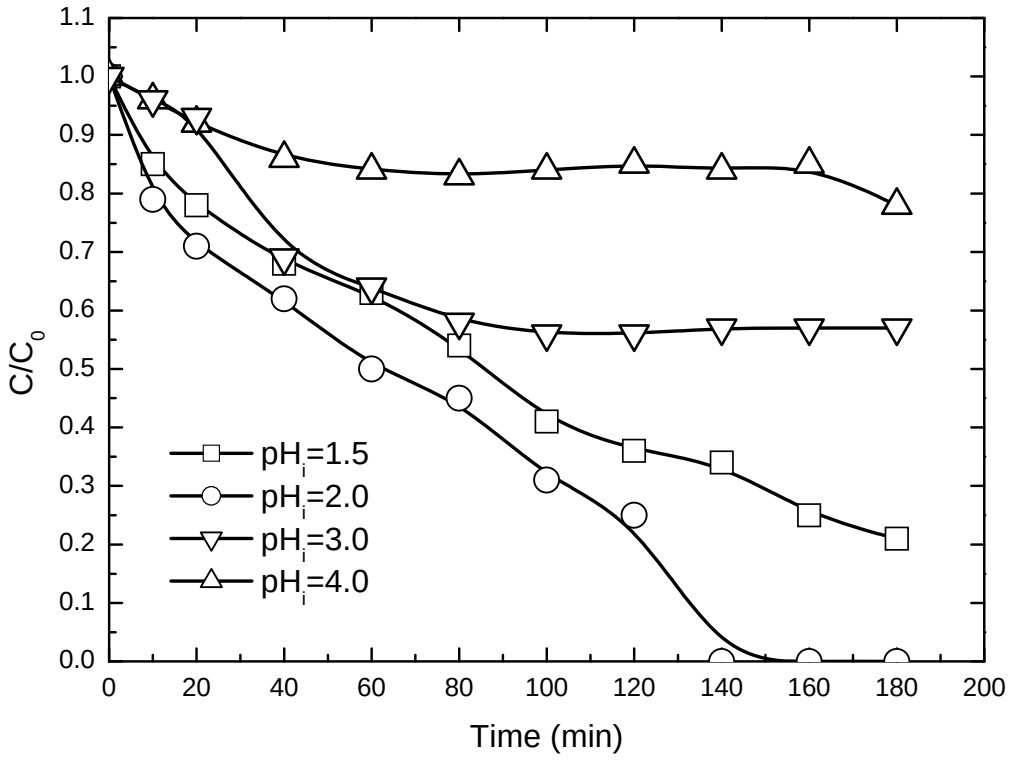

Figure 4.7 Effect of pH_i on the 2,6-DMA degradation.

([2,6-DMA] =1 mM; $[Fe^{2+}]$=1 mM; $[H_2O_2]$= 20 mM; $[NaClO_4]$= 50 mM; CD_a= 7.6 A/m^2; CD_c=7.1 A/m^2)

Table 4.2 Kinetic constant (k_{obs}) for 2,6-DMA degradation in electro-Fenton process ([2,6-DMA] =1 mM; $[Fe^{2+}]$=1 mM; $[H_2O_2]$= 20 mM; pH_i=2.0; $[NaClO_4]$= 50 mM; CD_a= 7.6 A/m^2; CD_c=7.1 A/m^2)

Initial pH (pH_i)	Final pH (pH_f)	$[Fe^{2+}]$ (mM)	$[H_2O_2]$ (mM)	Current density (A/m^2)	Remaining (%)	k_{obs} (min^{-1})	R
1.50	1.31	1.0	20	7.10	36	0.0084	0.996
2.00	1.89	1.0	20	7.10	25	0.0113	0.994
3.00	2.80	1.0	20	7.10	56	0.0079	0.946
4.00	3.50	1.0	20	7.10	85	0.0038	0.999
2.00	1.89	1.0	20	7.10	25	0.0113	0.994
2.00	1.93	1.5	20	7.10	19	0.0141	0.997
2.00	1.89	2.0	20	7.10	0	0.0158	0.998
2.00	1.93	1.0	10	7.10	46	0.0069	0.993
2.00	1.89	1.0	15	7.10	36	0.0086	0.985
2.00	1.89	1.0	20	7.10	25	0.0113	0.994
2.00	1.89	1.0	25	7.10	0	0.0152	0.991
2.00	1.89	1.0	30	7.10	35	0.0086	0.997
2.00	1.93	1.0	20	3.50	42	0.0067	0.977
2.00	1.89	1.0	20	7.10	25	0.0113	0.994
2.00	1.88	1.0	20	10.6	9	0.0204	0.977

To further compare the rate constant of 2,6-DMA degradation, all experimental data were analyzed using a simple first-order kinetic model; the values of rate constant, kobs, were obtained and are presented in Table 4.2. The first-order rate constants (k_{obs}) of the pH_i effect were determined from the slopes of the plots of $\ln([2,6\text{-DNA}]_t/[2,6\text{-DNA}]_0)$ vs. time and for reaction time ≤ 120 minutes (R≥0.95). The results in Table 4.2 show that the k_{obs} of 2,6-DMA degradation was significantly influenced by the pH_i value and that the optimal pHi was observed at pH 2.0. The value of k_{obs} increase when the pHi increase from 1.5 to 2.0, suddenly decrease when the pHi is raised from 2.0 to 3.0, and then slightly drops off with the increase of the pHi in the range of 3.0 to 4.0. The k_{obs} is limited in the low pH_i range (<2.0) due to the hydroxyl radical scavenging effects of the H^+ ion (Muruganandham and Swaminathan, 2004; Sun et al., 2007).

$$^{\bullet}OH + H^+ + e^- \rightarrow H_2O \tag{4.10}$$

The poor degradation of 2,6-DMA at a high pH range (>2.0) was caused by the formation of ferric and ferric hydroxide complexes with much lower catalytic capability than Fe^{2+} (Pignatello et al., 2006). Furthermore, a low pH also promotes hydrogen evolution, according to equation (4.6), reducing the number of active sites for generating ferrous ions.

On the cathode side:

$$Fe^{3+} + e^- \rightarrow Fe^{2+} \tag{1.4}$$

$$H_2O + e^- \rightarrow 1/2H_2 + OH^- \tag{4.5}$$

$$2H^+ + 2e^- \rightarrow H_2 \tag{4.6}$$

4.2.2. Effect of Fe^{2+} loading

The first-order rate constants (k_{obs}) were determined from the slopes of the plots of $\ln([2,6\text{-DNA}]_t/[2,6\text{-DNA}]_0)$ vs. time and for reaction time ≤ 120 minutes ($R \geq 0.99$). The effect of Fe^{2+} concentration on the kinetic rate constants, k_{obs}, for 2,6-DMA degradation was studied by varying $[Fe^{2+}]_0$ from 1.0 to 2.0 mM. The results are presented in Figure 4.8. It can be seen from Table 2 that the k_{obs} of 2,6-DMA degradation increased with increasing Fe^{2+} concentration from 1.0 to 1.5 mM. This is due to the fact that Fe^{2+} plays a very important role in initiating the decomposition of hydrogen peroxide to generate the hydroxyl radical in the Fenton process. When the concentrations of Fe^{2+} and hydroxyl radical are high, Fe^{2+} can react with the hydroxyl radical according to equation (2.3).

$$Fe^{2+} + {}^{\bullet}OH \rightarrow Fe^{3+} + OH^{-} \qquad k = 3.2\times10^{8}\ M^{-1}s^{-1} \quad (2.3)$$

$$H_2O_2 + Fe^{3+} \rightarrow Fe^{2+} + H_2O^{\bullet} + H^{+} \qquad k = 0.01\ M^{-1}s^{-1} \quad (1.2)$$

$$Fe^{3+} + e^{-} \rightarrow Fe^{2+} \qquad (1.4)$$

The k_{obs} does not increase significantly as the dosage of ferrous ions increased from 1.5 mM to 2.0 mM. The rate constant in equation (2.3) has a value of several orders of magnitude higher than that in equation (1.2) and (1.4). Hence, the excess ferrous ions consumed the hydroxyl radicals with a high oxidative potential. It caused the ferric reduction efficiency to be lower than in equation (2.3). However, it is not a good idea to use over high concentration of Fe^{2+}. Otherwise, a large quantity of ferric oxide sludge will be generated, resulting in much more requirement of separation and disposal of the sludge.

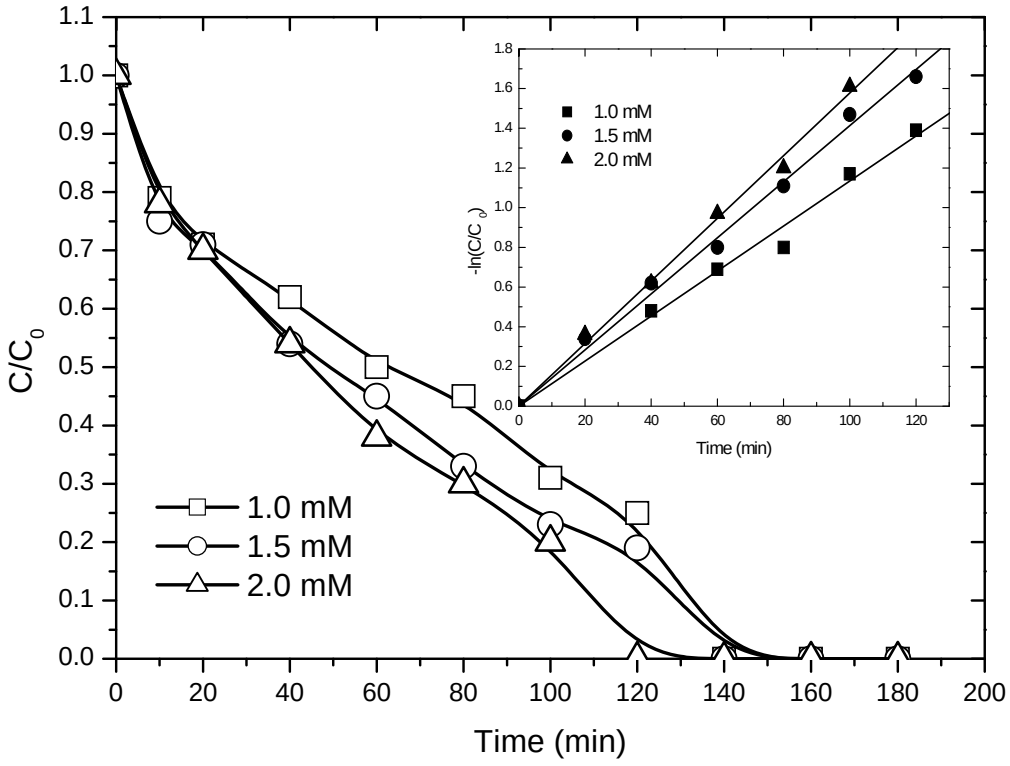

Figure 4.8 Effect of Fe^{2+} dosage on the 2,6-DMA degradation.

([2,6-DMA] =1 mM; $[H_2O_2]$= 20 mM; pH_i=2.0; $[NaClO_4]$= 50 mM; CD_a= 7.6 A/m^2; CD_c=7.1 A/m^2)

4.2.3. Effect of H_2O_2 molar concentration

The initial concentration of H_2O_2 plays an important role in the electro-Fenton process. The effect of the H_2O_2 concentration on the 2,6-DMA degradation is shown in Figure 4.9. Increasing the H_2O_2 concentration from 10 mM to 25 mM increased the removal efficiency, 46%, at 120 min. A further increase from 25 mM to 30 mM decreased the removal efficiency, 35%. The increase in the removal efficiency was due to the increase in hydroxyl radical concentration as a result of the addition of H_2O_2. However, at a high dosage of H_2O_2, the decrease in removal efficiency was due to the hydroxyl radical scavenging effect of H_2O_2 (equation (2.8) and (4.11)) and the recombination of the hydroxyl radical (equation (4.12)) (Muruganandham and Swaminathan, 2004).

$$HO^{\bullet} + H_2O_2 \rightarrow H_2O + HO_2^{\bullet} \qquad k = 3.3\times10^{7}\ M^{-1}s^{-1} \quad (2.8)$$

$$^{\bullet}HO_2 + {}^{\bullet}OH \rightarrow H_2O + O_2 \qquad k = 1.0\times10^{10}\ M^{-1}s^{-1} \quad (4.11)$$

$$^{\bullet}OH + {}^{\bullet}OH \rightarrow H_2O_2 \qquad k = 4.2\times10^{9}\ M^{-1}s^{-1} \quad (4.12)$$

The first-order rate constants (k_{obs}) were determined from the slopes of the plots of $\ln([2,6\text{-DNA}]_t/[2,6\text{-DNA}]_0)$ vs. time and for reaction time ≤ 120 minutes ($R \geq 0.97$). The results shown in Figure 4.9 indicates that from 10 mM to 25 mM, the reaction was first-order, reflecting equation (1.2) as the rate limiting step. Above 25 mM, the rate was inhibited by the hydroxyl radical scavenging effect of H_2O_2 and the recombination of the hydroxyl radical (Li et al., 2007).

$$Fe^{2+} + H_2O_2 \rightarrow Fe^{3+} + OH^{-} + {}^{\bullet}OH \quad (1.1)$$

$$H_2O_2 + Fe^{3+} \rightarrow Fe^{2+} + {}^{\bullet}H_2O + H^{+} \quad (1.2)$$

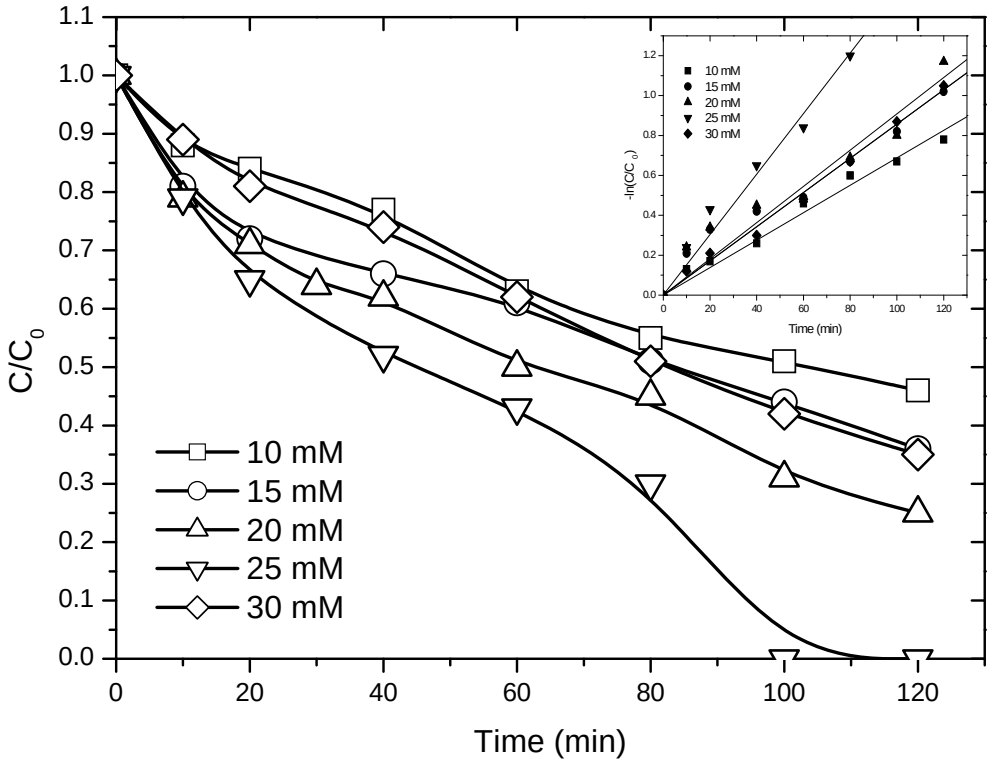

Figure 4.9 Effect of H_2O_2 concentration on the 2,6-DMA degradation.

([2,6-DMA] =1 mM; $[Fe^{2+}]$=1 mM; pH_i=2.0; $[NaClO_4]$= 50 mM; CD_a= 7.6 A/m^2; CD_c=7.1 A/m^2)

4.2.4. Effect of current density

Figure 4.10 shows the effect of current density for the 2,6-DMA degradation, which was significant. Increasing the current density increased the production rate of Fe^{2+} on the cathode. Therefore, the removal efficiency increased with increasing current density. In this work, the removal efficiency was 58%, 75% and 91% for current densities of 3.50, 7.10 and 10.6 A/m^2, respectively. The results further indicate that the effect of the apparent current density on the removal efficiency was significant indicating that the production rate of Fe^{2+} was increased with increasing current. It should be pointed out that the optimal current density also depends on the Fe^{3+} concentration because Fe^{3+} mass transfer also controls the ferric reduction efficiency (Chou et al., 1999; Qiang et al., 2005).

Figure 4.11 shows the effect of current density on the (a) remaining ratio (b) concentration of accumulated ferrous ion and (c) *k* value for the 2,6-DMA degradation in 60 minutes. The first-order rate constants (k_{obs}) were determined from the slopes of the plots of $\ln([2,6\text{-DNA}]_t/[2,6\text{-DNA}]_0)$ vs. time and for reaction time ≤ 120 minutes ($R \geq 0.97$). The effect of current density on the kinetic rate constants, k_{obs}, for 2,6-DMA degradation was studied by varying the current density from 3.5 to 10.60 A/m^2. The results are presented in Figure 4.10. It can be seen from k_{obs} that the 2,6-DMA degradation was increased with the increase of current density from 3.5 to 10.6 A/m^2. This was due to the higher electro-regeneration of ferrous ions from ferric ions (equation (1.4)) with increasing the current density, which increased the efficiency of the Fenton chain reactions.

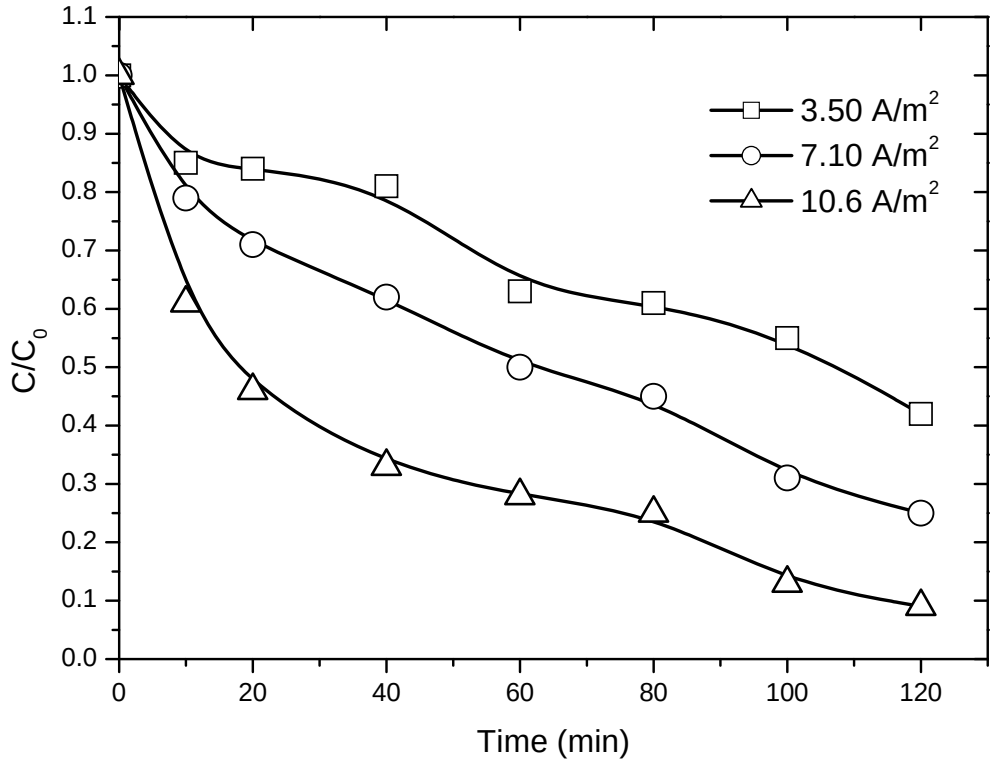

Figure 4.10 Effect of the current density for the 2,6-DMA degradation.

([2,6-DMA] =1 mM; [Fe^{2+}]=1 mM; [H_2O_2]= 20 mM; pH_i=2.0; [$NaClO_4$]= 50 mM)

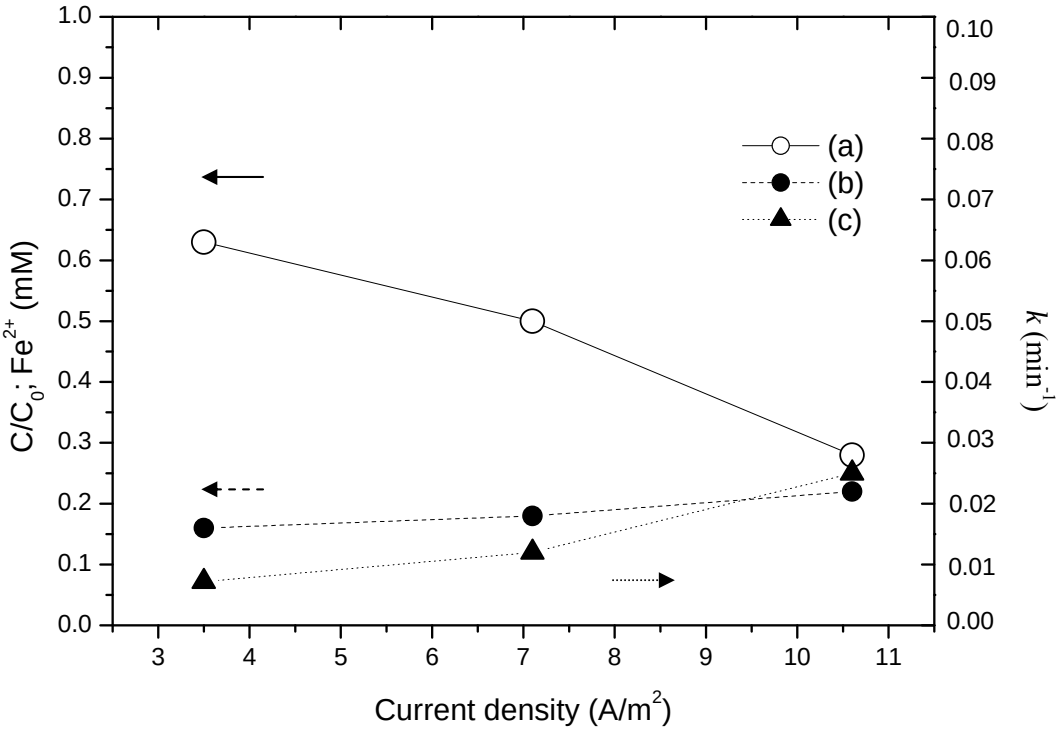

Figure 4.11 (a) Remaining ratio (b) concentration of accumulated ferrous ion and (c) *k* value vs. current density for the 2,6-DMA degradation.

([2,6-DMA] =1 mM; [Fe^{2+}]=1 mM; [H_2O_2]= 20 mM; pH_i=2.0; [$NaClO_4$]= 50 mM; reaction time=60 min)

4.2.5. Degradation performance

Three concentrations of hydrogen peroxide (15, 20 and 25 mM) were applied to study its effect on the 2,6-DMA oxidation. Fenton, electro-Fenton and photoelectro-Fenton processes were carried out for the comparison. Figure 4.12 shows that the Fenton reaction could hardly remove 2,6-DMA. In this method, hydrogen peroxide is catalyzed by ferrous ion to produce hydroxyl radicals (equation (1.1)). However, in the Fenton chain reactions, the rate constant of equation (1.1) is between 53 and 76 $M^{-1}s^{-1}$ (Walling, 1975; Rigg et al., 1954; Metelitsa et al., 1971), while that of equation (1.2) is only 0.01 $M^{-1}s^{-1}$ (Walling, 1973). This means that the ferrous ions have been fully consumed in the earlier reaction period of 5 min, and the ferric ions catalysis of hydrogen peroxide is not important.

$$Fe^{2+} + H_2O_2 \rightarrow Fe^{3+} + OH^- + {}^{\bullet}OH \quad (1.1)$$

$$H_2O_2 + Fe^{3+} \rightarrow Fe^{2+} + {}^{\bullet}H_2O + H^+ \quad (1.2)$$

As shown in the same figure, the concentration of hydrogen peroxide affected the efficiency of 2,6-DMA destruction obviously in electro-Fenton and photoelectro-Fenton processes. In the electro-Fenton process, hydroxyl radicals can be initiated by the reduction of ferric ion to ferrous ion at the cathode surface. Therefore, the residual ratios were 61%, 50% and 43% for the hydrogen peroxide concentrations of 15, 20 and 25 mM, 60 min, respectively. In photoelectro-Fenton process, the Fenton's reagent was utilized to produce hydroxyl radical in the electrochemical cell, and ferrous ion was regenerated via the reduction of ferric ion on the light source and cathode. Increasing the hydrogen peroxide concentration decreased the residual ratio of 2,6-DMA in photoelectro-Fenton process. In this work, the residual ratios were 28%, 12% and 9% for the hydrogen peroxide concentrations of 15, 20 and 25 mM, 60 min, respectively.

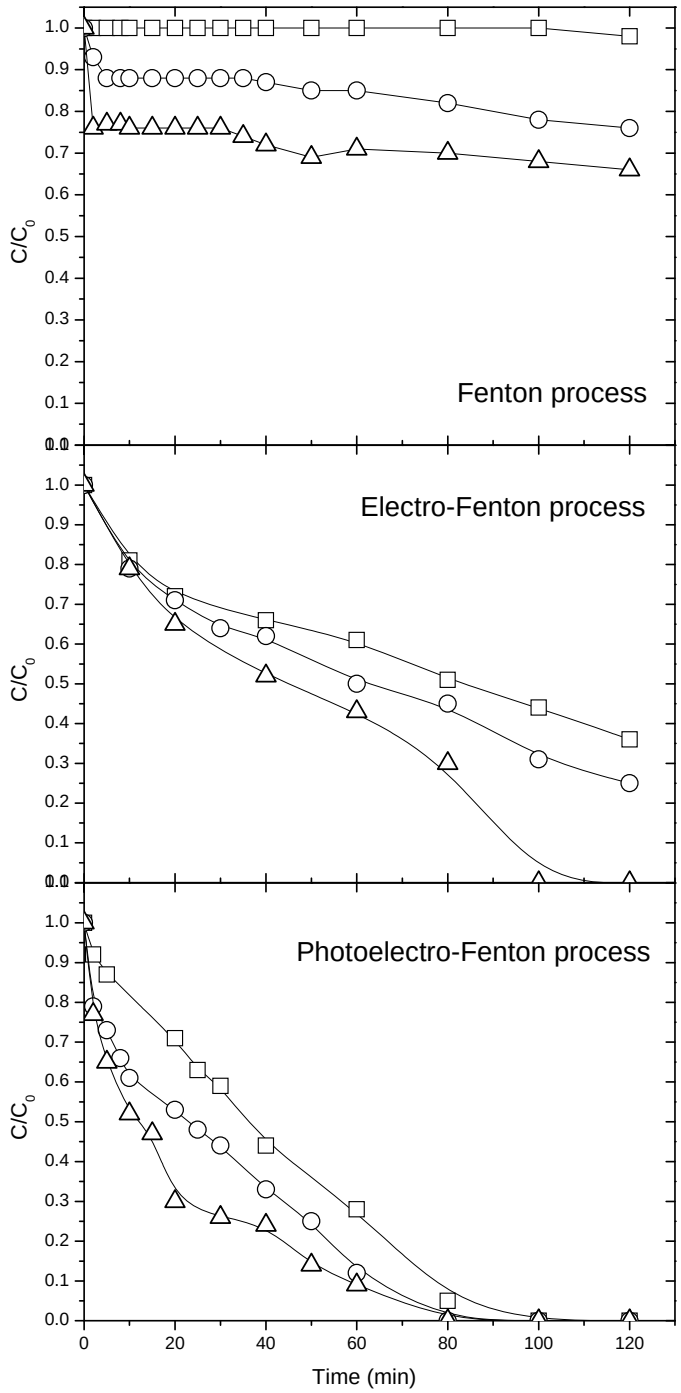

Figure 4.12 Effect of hydrogen peroxide concentration on the 2,6-DMA degradation. ([2,6-DMA] =1 mM; $[Fe^{2+}]$=1 mM; pH_i=2.0; $[NaClO_4]$= 50 mM; 48 W UVA irradiation; CD_a= 7.6 A/m^2; CD_c=7.1 A/m^2; CD_a and CD_c denote the current densities of anode and cathode, respectively; (□): 15 mM; (○): 20 mM; (Δ): 25 mM

4.2.6. The factors on the oxidation of 2,6-DMA

In this section the degradation of 2,6-DMA was explored by electro-Fenton and photoelectro-Fenton processes. To compare the performance of different oxidation processes, we evaluated three indexes: (i) the stoichiometric efficiency (E), (ii) the rate constant (k_{obs}) and (iii) UVA-promoted efficiency ($r_{PE\text{-}F}/r_{E\text{-}F}$). We define E as below (Valentine and Wang, 1998):

$$E\ (mM/mM) = \Delta[\text{pollutant}]/\Delta[H_2O_2] \quad (4.13)$$

When E is low, few radicals react with organic compounds, it substitutes for inefficient scavenging reaction. To evaluate the effect of UVA light on the degradation of 2,6-DMA, electro-Fenton and photoelectro-Fenton processes were compared at different concentrations of hydrogen peroxide (15, 20 and 25 mM). Table 4.3 indicates that higher hydrogen peroxide concentrations induce faster 2,6-DMA degradation, yet reduce E. These phenomena may be due to the hydroxyl radical scavenging effect of hydrogen peroxide (equation (2.8)) (Walling, 1975; Rigg et al., 1954).

$$H_2O_2 + {}^{\bullet}OH \rightarrow H_2O + {}^{\bullet}HO_2 \qquad k = 3.3\times10^7\ M^{-1}s^{-1} \quad (2.8)$$

The kinetic study of the electro-Fenton and photoelectro-Fenton processes follows pseudo-first-order kinetics in which the k value is determined by the following expression:

$$\ln C/C_0 = kt \quad (4.14)$$

Where C_0 represents the initial concentration of the organic compound, and C represents the concentration of the organic compound at time, t. The first-order rate constants (k_{obs}) were determined from the slopes of the plots of $\ln([2,6\text{-DNA}]_t/[2,6\text{-DNA}]_0)$ vs. time and for reaction time 60 minutes ($R \geq 0.95$). The k_{obs} value for 2,6-DMA degradation in each process is determined as show in Table 4.3. The degradation rate of the electro-Fenton with UVA irradiation would faster than the one without it. The photoelectro-Fenton process

exhibited good decomposition ability on the degradation of organic contaminants in this work. It is due to the fact that ferrous ion catalyst can be regenerated though the photoreduction of ferric ions. It then catalyzes hydrogen peroxide to produce highly reactive hydroxyl radicals. These findings confirm the significant contribution the additional generation of hydroxyl radicals in the photoelectro-Fenton process.

Table 4.3 Comparison of various oxidation processes by Stoichiometric efficiency (E) and kinetic constant (k_{obs}) ([2,6-DMA] =1 mM; [Fe^{2+}]=1 mM; [H_2O_2]= 20 mM; pH_i=2.0; [$NaClO_4$]= 50 mM; CD_a= 7.6 A/m^2; CD_c=7.1 A/m^2; 48 W UVA irradiation; reaction time=60 min)

[H_2O_2] (mM)	Electro-Fenton			Photoelectro-Fenton		
	C/C_0 (%)	E (mM/mM)	K_{obs} (min^{-1})	C/C_0 (%)	E (mM/mM)	K_{obs} (min^{-1})
15	61	0.0548	0.0096	28	0.1122	0.0194
20	50	0.0457	0.0123	12	0.0744	0.0314
25	43	0.0320	0.0153	9	0.0489	0.0408

Table 4.4 UVA irradiation promoting the efficiency of 2,6-DMA oxidation ([2,6-DMA] =1 mM; [Fe^{2+}]=1 mM; [H_2O_2]= 20 mM; pH_i=2.0; [$NaClO_4$]= 50 mM; CD_a= 7.6 A/m^2; CD_c=7.1 A/m^2; 48 W UVA irradiation)

[Fe^{2+}] (mM)	[H_2O_2] (mM)	$r_{E\text{-}F}$	$r_{PE\text{-}F}$	$r_{PE\text{-}F}/r_{E\text{-}F}$
1	15	0.0096	0.0194	2.01
1	20	0.0123	0.0314	2.56
1	25	0.0153	0.0408	2.66

The role of UVA irradiation in promoting the oxidation efficiency of 2,6-DMA could be clearly illustrated with the values obtained in Table 4.4. The ratios of UVA irradiation promoting the efficiency on the initial rates of 2,6-DMA could be obtained as follows:

$r_{PE\text{-}F}/r_{E\text{-}F}$ = Initial rate of PE-F /Initial rate of E-F (4.15)

Where $r_{PE\text{-}F}$ represents the initial rate of the photoelectro-Fenton process and $r_{E\text{-}F}$ represents the initial rate of the electro-Fenton process. The initial oxidation rate by hydroxyl radicals of organic compound in the electro-Fenton and photoelectro-Fenton processes can be expresses as equation (4.16) and (4.17), respectively (Benitez et al., 2001):

$$-d[C_{E-F}]/dt = k_{OH}[^{\bullet}OH][C_{E-F}] = r_{E-F} \quad (4.16)$$

$$-d[C_{PE-F}]/dt = k_{OH}[^{\bullet}OH][C_{PE-F}] = r_{PE-F} \quad (4.17)$$

Where $C_{E\text{-}F}$ and $C_{PE\text{-}F}$ are the concentration of organic compounds in the electro-Fenton and photoelectro-Fenton processes, and the k_{OH} represents the rate constants for the reaction between hydroxyl radicals and organic compound. The rations ($r_{PE\text{-}F}/r_{E\text{-}F}$) of UVA promoting the efficiency on the initial rates of 2,6-DMA were 2.01, 2.56 and 2.66 while the initial concentration of hydrogen peroxide increased from 15 to 20 and 25 mM, respectively. It can be concluded that the highest benefit of UVA irradiation was achieved at 25 mM of hydrogen peroxide.

4.2.7. Summary

The effect of initial pH, Fe^{2+} loading, H_2O_2 concentration and current density were investigated to evaluate the degradation and mineralization efficiency of electrolysis, Fenton, electro-Fenton and photoelectro-Fenton processes. The optimal pH_i in this study was 2. When above this pH, Fe^{3+} started to be precipitated in the form of amorphous $Fe(OH)_{3(s)}$. The formation of $Fe(OH)_{3(s)}$ not only decreased the dissolved Fe^{3+} concentration, but also inhibited Fe^{2+} regeneration by partially coating the electrode surface. Increasing ferrous ions increased the hydroxyl radicals and then promote the oxidation efficiency of 2,6-DMA. The optimal hydrogen peroxide concentration for 2,6-DMA degradation in this study was 25 mM. Higher hydrogen peroxide concentrations induce faster 2,6-DMA degradation, yet reduce E. These phenomena may be due to the hydroxyl radical scavenging effect of hydrogen peroxide. The reason is may be either the reaction of hydroxyl radical and hydrogen peroxide, or the combination of two hydroxyl radicals to form hydrogen peroxide. The 2,6-DMA degradation was increased as the current density was increased from 3.5 to 10.6 A/m^2. This was due to the higher electro-regeneration of ferrous ion from ferric ion with an increase in the current density, which increased the efficiency of the Fenton chain reactions.

The kinetic study of the electro-Fenton and photoelectro-Fenton processes follows pseudo-first-order kinetics. The electro-Fenton oxidation under UVA irradiation conditions would accelerate degradation faster than electro-Fenton method alone. These findings confirm the significant contribution of the radical pathway due to the additional generation of hydroxyl radicals in the photoelectro-Fenton process.

4.3. Treatment of BSA and 2,6-DMA by Different Oxidation Processes

According to the summary mentioned above, we know that the double cathode electrochemical cell has more potential for the improvement of the efficiency of electricity utilization. Therefore, in this part of study, we employed a novel photoelectro-Fenton method, in which ferrous ion was regenerated via the reduction of ferric ion by the light source and also on the double cathode. Furthermore, the electrolysis, Fenton, electro-Fenton and photoelectron-Fenton experiments were conducted to investigate the synergistic effect of combined photo and electrochemical methods.

4.3.1. Oxidation of BSA in different processes

Based on the results of current efficiency and energy consumption, the double cathode device (Figure 3.3 (a)) should be used for further oxidation research. Electrolysis, Fenton, electro-Fenton and photoelectron-Fenton experiments were conducted to investigate the synergistic effect of combined photo and electrochemical methods. Figure 4.13 showed that the electrochemical method could only slightly remove COD from the benzene sulfonic acid solution. In the electro-Fenton process, COD was removed rapidly during the first 20 minutes. The final COD removal efficiency achieved by the electro-Fenton process was nearly 17 % higher than that of the Fenton's reagent alone. Meanwhile, the photoelectron-Fenton process achieved a COD removal efficiency that was 14 % higher than that of the electro-Fenton process. This indicated that the photoelectro-Fenton method had synergistic effect for COD removal.

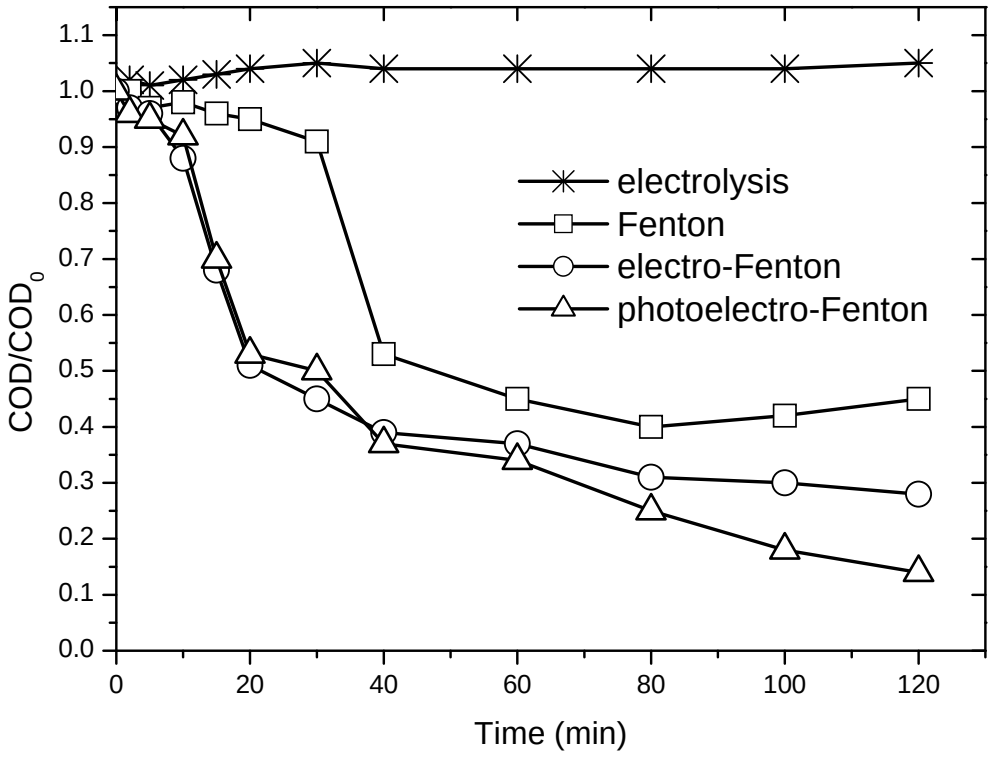

Figure 4.13 Effect of different processes on COD removal efficiency.

([$C_6H_5SO_3H$]=10 mM; [Fe^{2+}]=8 mM; [H_2O_2]=166 mM; pH_i=2.0; CD_a= 75.8 A/m^2; CD_c=71.0 A/m^2; H_2O_2 feeding time= 0, 5, 10, 15, 20, 30, 40, 60, 80, 100 min)

4.3.2. Mineralization of BSA in different processes

To investigate the synergistic effect of combined irradiation, electrochemical method and Fenton's reagent, 720 mg/L TOC of BSA solution was treated with Fenton reagent alone, the electro-Fenton method alone and the photoelectro-Fenton method, respectively. Figure 4.14 show that the Fenton process could only slightly remove TOC from the BSA solution. Furthermore in both the electro-Fenton and the photoelectro-Fenton processes, TOC was removed faster during the first hour. After that, only slow changes in TOC were observed because ferric ion was complexed by oxidation products such as oxalic acid. The degradation of aromatic compounds often leads to the formation of intermediates such as glyoxylic, maleic, oxalic, acetic and formic acids (Pignatello et al,. 2006; Sirés et al,. 2007a). These complexes typically have higher molar absorption coefficients up to 500 nm in the near-UV and visible regions leading to the generation of ferrous ion (Safarzadeh-Amiri et al., 1996). Meanwhile, the ferrous ion is regenerated via the reduction of ferric ion on the cathode.

The photochemistry of Fe^{3+} is advantageous to the Fenton process because the reduced iron can react with H_2O_2 to produce hydroxyl radical. The final TOC removal efficiency achieved by the electro-Fenton method was 64%, nearly 20% higher than Fenton's reagent alone. Meanwhile the final TOC removal efficiency achieved by the photoelectro-Fenton method was 72 %. This indicates that irradiation and electrochemical methods had a synergistic effect for TOC removal because the photoelectro-Fenton reaction takes advantage of the photo-reduction of Fe(Ⅲ)-oxalate complexes (Pignatello et al,. 2006). Bolton and coworkers added oxalate to the reaction solution and observed the photoreduction of the resulting ferrioxalate complexes, such as

$$[Fe(C_2O_4)_3]^{3-} \xrightarrow{h\nu} Fe^{2+} + 2C_2O_4^{2-} + C_2O_4^{-\bullet} \qquad (2.23)$$

and obtained degradation of aromatic and chlorinate aromatic hydrocarbons

(Safarzadeh-Amiri et al., 1996). However, photodecomposition of Fe^{3+} complexes produced some short organic acids, which are produced in the last degradation steps before total conversion to CO_2 (Brillas et al., 2000). As shown in equation (2.23), this is especially relevant with regard to the oxalic acid mineralization. The ferric complexes would be reduced to ferrous ion from the photo-reduction and by reduction in the cathode. This would induce the Fenton chain reaction efficiently.

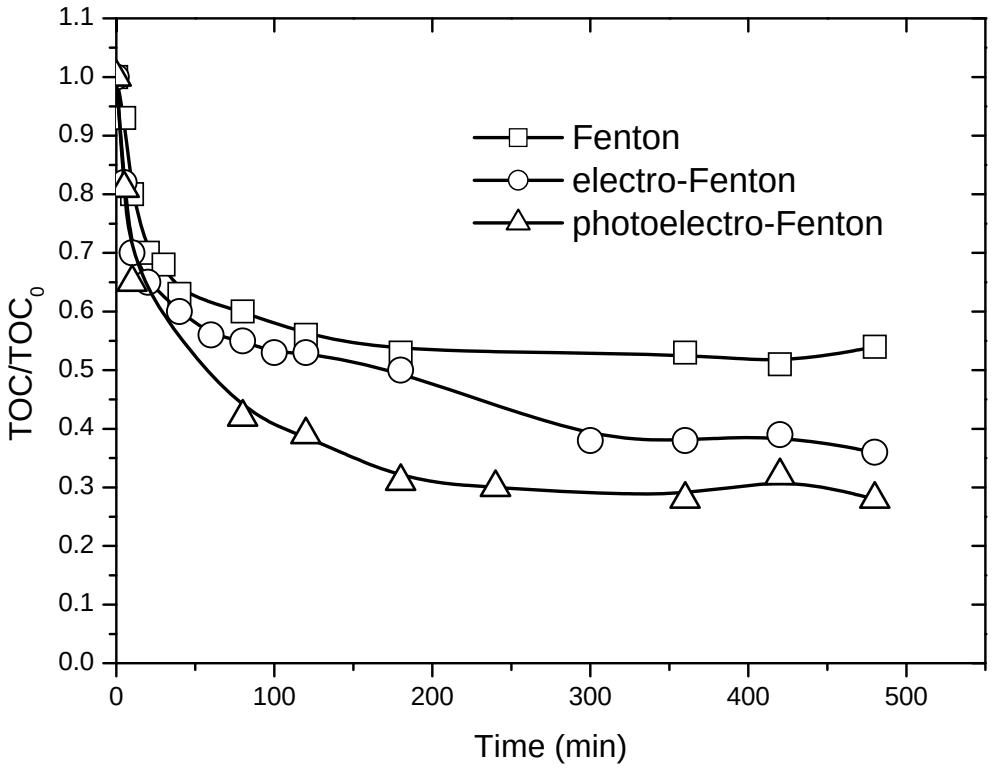

Figure 4.14 Mineralization of benzene sulfonic acid with different processes. ([$C_6H_5SO_3H$]=10 mM; [Fe^{2+}]=8 mM; [H_2O_2]=166 mM; pH_i=2.0; CD_a= 75.8 A/m^2; CD_c=71.0 A/m^2)

4.3.3. Intermediate products of BSA

The degradation of aromatic compounds often leads to the formation of intermediates such as glyoxylic, maleic, oxalic, acetic and formic acids (Pignatello et al,. 2006; Sirés et al,. 2007a).

Figure 4.15 indicates the formation of organic acid. The photo-reactivity of Fe(Ⅲ)-carboxylate or Fe(Ⅲ)-polycarboxylate complexes usually leads to decarboxylation of the organic ligand (Boye et al,. 2002).

$$R(CO_2) - Fe(\text{Ⅲ}) + h\nu \rightarrow R(CO_2^{\bullet}) + Fe(\text{Ⅱ}) \rightarrow R^{\bullet} + CO_2 \quad (1.7)$$

The use of long wave UV light and electric current as electron donors can efficiently initiate the Fenton reaction. Oxalic acid, the major intermediate of aromatic compound degradation, can complex with ferric ions. These complexes typically have higher molar absorption coefficients up to 500 nm in the near-UV and visible regions leading to the generation of ferrous ion (Safarzadeh-Amiri et al., 1996). Meanwhile, the ferrous ion is regenerated via the reduction of ferric ion on the cathode. The photochemistry of Fe^{3+} is advantageous to the Fenton process because the reduced iron can react with H_2O_2 to produce hydroxyl radical.

Bolton and coworkers added oxalate to the reaction solution and observed the photoreduction of the resulting ferrioxalate complexes, such as

$$[Fe(C_2O_4)_3]^{3-} \xrightarrow{h\nu} Fe^{2+} + 2C_2O_4^{2-} + C_2O_4^{-\bullet} \quad (2.23)$$

and obtained degradation of aromatic and chlorinate aromatic hydrocarbons (Safarzadeh-Amiri et al., 1996). However, photodecomposition of Fe^{3+} complexes produced some short organic acids, which are produced in the last degradation steps before total conversion to CO_2 (Brillas et al., 2000). As shown in equation (2.23), this is especially relevant with regard to the oxalic acid mineralization. The ferric complexes would be reduced to ferrous ion from the photo-reduction and by reduction in the cathode. This would induce the Fenton chain reaction efficiently.

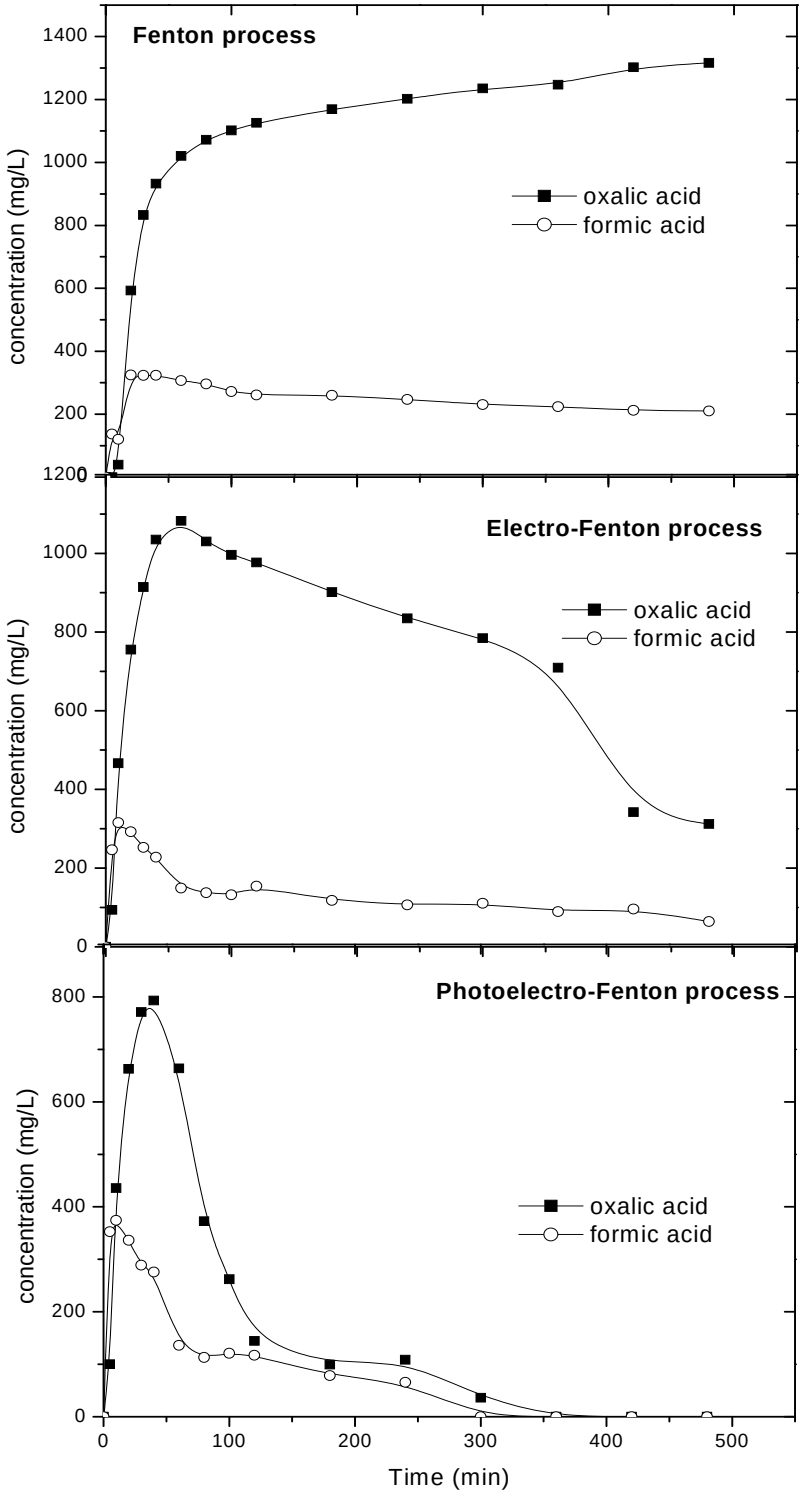
Fenton process
oxalic acid
formic acid
concentration (mg/L)
Electro-Fenton process
oxalic acid
formic acid
concentration (mg/L)
Photoelectro-Fenton process
oxalic acid
formic acid
concentration (mg/L)
Time (min)

Figure 4.15 Formation of organic acid by the degradation of benzene sulfonic acid. ([$C_6H_5SO_3H$]=10 mM; [Fe^{2+}]=8 mM; [H_2O_2]=166 mM; pH_i=2.0; CD_a= 75.8 A/m^2; CD_c=71.0 A/m^2)

4.3.4. Degradation of 2,6-DMA in different processes

Electrolysis, Fenton, electro-Fenton and photoelectron-Fenton experiments were conducted to investigate the synergistic effect of combined photo and electrochemical methods. As shown in Figure 4.16, the electrochemical method alone could remove 18% of 2,6-DMA in 2 hr. In the electrolysis method, 2,6-DMA would be destroyed by reaction with adsorbed hydroxyl radical generated at the surface of a high oxygen-overvoltage anode from water oxidation (Zhang et al., 2007; Sirés et al., 2007b), according to equation (4.1).

$$H_2O \rightarrow {}^{\bullet}OH + H^+ + e^- \quad (4.1)$$

The same tendency can be found in the research of Brillas et al (Brillas et al., 1998; Brillas et al., 2007). The removal ratio reached 24% with Fenton's reagent, showing that the Fenton process could only remove 2,6-DMA slightly. The main reason is that ferrous ions reacted very quickly with hydrogen peroxide to produce some hydroxyl radicals (equation (1.1)), and it is a Fe^{2+}/H_2O_2 reaction ($t \leq 5$ minutes). The rate constant of ferrous ions reacting with hydrogen peroxide to produce hydroxyl radicals is 53 $M^{-1}s^{-1}$, and the rate constant of ferric ions reacting with hydrogen peroxide to form ferrous is 0.01 $M^{-1}s^{-1}$ (equation (1.1) and (1.2)) (Pignatello et al., 2006; Walling, 1973). As literature reported (Pignatello et al., 2006; Lu et al., 1999), Fe^{3+} has a lower catalytic activity than Fe^{2+} and may complex with intermediates. It means that the ability of Fenton method without electrical or photo reduction to promote the ferrous concentration is too low for generating hydroxyl radicals.

The 75% removal efficiency achieved by the electro-Fenton process was nearly 51%

higher than that of the Fenton's reagent alone. Meanwhile, in the photoelectro-Fenton process, 2,6-DMA was removed completely during the first 100 minutes. The photoelectron-Fenton process achieved a removal efficiency that was 25% higher than that of the electro-Fenton process. This indicates that the photoelectro-Fenton method had a synergistic effect for 2,6-DMA degradation.

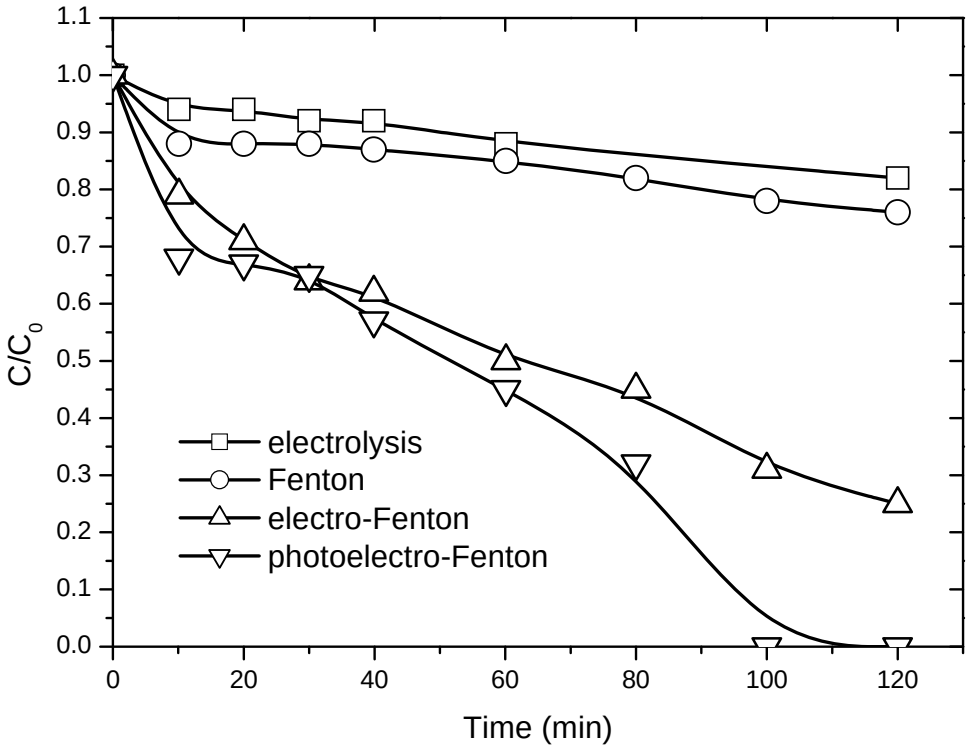

Figure 4.16 Effect of different processes on the 2,6-DMA degradation.

([2,6-DMA] =1 mM; $[Fe^{2+}]$=1 mM; $[H_2O_2]$= 20 mM; pH_i=2.0; $[NaClO_4]$= 50 mM; CD_a= 7.6 A/m^2; CD_c=7.1 A/m^2)

4.3.5. Mineralization of 2,6-DMA in different processes

To investigate the synergistic effect of combined irradiation, electrochemical method and Fenton's reagent, 96 mg/L TOC of 2,6-DMA solution was treated with Fenton reagent, the electro-Fenton method and the photoelectro-Fenton method, respectively.

Figure 4.17 shows that the electrochemical method could only remove 10% of TOC from the 2,6-DMA solution via reaction with adsorbed hydroxyl radical (equation (4.1)). Furthermore in the Fenton process, only 8 % of the TOC was removed in the first 10 minutes. After that, no obvious change in TOC was observed in the end of 8 hours of treatment (15% mineralization) because ferrous ions were precipitated. In the electro-Fenton and the photoelectro-Fenton processes, TOC removal tendencies during the first 30 minutes were similar. After that, slow changes in TOC were observed in the electro-Fenton and photoelectro-Fenton processes because ferric ion was complexed by oxidation products such as oxalic acid. These complexes typically have higher molar absorption coefficients up to 500 nm in the near-UV and visible regions leading to the generation of ferrous ions (Pignatello et al., 2006). The photochemistry of Fe^{3+} is advantageous to the Fenton process because the reduced iron can react with H_2O_2 to produce hydroxyl radical. The final TOC removal efficiency by the electro-Fenton method was 60%, nearly 45% higher than with Fenton's reagent alone. Meanwhile, the final TOC removal efficiency by the photoelectro-Fenton method was 84%. This indicates that irradiation and electrochemical methods had a synergistic effect for TOC removal.

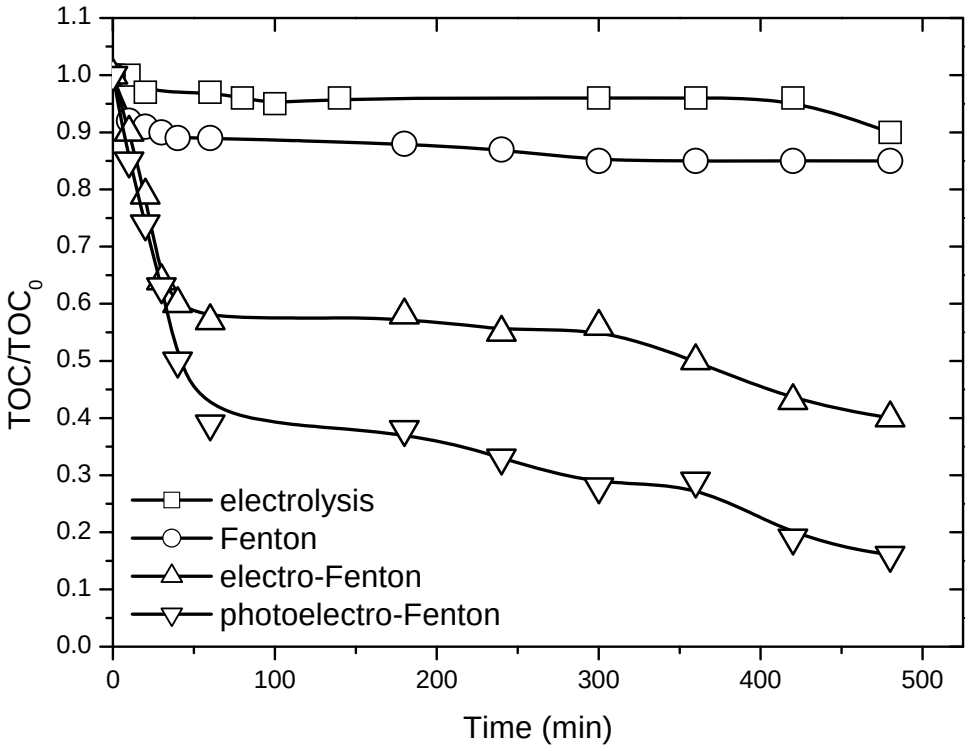

Figure 4.17 Effect of different processes on the 2,6-DMA mineralization. ([2,6-DMA] =1 mM; [Fe^{2+}]=1 mM; [H_2O_2]= 20 mM; pH_i=2.0; [$NaClO_4$]= 50 mM; CD_a= 7.6 A/m^2; CD_c=7.1 A/m^2)

4.3.6. Intermediate products of 2,6-DMA

The degradation of aromatic compounds often leads to the formation of intermediates such as glyoxylic, maleic, oxalic, acetic and formic acids (Lu et al., 2003; Casado et al., 2005). Here, the oxalic acid has been detected in the degradation solution by ion-exclusion chromatography in order to get a further understanding of the oxidative ability for electrolysis, Fenton, electro-Fenton and photoelectro-Fenton processes. Figure 4.18 indicates the formation of oxalic acid. Result indicates that the electrolysis and Fenton methods displayed worse oxidative ability with regard to the production of the oxalic acid, and it is obvious that photoelectro-Fenton process showed the best performance. The electro-Fenton method resulted in an accumulation of oxalic acid, almost reaching a constant concentration of 23.11 mg/L.

$$R(CO_2) - Fe(\text{Ⅲ}) + h\nu \rightarrow R(CO_2^{\bullet}) + Fe(\text{Ⅱ}) \rightarrow R^{\bullet} + CO_2 \quad (1.7)$$

Oxalic acid is rapidly produced and destroyed by photoelectro-Fenton. As shown in equation (1.7), the photo-reactivity of Fe(Ⅲ)-carboxylate or Fe(Ⅲ)-polycarboxylate complexes usually leads to decarboxylation of the organic ligand (Pignatello et al., 2006; Brillas et al., 2003). The use of UVA light and electric current as electron donors can efficiently initiate the Fenton reaction. Oxalic acid, the major intermediate of aromatic compound degradation, can complex with ferric ions. These complexes typically have higher molar absorption coefficients up to 500 nm in the near-UV and visible regions, leading to the generation of ferrous ion (Pignatello et al., 2006). The photochemistry of Fe^{3+} is advantageous to the Fenton process because the reduced iron can react with H_2O_2 to produce hydroxyl radicals. However, photodecomposition of Fe^{3+} complexes produced some simple organic acids, which are produced in the last degradation steps before total conversion to CO_2 (Brillas et al., 2003). This is especially relevant with regard to the oxalic

acid mineralization. The ferric complexes would be reduced to ferrous ions from the photo-reduction and by reduction in the cathode. This would induce the Fenton chain reaction efficiently.

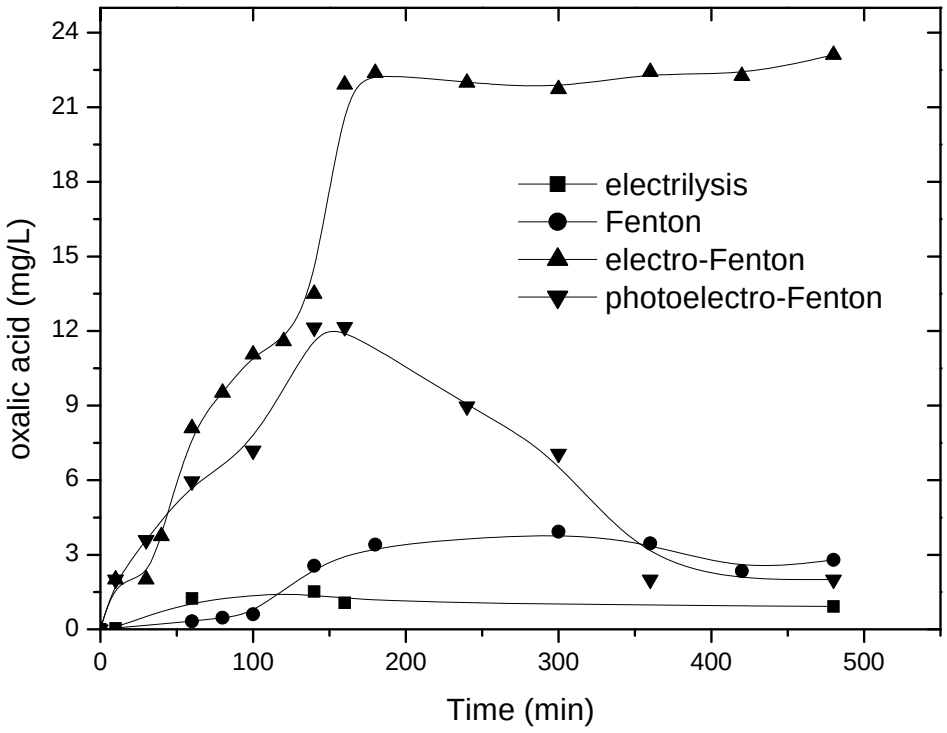

Figure 4.18 Formation of oxalic acid by the degradation of 2,6-DMA.

([2,6-DMA] =1 mM; $[Fe^{2+}]$=1 mM; $[H_2O_2]$= 20 mM; pH_i=2.0; $[NaClO_4]$= 50 mM; CD_a= 7.6 A/m^2; CD_c=7.1 A/m^2)

4.3.7. Summary

This part of study has demonstrated that the performances of the electro-Fenton and photoelectro-Fenton methods are significantly superior to the oxidative ability of a Fenton process in the degradation of BSA and 2,6-DMA. The same tendency was shown in the TOC removal. This indicates that the photoelectro-Fenton method had a synergistic effect for mineralization. Oxalic acid, the major intermediate of aromatic compound degradation, can complex with ferric ions. The ferric complexes would be reduced to ferrous ion from photo-reduction and by reduction in the cathode. This would induce the Fenton chain reaction efficiently.

4.4. Contribution of the Fenton, Electro-Fenton and Photoelectro-Fenton Processes to the Biodegradation of 2,6-DMA

As mentioned in this study, the photoelectro-Fenton process is a successful one for the 2,6-DMA degradation. In this part, the intermediates were detected and the biodegradable efficiency of Fenton, electro-Fenton and photoelectro-Fenton processes was examined. The variation of biodegradability as a function of the chemical reaction conditions was determined. BOD, BOD/COD and BOD/TOC were used for measuring biodegradability.

4.4.1. Biodegradability of 2,6-DMA in different oxidation processes

Fenton, electro-Fenton and photoelectro-Fenton processes were conducted for 2 hours to investigate the biodegradability of the effluent of reaction solutions. As show in

Figure 4.19, the Fenton oxidations of BOD, COD and TOC were steady around 90, 339 and 85 mg/L, respectively. The ferrous ions were limited as a result of the slow regeneration rate of reactions (1.1) and (1.2), the final BOD, COD and TOC values could be increased by the electro-Fenton process.

$$Fe^{2+} + H_2O_2 \rightarrow Fe^{3+} + OH^- + {}^{\bullet}OH \quad (1.1)$$

$$H_2O_2 + Fe^{3+} \rightarrow Fe^{2+} + {}^{\bullet}H_2O + H^+ \quad (1.2)$$

This combination (electrochemical/Fenton regent) leads to the formation of additional recycling of ferrous catalyst and hydroxyl radicals. It is very interesting to observe that in the electro-Fenton process, the degradation of 2,6-DMA was retarded after 1 hour. A possible explanation for this observation is the formation of Fe^{3+} with organic

intermediates in the solution, yielding iron complex species which could interfere with the electrochemical regeneration of Fe^{2+}. The photo-reactivity of Fe(Ⅲ)-carboxylate or Fe(Ⅲ)-polycarboxylate complexes usually leads to decarboxylation of the organic ligand (Pignatello et al., 2006). Hence, the photoelectro-Fenton process has significant oxidation capacity compared with the Fenton and electro-Fenton processes.

$$R(CO_2) - Fe(\text{Ⅲ}) + h\nu \rightarrow R(CO_2^{\bullet}) + Fe(\text{Ⅱ}) \rightarrow R^{\bullet} + CO_2 \quad (1.7)$$

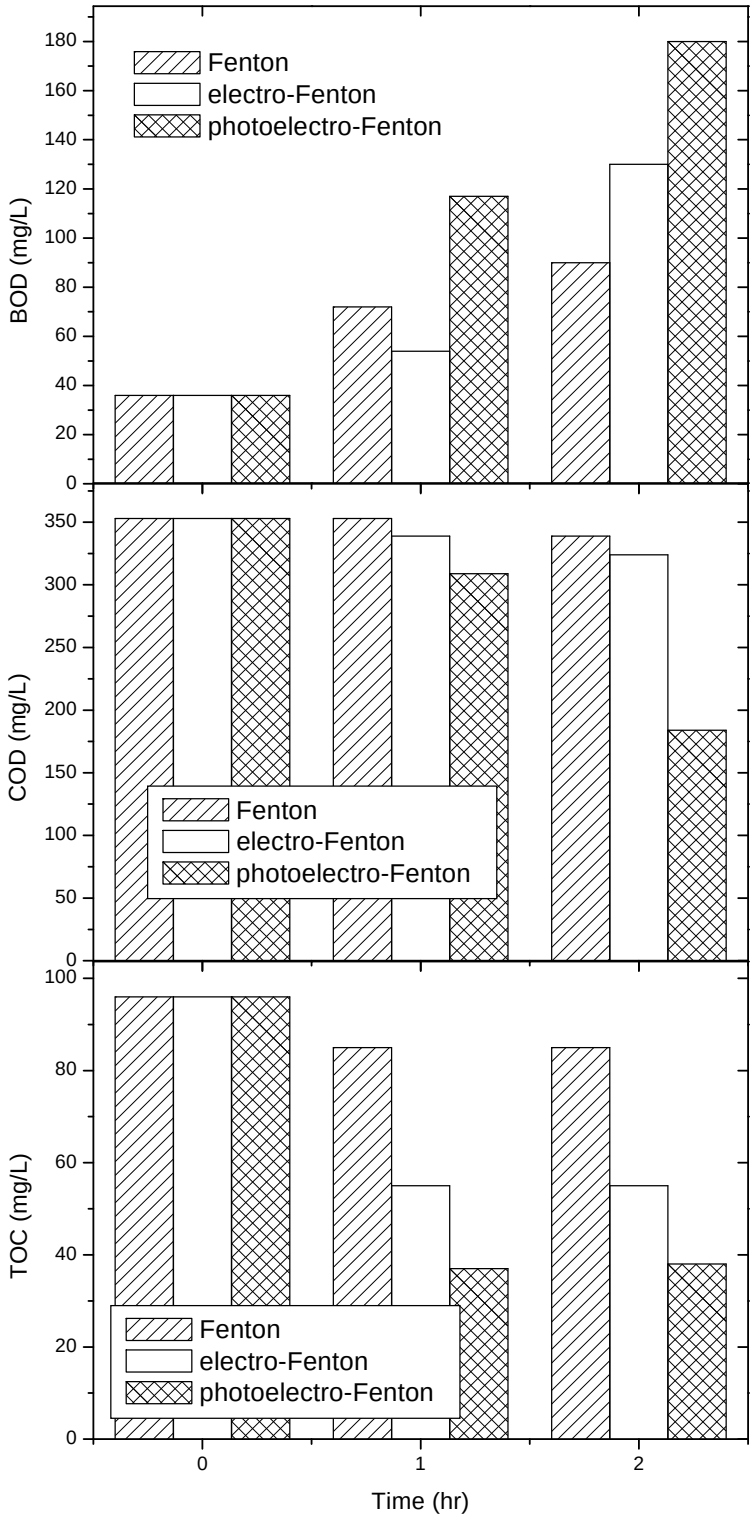

Figure 4.19 Comparison between Fenton, electro-Fenton and photoelectro-Fenton processes at 1 mM of 2,6-DMA, 1 mM of Fe^{2+}, 20 mM of H_2O_2, 48 W UVA irradiation, CD_a= 7.6 A/m^2 and CD_c=7.1 A/m^2.

The biodegradability of the solution was also tested in the experiment. BOD_5/COD and BOD_5/TOC ratios were chosen as biodegradability indicators. BOD_5/COD ratios are plotted in

Figure 4.20. In the Fenton process, the ratio barely increased in the range of 0.1 to 0.3. A BOD/COD ratio of 0.4 is generally considered the cut-off point between biodegradable and difficult to biodegrade waste. Domestic wastewater typically has a BOD_5/COD ratio of between 0.4 and 0.8 (Metcalf and Eddy Inc, 1985).

For electro-Fenton and photoelectro-Fenton processes, the ratio of BOD_5/COD was increased to 0.4 and 1.0, respectively. The same tendency was observed for BOD_5/TOC ratios for each process.

Figure 4.21 shows the biodegradability of BOD_5/TOC in each process for various reaction times. The BOD test measures organic pollutant concentrations indirectly in terms of an equivalent oxygen demand by biological oxidation of the organic matter. However, not all organic materials are biologically degradable. Conversely, the BOD/TOC (molar ratio) evaluation measures the amount of total organic carbon decomposable by microorganisms. A high BOD/TOC ratio means a high degree of biodegradation. An increase in the BOD_5 of a sample due to different treatment would indicate a greater amenability to biodegradation. Thus, an increase in the BOD_5/TOC ratio after Fenton, electro-Fenton and photoelectro-Fenton processes are indicative of improved biodegradability due to an enhancement in the proportion of TOC amenable to biological mineralization. The BOD_5/TOC ratio could exceed 1.0. This is because the oxygen demand by microorganisms not only applies from organic carbon (i.e. nitrification).

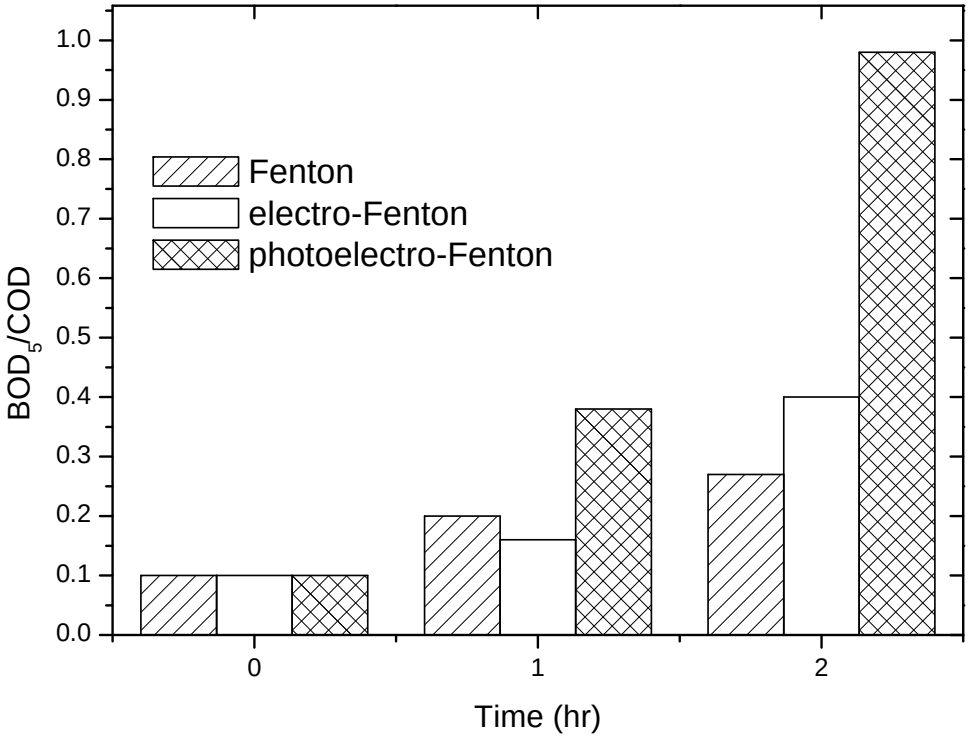

Figure 4.20 Comparison of BOD_5/COD ratios by Fenton, electro-Fenton and photoelectro-Fenton processes at 1 mM of 2,6-DMA, 1 mM of Fe^{2+}, 20 mM of H_2O_2, 48 W UVA irradiation, CD_a= 7.6 A/m^2 and CD_c=7.1 A/m^2.

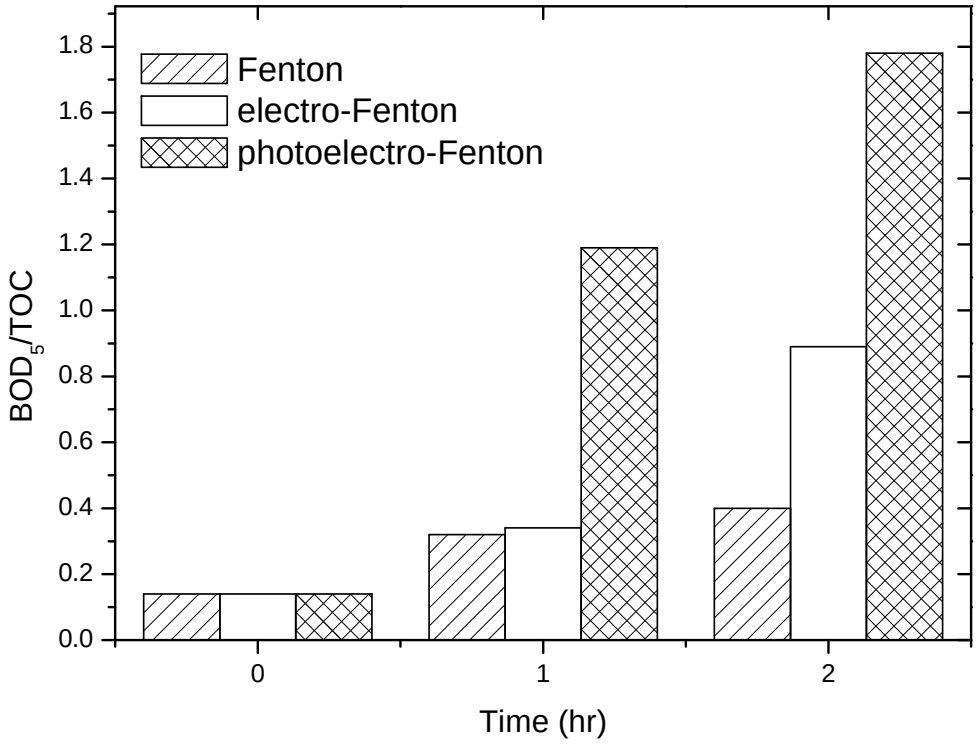

Figure 4.21 Comparison of BOD_5/TOC ratios by Fenton, electro-Fenton and photoelectro-Fenton processes at 1 mM of 2,6-DMA, 1 mM of Fe^{2+}, 20 mM of H_2O_2, 48 W UVA irradiation, CD_a= 7.6 A/m^2 and CD_c=7.1 A/m^2.

4.4.2. Reaction pathway for 2,6-DMA mineralization

The formation of aminobenzene, nitrobenzene, 2,6-dimethylphenol, phenol and oxalic acid were observed by GC-Mass. Therefore, the degradation mechanism of 2,6-DMA was proposed in Figure 4. 22. Hydroxyl radicals react with organic compounds by the addition to double bonds possessing sufficient electron density, by hydrogen abstraction from alkyl groups or hydroxyl groups, or by electron transfer (Figure 4.23). Therefore, aminophenols should be generated during the addition reaction with hydroxyl radicals. Bossmann et al. (1998) reported that the aromatic amine group of 2,4-DMA leaves as hydroxylamine and 2,4-dimethylphenol can be formed. The concentration of these products may strongly depend on the reaction conditions and different processes, but their presence supports a hydroxyl radical mechanism (Neyens and Baeyens, 2003; Pignatello et al., 2006).

Brillas et al. (1998) reported that different oxidation reactions led to the formation of nitrobenzene and benzoquinonimine. Benzoquinonimine produced benzoquinone. The oxidation of phenol leads to hydroquinone, which can be further degraded to either benzoquinone. The destruction of nitrobenzene with the release of NO_3^-, benzoquinone and 1,3,4-trihydroxybenzene gives maleic, fumaric and oxalic acids.

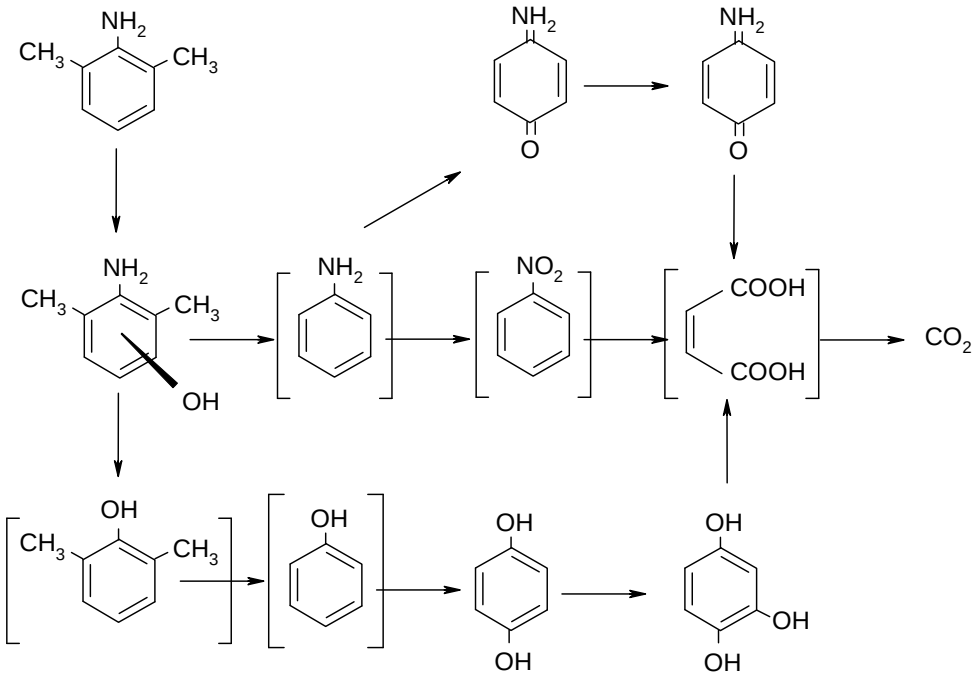

Figure 4. 22 Proposed reaction pathways for the mineralization of 2,6-DMA by Fenton, electro-Fenton and photoelectro-Fenton processes.

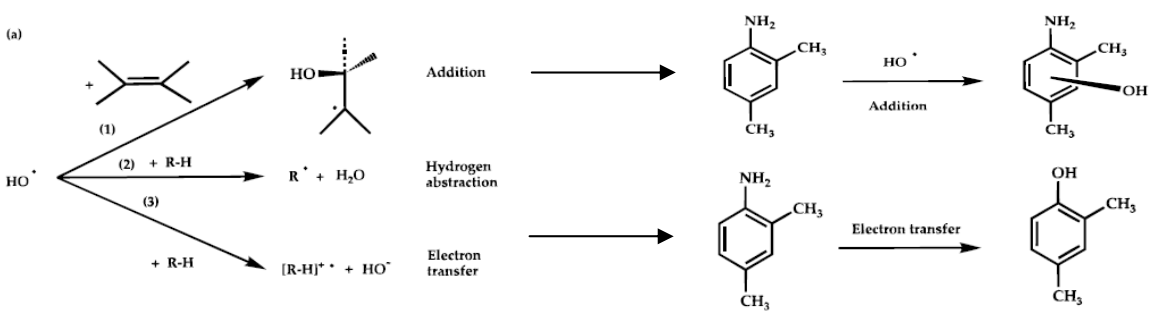

Figure 4.23 Possible reaction pathways involving hydroxyl radicals (Bossmann et al., 1998).

4.4.3. Summary

This study has demonstrated that the performances of electro-Fenton and photoelectro-Fenton methods are significantly superior to the oxidative ability of a Fenton process in the degradation of 2,6-DMA. After Fenton, electro-Fenton and photoelectro-Fenton treatments, the biodegradability was measured using BOD/COD and BOD/TOC. The BOD/COD values increased from 0.27, 0.40 to 0.98. Photoelectro-Fenton process is thought to be a successful treatment for both the abatement and the improvement of the biodegradability. The photoelectro-Fenton method could apply enough acute detoxicity and no inhibition effects on 2,6-DMA as well as a BOD_5/COD higher than 0.95. These conclusions would allow us to suggest integrating the technology of photoelectro-Fenton process and biological treatment as an optimal strategy for 2,6-DMA removal in industrial wastewater. Gas chromatography and mass spectrometry allows to detect some organic intermediates; aminobenzene, nitrobenzene, 2,6-dimethylphenol, phenol and oxalic acid in the different oxidation processes.

CHAPTER 5 CONCLUSIONS AND RECOMMENDATIONS

5.1. Conclusions

Using the results and discussion in Chapters 4, we can make the following conclusions:

(1) Considering the effects of electrode geometry and different oxidation methods, it should be pointed out that the double cathode electrochemical cell has more potential for improving the efficiency of electricity utilization. The results also suggest that a small electrode distance device can provide more economical operation.

(2) Considering the effect of different oxidation methods to mineralize BSA, the final COD removal efficiency achieved by the photoelectro-Fenton process was 17 % higher than that using the Fenton's reagent alone. The photoelectro-Fenton process achieved a COD removal efficiency that was 14 % higher than that of the electro-Fenton process. The same trend was shown in the TOC removal.

(3) In the degradation of 2,6-DMA, the performances of the electro-Fenton and photoelectro-Fenton methods are significantly superior to that of the Fenton process. The final TOC removal efficiencies were 10%, 15%, 60% and 84% using the electrolysis, Fenton, electro-Fenton and photoelectro-Fenton processes, respectively.

(4) The investigation of E, k_{obs} and $r_{PE\text{-}F}/r_{E\text{-}F}$ in the electro-Fenton and photoelectro-Fenton processes show that higher hydrogen peroxide concentrations induce faster 2,6-DMA degradation, yet reduce E. This may be due to the hydroxyl radical scavenging effect of hydrogen peroxide.

(5) The kinetic study of the electro-Fenton and photoelectro-Fenton processes follows pseudo-first-order kinetics. The electro-Fenton oxidation under UVA irradiation conditions accelerates degradation faster than does the electro-Fenton method alone.

(6) After treatment, the BOD/COD values of Fenton, electro-Fenton and photoelectro-Fenton processes were 0.27, 0.40 and 0.98, respectively.

(7) Some organic intermediates; i.e. aminobenzene, nitrobenzene, 2,6-dimethylphenol, phenol and oxalic acid were detected in the different oxidation processes using GC-Mass.

(8) Oxalic acid, the major intermediate of aromatic compound degradation, can complex with ferric ions. The ferric complexes are reduced to ferrous ions from photo-reduction and electrogeneration in the cathode. This efficiently induces the Fenton chain reaction.

5.2. Recommendations

The electro-Fenton and photoelectro-Fenton processes have been demonstrated to be effective in degrading organic compounds. Further research can focus on the following areas:

(1) To save costs, we suggest that wastewater can be treated with the electro-Fenton or photoelectro-Fenton process. Biotreatment can then be used.
(2) The anion effect of 2,6-DMA and BSA was roughly investigated in this study. The effect for oxidation of wastewater should be further studied.
(3) Based on the data obtained from the study, a pilot reactor can be designed and setup. The cost of the electro-Fenton and photoelectro assisted Fenton process can be evaluate with the pilot reactor.
(4) The integral, initial rate and excess methods can be used to determine the kinetics of the reaction.

REFERENCES

Abad, L.V., Saiki, S., Kudo, H., Muroya, Y., Katsumura, Y., de la Rosa, A.M., Rate constants of reactions of κ-carrageenan with hydrated electron and hydroxyl radical, Nucl. Instrum. Meth. B. 265, 410-413, 2007.

Alonso, M.C., Tirapu, L., Ginebreda, A., Barcelo, D., Monitoring and toxicity of sulfonated derivatives of benzene and naphthalene in municipal sewage treatment plants, Environ. Pollut. 137, 253-262, 2005.

Al Momani, F., Shawaqfeh, A., Shawaqfeh, M., Solar wastewater treatment plant for aqueous solution pf pesticide, Sol. Energy. 81, 1213-1218, 2007.

Andreozzi, R., Caprio, V., Insola, A., Marotta, R., Advanced oxidation processes (AOP) for water purification and recovery, Catal. Today. 53, 51-59, 1999.

Andrianirinaharivelo, S., Mailhot, G., and Bolte, M., Photodegradation of organic pollutants induced by complexation with transition metals (Fe^{3+} and Cu^{2+}) present in natural waters, Solar Energy Mater. Solar Cells. 38, 459-474, 1995.

APHA, Standard methods for the examination of water and wastewater, 20^{th} ed., American Public Health Association, Washington, D.C., USA, 1998.

Arienzo, M., Chiarenzelli, J., Scrudato, R., Remediation of metal-contaminated queous systems by electrochemical peroxidation: An experimental investigation, J. Haz. Mater. 87, 187-198, 2001a.

Arienzo, M., Chiarenzelli, J., Scrudato, R., Pagano, J., Falanga, L., Connor, B., Iron-mediated reactions of polychlorinated biphenyls in electrochemical peroxidation rocess (ECP), Chemosphere. 44, 1339-1346, 2001b.

Badellino, C., Rodrigues, C.A., Bertazzoli, R., Oxidation of pesticides by in situ electrogenerated hydrogen peroxide: Study for the degradation of

2,4-dichlorophenoxyacetic acid, J. Hazard. Mater. 137, 856-864, 2006.

Baeyens, J., Hosten, L., Van Vaerenbergh, E., Wastewater Treatment, Kluwer Academic Publishers, The Netherlands, 876, 1997.

Baeyens, J., Van Puyvelde, F., The incineration of sewage sludge: a strategy for the design, J. Hazard. Mater. 37179-190, 1994.

Balzani, V., Carassiti, V., Photochemistry of coordination compounds, Academic ress, New York, 1970.

Balanosky, E., Herrera, F., Lopez, A., Kiwi, J., Oxidative degradation of textile aste water. Modeling reactor performance, Wat. Res. 34, 582-596, 2000.

Bandara, J., Morrison, C., Kiwi, J., Pulgarin, C., Peringer, P.J., Degradation/ decoloration of concentrated solutions of orange II. Kinetics and quantum yield for sunlight induced reactions via Fenton type reagents, Photochem. Photobiol. A Chem. 99, 57-66, 1996.

Bandara, J., Nadtochenko, V. Kiwi, J., Pulgarin, C., Dynamics of oxidant addition s a parameter in the modelling of dye mineralization (orange II) via advanced oxidation technologies, Water Sci. Technol. 35, 87-93, 1997.

Benitez, F.J., Acero, J.L., Real, F.J., Rubio, F.J., Leal, A.I., The role of hydroxyl radicals for the decomposition of p-hydroxy phenylacetic acid in aqueous solutions, Wat. Res. 35, 1338-1343, 2001a.

Benitez, F.J., Beltran-Heredia, J., Rea, F., Acero, J.L., Phenolic contaminant acids oxidation by Fenton's reagent, Fresenius Environ. Bull. 9, 144-151, 2000b.

Benkelberg, H.J., Warneck, P., Photodecomposition of iron(III) hydroxo and sulfato complexes in aqueous solution: Wavelength dependence of OH and SO" quantum yields, J. Phys. Chem. 99, 5214-5221, 1995.

Bielski, B.H.J., Cabelli, D.E., Arudi, R.L., Reactivity of H_2O_2/O_2-radicals in aqueous

solution, J. Phys. Chem. Ref. Data 14, 1041-1100, 1985.

Bonfatti, F., Ferro S., Lavezzo, F., Malacarne, M., Lodi, G., De Battisti, A., Electrochemical incineration of glucose as a model organic subtrate. Part 2: Role of the active chlorine mediation, Electrochem. Soc. 147, 592-596, 2000.

Bossmann, S.H., Oliveros, E., Göb, S., Siegwart, S., Dahlen, E.P., Payawan, L., Straub, J.M., Wörner, M., Braun, A.M., New evidence against hydroxyl radicals as reactive intermediates in the thermal and photochemically enhanced Fenton reactions, J. Phys. Chem. A. 102, 5542-5550, 1998.

Boudenne, J.L., Cerclier, O., Galea, J., Vlist, E.V., Appl. Catal. A-Gen. 143, 185-202, 1996.

Boudenne, J.L., Cerclier, O., Performance of carbon black slurry electrodes for 4-chlorophenol oxidation, Water Res. 33, 494-504, 1999.

Boye, B., Dieng, M.M., Brillas, E., Degradation of herbicide 4-chlorophenoxyacetic acid by advanced electrochemical oxidation methods, Environ. Sci. Technol. 36, 3030-3035, 2002.

Boye, B., Dieng, M.M., Brillas, E., Anodic oxidation, electro-Fenton and photoelectro-Fenton treatments of 2,4,5-trichlorophenoxyacetic acid, J. Electroanal. Chem. 557, 135–146, 2003.

Boye, B., Brillas, E., Buso, A., Farnia, G., Flox, C., Giomo, M., Sandona, G., Electrochemical removal of gallic acid from aqueous solutions, Electrochim. Acta 52, 256–262, 2006.

Brand, N., Mailhot, G., Bolte, M., Degradation photoinduced by Fe(III): Method of alkylphenolethoxylates removal in water, Environ. Sci. Tecbnol. 32, 2715-2720, 1998.

Braun, A.M., Maurette, M.T., Oliveros, E., Photochemical Technology, Wiley & Sons,

New York, 77-81, 1991 (and references cited therein.)

Brillas, E., Mur, E., Sauleda, R., Sanchez, L., Peral, J., Domenech, X., Casado, J., Aniline mineralization by AOP's: anodic oxidation, photocatalysis, electro-Fenton and photoelectro-Fenton processes, Appl. Catal. B: Environ. 16, 31-42, 1998.

Brillas, E., Calpe, J.C., Casado, J., Mineralization of 2,4-D by advanced electrochemical oxidation processes, Wat. Res. 34, 2253-2262, 2000.

Brillas, E., Casado, J., Aniline degradation by Electro-Fenton$^{(R)}$ and peroxi-coagulation processes using a flow reactor for wastewater treatment, Chemosphere. 47, 241-248, 2002.

Brillas, E., Baños, M.Á., Garrido, J.A., Mineralization of herbicide 3,6-dichloro-2-methoxybenzoic acid in aqueous medium by anodic oxidation, electro-Fenton and photoelectro-Fenton, Electrochimica. Acta. 48, 1697-1705, 2003a.

Brillas, E., Boye, B., Dieng, M.M., General and UV-assisted cathodic Fenton treatments for the mineralization of herbicide MCPA, J. Electrochem. Soc. 150, 583–589, 2003b.

Brillas, E., Baños, M.Á., Skoumal, M., Cabot, P.L., Garrido, J.A., Rodríguez, R.M., Degradation of the herbicide 2,4-DP by anodic oxidation, electro-Fenton and photoelectro-Fenton using platinum and boron-doped diamond anodes, Chemosphere. 68, 199-209, 2007.

Buxton, G.V., Greenstock, C.L., Critical review of rate constants for reactions of hydrated electrons, J. Phys. Chem. Ref. Data 17, 513-886, 1988.

Calabrese, E.J., Kostecki, P.T., Petroleum contaminated soil, remediation technologies, Environmental Fate, Risk Assessment, Analytical Methodologies, vol. 2, Lewis Publishers Inc., Chelsea, MI, 1989.

Casado, J., Fornaguera, J., Galán, M.I., Mineralization of aromatics in water by sunlight-assisted electro-Fenton technology in a pilot reactor, Environ. Sci. Technol. 39, 1843-1847, 2005.

Comninellis, Ch., Electro catalysis in the electrochemical conversion/combustion of organic pollutants for wastewater treatment, Electrochimica Acta. 39, 1857-1862, 1994.

Comninellis, Ch., Nerini, A., Anode oxidation of phenol in the presence of NaCl for wastewater treatment, Appl. Electrochem. 25, 23-28, 1995.

Comninellis, Ch., De Battisti, A., Electrocatalysis in anodic oxidation of organics with simultaneous oxygen evolution, Chim. Phys. 93, 673-679, 1996.

Comninellis, Ch., Plattner, E., Electrochemical wastewater treatment, Chimia. 42, 250-252, 1988.

Contreras, S., Rodríguez, M., Al Momani, F., Sans, C., Esplugas, S., Contribution of the ozonation pre-treatment to the biodegradability of aqueous solution of 2,4-dichlorophenol, Wat. Rew. 13, 3164-3171, 2003.

Chamarro, E., Marco, A., Esplugas, S., Use of Fenton reagent to improve organic chemical biodegradability. Wat. Res. 35, 1047-1051, 2001.

Chen, R., Pignatello, J.J., Role of quinone intermediates as electron shuttles in Fenton and photoassisted Fenton oxidations of aromatic compounds, Environ. Sci. Technol. 31, 2399-2406, 1997.

Chen, G., Electrochemical technologies in wastewater treatment, Sep. Purif. Technol. 38, 11-41, 2004.

Chou, S., Huang, Y.H., Lee, S.N., Huang, G.H., Huang, C., Treatment of high strength hexamine-containing wastewater by electro-Fenton method, Water Res. 33, 751-759, 1999.

De Laat, J., Gallard, H., Catalytic decomposition of hydrogen peroxide by Fe(III) in homogeneous aqueoussolutions: mechanism and kinetic modelling, Environ. Sci. Technol. 33, 2726-2732, 1999.

Elizardo, K., Fighting pollution with hydrogen peroxide, Pollution Engineering. September, 106-109, 1991.

Esplugas, S., Ollis, D.F., Economic aspects of integrated (chemical+biological) processes for water treatment, J. Adv. Oxid. Technol. 2, 197-186, 1997.

Exposito, E., Sanchez-Sanchez, C.M., Montiel, V., Mineral iron oxides as iron source in electro-Fenton and photoelectro-Fenton mineralization processes, J. Electrochem. Soc. 154, E116-E122, 2007.

Faust, B.C., Hoigne, J., Photolysis of Fe(III)-hydroxyl complexes as sources of OH radicals in clouds, fog, and rain, Atmos. Environ. 24A, 79-89, 1990.

Flox, C., Ammar, S., Arias, C., Brillas, E., Vargas-Zavala, A.V., Abdelhedi, R., Electro-Fenton and photoelectro-Fenton degradation of indigo carmine in acidic aqueous medium, Appl. Catal. B: Environ. 67, 93–104, 2006.

Flox, C., Garrido, J.A., Rodríguez, R.M., Cabot, P.L., Centellas, F., Arias, C., Brillas, E., Mineralization of herbicide mecoprop by photoelectro-Fenton with UVA and solar light, Catal. Today. 129, 29-36, 2007.

Foti, G., Gandini, D., Comninellis, Ch., Anodic oxidation of organics on. thermally prepared oxide electrodes, Curr. Top. Electrochem. 5, 71-91, 1997.

Grimm J., Bessarabov D.G., Maier W., Storck S., Sanderson R.D., Sol-gel film-preparation of novel electrodes for the electrocatalytic oxidation of organic pollutants in water, Desalination. 115, 295-302, 1998.

Harrington, T., Pletcher, D., The removal of low levels of organics from aqueous solutions using Fe(II) and hydrogen peroxide formed in situ at gas diffusion electrodes, J.

Electrochem. Soc. 146, 2983-2989, 1999.

Hatchard, C.G., Parker, C.A., A new sensitive chemical actinometer. II. Potassium ferrioxalate as a standard chemical actinometer, Proc. Roy. Soc. A235, 518-536, 1956.

Hislop, K.A., Bolton, J.R., The photochemical generation of hydroxyl radicals in the UV-vis/ferrioxalate/H_2O_2 System, Environ. Sci. Technol. 33, 3119-3126, 1999.

Hickey, W.J., Arnold, S.M., Harris, R.F., Degradation of atrazine by Fenton's reagent: condition optimization and product quantification, Environ. Sci. Technol. 29, 2083-2089, 1995.

Hofseth, C.S., Chapman, T.W., Electrochemical destruction of dilute cyanide by copper-catalyzed oxidation in a flow-through porous electrode, Electrochem. Soc. 146, 199-207, 1999.

Houghton, J.I., Quarmby, J., Stephenson, T., Municipal wastewater sludge dewaterability and the presence of microbial extracellular polymer, Wat. Sci. Technol. 44, 373-379, 2001.

Hsaio, Y.L., Nobe, K., Oxidative reactions of phenol and chlorobenzene with in situ electrogenerated Fenton's reagent, Chem. Eng. Commun. 126, 97-110, 1993.

Huang, C.P., Dong, C., Tang, Z., Advanced chemical oxidation: its present role and potential future in hazardouswaste treatment, Waste Mgmt. 13, 361–377, 1993.

Huang, Y.H., Chou, S., Perng, M.G., Huang, G.H., Cheng, S.S., Case study on the bioeffluent of petrochemical wastewater by electro-Fenton method, Water Sci. Technol. 39, 145-149, 1999.

Huston, P.L., Pignatello, Jj., Reduction of perchloroalkanes by ferrioxalategenerated carboxylate radical preceding mineralization by the photo-Fenton reaction, Environ. Sci. Technol. 30, 3457-3463, 1996.

Irmak, S., Yavuz, H.I., Erbatur, O., Degradation of 4-chloro-2-methylphenol in aqueous solution by electro-Fenton and photoelectro-Fenton processes, Appl. Catal. B: Environ. 63, 243–248, 2006.

Jorand, F., Bouge-Bigne, F., Block, J.C., Urbain, V., Hydrophobic/hydrophilic properties of activated sludge exopolymeric substances, Wat. Sci. Technol. 37, 307-316, 1998.

Juttner, K., Galla, U., Schmieder, H., Environmental Electrochemistry: Fundamentals and applications in pollution abatement, Electrochim. Acta. 45, 2575-2594, 2000.

Kang, S.F., Liao, C.H., Hung, H.O., Peroxidation treatment of dye manufacturing wastewater in the presence of ultraviolet light and ferrous ions, J. Hazard. Mater. 65, 317-333, 1999.

Kannan, N., Karthikeyan, G., Tamilselvan, N., Comparison of treatment potential of electrocoagulation of distillery effluent with and without activated Areca catechu nut carbon, J. Hazard. Mater. 137, 1803-1809, 2006.

Kawaguchi, H., Inagaki, A., Kinetics of ferric ion promoted photodecomposition of 2-chlorophenol, Chemosphere 28, 57-62, 1994.

Kitis, M., Adams, C.D., Daigger, G.T., The effects of Fenton's reagent pretreatment on the biodegradability ofnon-ionic surfactants, Wat. Res. 33, 2561-2568, 1999.

Kiwi, J., Pulagarin, C., Peringer, P., Effect of Fenton and photo-Fenton reactions on the degradation and biodegradability of 2- and 4-nitrophenols in water treatment, Appl. Catal. B Environ. 3, 335-350, 1994.

Kurt, U., Apaydin, O., Gonullu, M.T., Reduction of COD in wastewater from an organized tannery industrial region by Electro-Fenton process, J. Hazard. Mater. 143, 33-40, 2007.

Kusvuran, E., Irmak, S., Yavuz, H.I., Samil, A., Erbatur, O., Comparison of the treatment

methods efficiency for decolorization and mineralization of Reactive Black 5 azo dye, J. Hazard. Mater. 119, 109-116, 2005.

L'air Liquide, Department Chimique, H_2O_2, Antipollution Clean Technology, Paris, France.

Larson, R.A., Schlauch, M.B., Marley, K.A., Ferric ions promoted photodecomposition of triazines, J. Agric. Food Chem. 39, 2057-2062, 1991.

Langford C.H., Carey, J.H., The charge transfer photochemistry of the hexaaquoiron(III) ion, the chloropentaaquoiron(III) ion, and the /-dihydroxy dimer explored with tert-butyl alcohol scavenger, Can. J. Chem. 53, 2430-2435, 1975.

Lei, L., Hu, X., Yue, P.L., Bossmann, S.H., G6b, S., Braun, A.M., Oxidative degradation of polyvinyl alcohol by the photochemically enhanced Fenton reaction, J. Photocbem. Photobiol. A Chem. 116, 159-166, 1998.

Li, C.W., Chen, Y.M., Chiou, Y.C., Liu, C.K., Dye wastewater treated by Fenton process with ferrous ions electrolytically generated from iron-containing sludge, J. Hazard. Mater. 144, 570-576, 2007.

Lin, S.H., Wu, C.L., Electrochemical nitrite and ammonia oxidation in sea water, Environ. Sci. Health, Part A. 32, 2125-2138, 1997.

Lipczynska-Kochany, E., Sprah, G., Harms, S., Influence of some groundwater and surface waters constituents on the degradation of 4-chlorophenol by the Fenton reaction, Chemosphere, 9-20, 1995.

Lu, M.C., Chen, J.N., Chang, C.P., Oxidation of dichlorvos with hydrogen peroxide using ferrous ion as catalyst, J. Hazard. Mater. B65, 277-288, 1999.

Lu, M.C., Lin, C.J., Liao, C.H., Ting, W.P., Huang, R.Y., Influence of pH on the dewatering of activated sludge by Fenton's reagent, Water. Sci. Technol. 44, 327-332, 2001.

Lu, M.C., Lin, C.J., Liao, C.H., Huang, R.Y., Ting, W.P., Dewatering of activated sludge by Fenton's reagent, Adv. Environ. Res. 7, 667-670, 2003.

Lu, M.C., Ting, W.P., Huang, Y.H., A new approach for double cathode reactor design of wastewater treatment by photoelectro-chemical method, ROC patent: 323472, 2007.

Mailhot, G., Astruc, M., Bolte, M., Degradation of tributyltin chloride in water photoinduced by iron(III), Organomet. Chem. 13, 53-61, 1999.

Manahan, S.E., Environmental chemistry, Lewis Publishers, Boca Raton, USA. 223-240, 1994.

Marselli, B., Garcia-Gomez, J., Michaud P.A., Rodrigo, M.A., Comninellis, Ch., Electrochemical synthesis and engineering electrogeneration of hydroxyl radicals on boron-doped diamond electrodes, Journal of the Electrochemical Society. 150, 79-83, 2003.

Mazellier, P., Mailhot, G., Bolte, M., Photochemical behavior of the iron(III)/2,6-dimethylphenol system, N.J. Chem. 21, 389-397, 1997.

Mazellier, P., Sulzberger, B., Diuron degradation in irradiated, heterogeneous iron/oxalate systems: The rate-determining step, Environ. Sci. Tecbnol. 35, 3314-3320, 2001.

Metelitsa, D.I., Mechanisms of the hydroxylation of aromatic compounds, Russ. Chem. Rev. 40, 563-580, 1971.

Metcalf and Eddy Inc, Wastewater engineering treatment, disposal and reuse, 3rd ed. New York, USA: McGraw-Hill, 1985.

Muruganandham, M., Swaminathan, M., Decolourisation of reactive orange 4 by Fenton and photo-Fenton oxidation technology, Dyes. Pigments. 63, 315-321, 2004.

Murphy, O.J., Hitchens, G.D., Kaba, L., Verostko, C.E., Direct electrochemical oxidation of organics for wastewater treatment, Wat.Res. 26, 443-451, 1992.

Mustranta, A., Viikari, L., Dewatering of activated sludge by an oxidative treatment, Wat. Sci. Technol. 28, 213–221, 1993.

Naumczyk, J., Szpyrkowicz, L., Grandi, F.Z., Electrochemical treatment of texitile wasterwater, Water Sci. Technol. 33, 17-24, 1996.

Neyens, E., Baeyens, J., Weemaes, M., De heyder, B., Advanced biosolids treatment using H_2O_2-oxidation, Environ. Eng. Sci. 19, 27-35, 2002.

Ollis D.F. and Al-Ekabi, H., Removal of Low concentration Air pollutions through photoassisted heterogeneous catalysis, Photocatalytic purification and treatment of water and air, Elsevier: Amsterdam, 375-379, 1993.

Oturan, M.A., Oturan, N., Lahitte, C., Trevin, S., Production of hydroxyl radicals by electrochemically assisted Fenton's reagent-Application to the mineralization of an organic micropollutant, pentachlorophenol, J. Electroanal. Chem. 507, 96-102, 2001.

Pere, J., Alen, R., Viikari, L., Eriksson, L., Characterisation and dewatering of activated sludge from the pulp and paper industry, Water Sci. Technol. 28, 193-201, 1993.

Pignatello, J.J., Dark and photoassisted Fe^{3+}-catalyzed degradation of chlorophenoxy herbicides by hydrogen peroxide, Environ. Sci. Technol. 26, 944-951, 1992.

Pignatello, J.J., Oliveros, E., Mackay, A., Advanced oxidation processes for organic contaminant destruction based on the Fenton reaction and related chemistry, Crit. Rev. Env. Sci. Tec. 36, 1-84, 2006.

Pletcher, D., Indirect oxidations using electrogenerated hydrogen peroxide, Acta Chem. Scand. 53, 745-750, 1999.

Polcaro, A.M., Palmas, S., Electrochemical oxidation of chlorophenols, Ind. Eng. Chem. Res. 36, 1791-1798, 1997.

Pratap, K., Lemley, A.T., Electrochemical peroxide treatment of aqueous herbicide

solutions, J. Agric. Food Chem. 42, 209-215, 1994.

Pratap, K., Lemley, A.T. Fenton electrochemical treatment of aqueous atrazine and metachlor, J. Agric. Food Chem. 46, 3285-3291, 1998.

Qiang, Z., Chang, J.H., Huang, C.P., Electrochemical regeneration of Fe^{2+} in Fenton oxidation processes, Water Res. 37, 1308-1319, 2003.

Rao, N.N., Bose, G., Khare, P., Kaul, S.N., Fenton and electro-Fenton methods for oxidation of H-acid and Reactive Black 5, J. Environ. Eng.-ASCE. 132, 367–376, 2006.

Rao, N.N., Somasekhar, K.M., Kaul, S.N. Szpyrkowicz, L.J., Electrochemical oxidation of tannery wastewater, Chem. Technol. Biotechnol. 76, 1124-1131, 2001.

Rajalo, G., Petrovskaya, T., Selective electrochemical oxidation of sulphides in tannery wastewater, Environ. Technol. 17, 605-612, 1996.

Rajeshwar, K., Ibanez, J.G., Electrochemistry and environment. Appl. Electrochem. 24, 1077-1091, 1994.

Rajeshwar, K., Ibanez, J.G., Environmental Electrochemistry: Fundamentals and applications in pollution abatement; Academic Press: San Diego, CA, 1997.

Rigg, T., Taylor, W., Weiss, J., The rate constant of the reaction between hydrogen peroxide and ferrous ions, J. Chem. Phys. 22, 575-577, 1954.

Roe, B.A., Lemnley, A.T., Treatment of two insecticides in an electrochemical Fenton system, J. Environ. Sci. Health. 32, 261-281, 1997.

Ronco, S.E., Aymonino, P.J., Kinetics of the thermal and photochemical decomposition of aquapentacyanoferrate(III) in aqueous solution, Transition Met. Chem. 12, 174-178, 1987.

Roland, S., Ingbert, S., Hans-Henning, S., Fluorometric determination of low concentrations of H_2O_2 in water: Comparison with two other methods and

application to environmental samples and drinking-water treatment, Wat. Res. 31, 1371–1378, 1997.

Ruppert, G., Bauer, R., Mineralization of cyclic organic water contaminants by the photo-Fenton reaction: influence of structure and substituents, Chemosphere, 271339-1347, 1993.

Safarzadeh-Amiri, A., Bolten, J.R., Cater, S.R., The use of iron in advanced oxidation processes, J. Adv. Oxid. Technol. 1, 18-26, 1996.

Safarzadeh-Amiri, A., Bolton, J.R., Cater, J.R., Ferrioxalate-mediated photodegradaation of organic pollutants in contaminated water, Wat. Res. 31, 787-798, 1997.

Savall, A. Electrochemical treatment of industrial organic effluents, Chimia 49, 23-27, 1995.

Sengil, I.A., ozacar, M., Treatment of dairy wastewaters by electrocoagulation using mild steel electrodes, J. Hazard. Mater. 137, 1197-1205, 2006.

Shen, Z., Yang, J., Hu, X., Lei, Y., Ji, X., Jia, J., Wang, W., Dual electrodes oxidation of dye wastewater with gas diffusion cathode, Environ. Sci. Tecbnol. 39, 1819-1826, 2005.

Sima, J., Makanova, J., Photochemistry of iron(III) complexes, Coord. Chem. Rev. 160, 161-189, 1997.

Sirés, I., Arias, C., Cabot, P.L., Centellas, F., Garrido, J.A., Rodríguez, R.M., Brillas, E., Degradation of clofibric acid in acidic aqueous medium by electro-Fenton and photoelectro-Fenton, Chemosphere. 66, 1660-1669, 2007a.

Sirés, I., Garrido, J.A., Rodrígues, R.M., Brillas, E., Oturan, N., Oturan, M.A., Catalytic behavior of the Fe^{3+}/Fe^{2+} system in the electro-Fenton degradation of the antimicrobial chlorophene, Appl. Catal. B-Environ. 72, 382-394, 2007b.

Snoeyink, V.L., Jenkins, D., Water Chemistry, Wiley, New York, 1982.

Sudoh, M., Kodera, T., Sakai, K., Zhang, J.Q., Koide, K., Oxidative degradation of aqueous phenol effluent with electrogenerated Fenton's reagent, J. Chem. Eng. Jpn. 19, 513-518, 1986.

Sun, Y., Pignatello, J.J., Activation of hydrogen peroxide by iron(III) chelates for abiotic degradation of herbicides and insecticides in water,J. Agric. Food Chem. 41,308-312, 1993a.

Sun, Y., Pignatello, J.J., Organic intermediates in the degradation of 2,4-dichlorophenoxyacetic acid by Fe^{3+}/H_2O_2 and $Fe^{3+}/ H_2O_2/UV$, J. Agric. Food Chem. 41, 1139-1142, 1993b.

Sun, Y., Pignatello, J.J., Photochemical reactions involved in the total mineralization of 2,4-D by $Fe^{3+}/H_2O_2/UV$, Environ. Sci. Tecbnol. 27, 304-310, 1993c.

Sun, J.H., Sun, S.P., Fan, M.H., Guo, H.Q., Qiao, L.P., Sun, R.X., A kinetic study on the degradation of *p*-nitroaniline by Fenton oxidation process, J. Hazard. Mater. 148, 172-177, 2007.

Takada H. and Ishiwatari R., Biodegradation experiments of linear alkylbenzenes (LABs): isomeric composition LABs as an indicator of the degree of LAB degradation in the aquatic environment, Environ. Sci. Technol. 24, 86-91, 1990.

Takeo, M., Nagayama, T., Takatani, K., Maeda, Y., Nakaoka, M., Mineralization and desulfonation of 3-nitrobenzenesulfonic acid by alcaligenes sp. GA-1, J. Ferment. Bioeng. 83, 505-509, 1997.

Tahar, N.B., Savall, A., Mechanistic aspects of phenol electrochemical degradation by oxidation on Ta/PbO_2 anode, Electrochem Soc. 145, 3427-3434, 1998.

Tang, W.Z., Tassos, S., Oxidation kinetics and mechanisms of trihalomethanes by Fenton's reagent,Wat. Res. 31, 1117-1125, 1997.

Ting, W.P., Huang, Y.H., Lu, M.C., Catalytic treatment of petrochemical wastewater by

electroassisted Fenton technologies, React. Kinet. Catal. L. 92, 41-48, 2007.

Ting W.P., Lu, M.C., Huang, Y.H., The reactor design and comparison of Fenton, electro-Fenton and photoelectro-Fenton processes for mineralization of benzene sulfonic acid (BSA), J. Hazard. Mater. doi:10.1016/j.jhazmat.2007.12.031, 2006.

Ting, W.P., Huang, Y.H., Lu, M.C., A double cathode reactor design of wastewater treatment by electro-chemical method, ROC patent: 316259, 2007.

Urbain, V., Block, J.C., Manem, J., Bioflocculation in activated sludge: an analytical approach, Water Res. 27, 829-838, 1993.

Van der Zee, J., Krootjes, B.B.H., Chignell, C.F., Dubbelman, T.M.A.R., Van Steveninck, J., Hydroxyl radical generation by a light dependent Fenton reaction, Free Radical Biol. Med. 14, 105-113, 1993.

Valentine, R.L., Wang, H.C.A., Iron oxide surface catalyzed oxidation of quinoline by hydrogen peroxide, J. Environ. Eng. 124, 31-38, 1998.

Venkatadri, R., Peters, R.W., Chemical oxidation technologies: ultraviolet light/hydrogen peroxide, Fenton'sreagent and titanium dioxide-assisted photocatalysis, Hazard. Waste. Hazard. Mater. 10, 107-149, 1993.

Walling, C., Kato, S., The oxidation of alcohols by Fenton's reagent: the effect of copper ion, J. Am. Chem.Soc. 93, 4275-4281, 1971.

Walling, C., Mechanism of the ferric ion catalyzed decomposition of hydrogen peroxide: effects of organic substrate, J. Am. Chem. Soc. 95, 2987-2991, 1973.

Walling, C., Fenton's reagent revisited, Acc. Chem. Res. 8, 121-131, 1975.

Wagner, R., Ruck, W., Determination of hydrogen peroxide and other peroxo compounds, Z. Wasser. Abwass. For. 17, 262-267, 1984.

Wang, Q.Q., Lemley, A.T., Kinetic model and optimization of 2,4-D degradation by anodic Fenton treatment, Environ. Sci. Technol. 35, 4509-4514, 2001.

Wells, C.F., Salam, M.A., Complex formation between iron(II) and inorganic anions. Part I. Effect of simple and complex halide ions on the reaction of Fe(II)+H_2O_2 reaction, Trans. Faraday Soc. 63, 620-629, 1967.

Wells, C.F., Salam, M.A., The effect of pH on the kinetics of the reaction of iron(II) with hydrogen peroxide in perchlorate media, J. Chem. Soc. A 24-29, 1968a.

Wells, C.F., Salam, M.A., Complex formation between iron(II) and inorganic anions. Part II. The effect of oxyanions on the reaction of iron(II) with hydrogen peroxide, J. Chem. Soc. A 308-315, 1968b.

Yoon, J., Cho, S., Cho, Y., Kim, S., The characteristics of coagulation of Fenton reaction in the removal of landfill leachate organics, Wat. Sci. Technol. 38, 209-214, 1998.

Yoon, J., Lee, Y., Kim, S., Investigation of the reaction pathway of OH radicals produced by Fenton oxidation in the conditions of wastewater treatment, Wat. Sci. Technol. 44, 15-21, 2001.

Zhang, H., Zhang, D., Zhou, J., Removal of COD from landfill leachate by electro-Fenton method, J. Hazard. Mater. 135, 106-111, 2006.

Zhang, H., Fei, C., Zhang, D., Tang, F., Degradation of 4-nitrophenol in aqueous medium by electro-Fenton method, J. Hazard. Mater. 145, 227-232, 2007.

Zhan, X.M., Wang, J.L., Wen, X.H., Qian, Y., Indirect electrochemical treatment of saline dye stuff wastewater, Environ. Technol. 22, 1105-1111, 2001.

APPENDIX

The GC-Mass spectra:

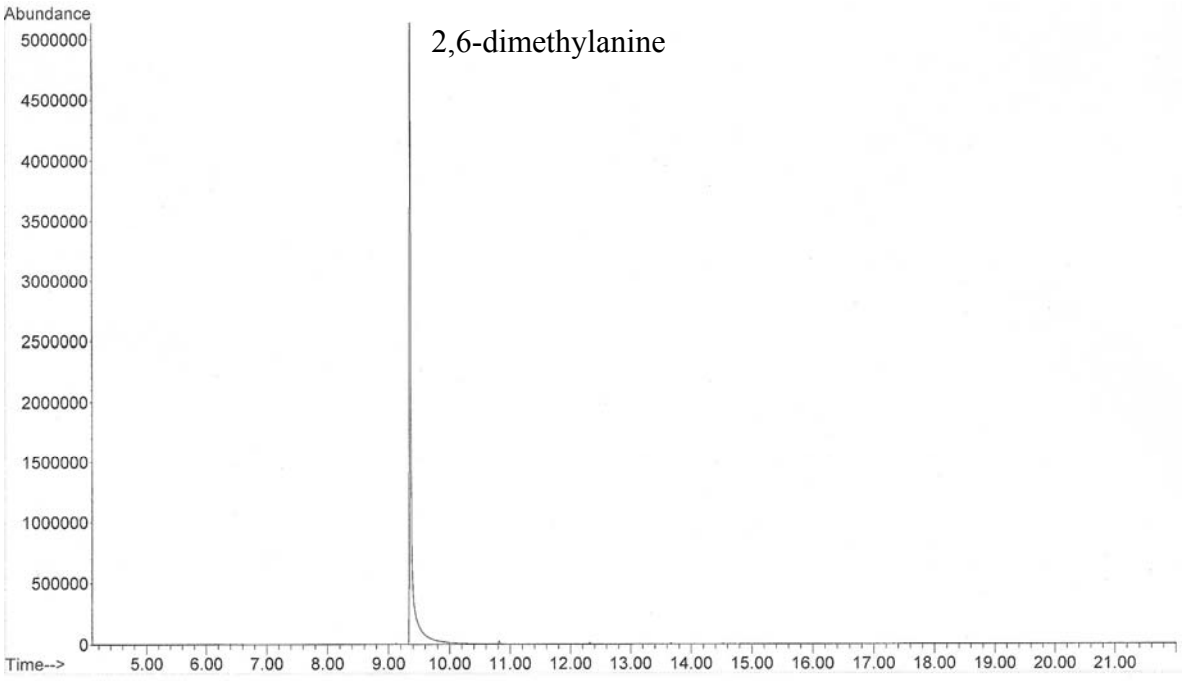

[2,6-DMA]= 1 mM, $[Fe^{2+}]$ =1 mM, $[H_2O_2]$=20 mM, 48 W UVA irradiation,

CD_a= 7.6 A/m^2 and CD_c=7.1 A/m^2

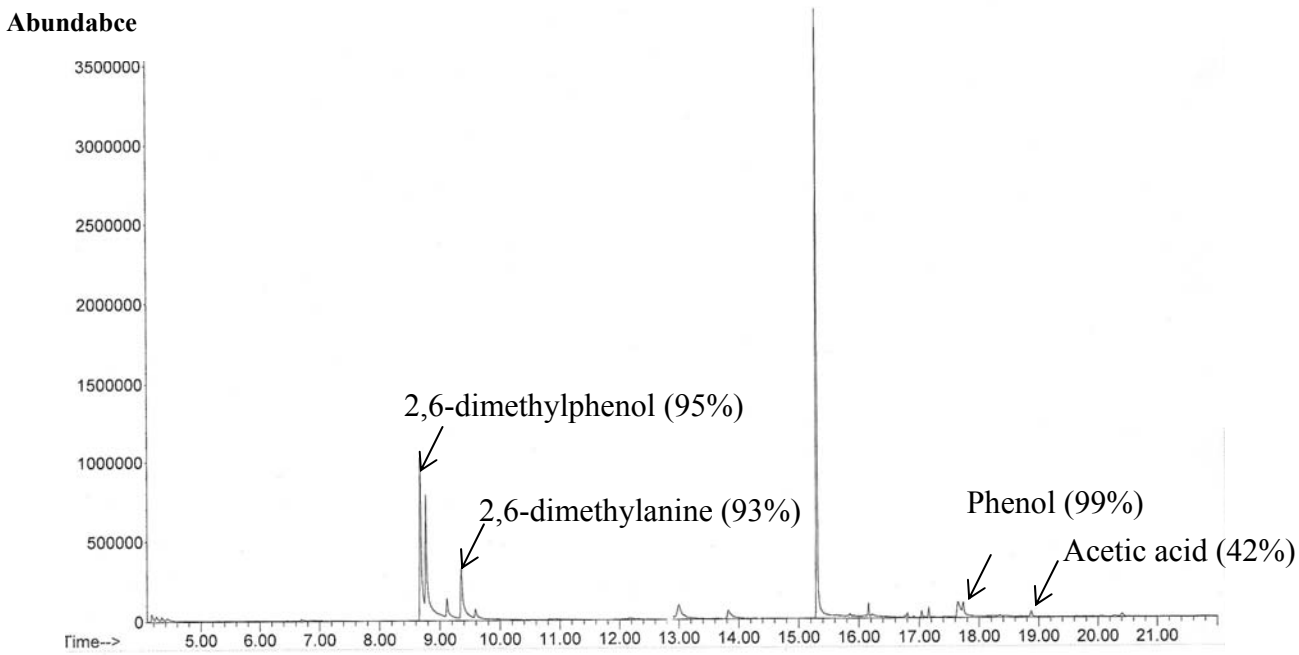

[2,6-DMA]= 1 mM, $[Fe^{2+}]$ =1 mM, $[H_2O_2]$=20 mM, 48 W UVA irradiation,

CD_a= 7.6 A/m^2 and CD_c=7.1 A/m^2

The IC spectra:

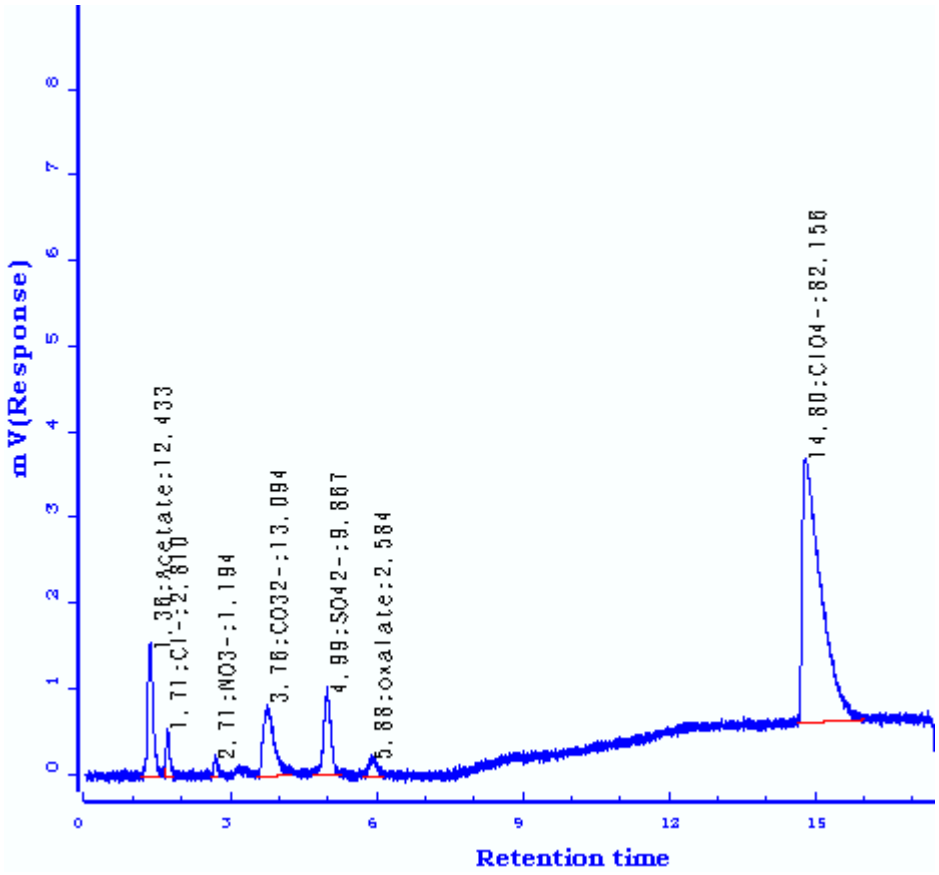

[2,6-DMA]= 1 mM, [Fe^{2+}] =1 mM, [H_2O_2]=20 mM, 48 W UVA irradiation,

CD_a= 7.6 A/m^2 and CD_c=7.1 A/m^2